ISBN 978-82-326-5168-9 (printed ver.)
ISBN 978-82-326-6258-6 (electronic ver.)
ISSN 1503-8181 (printed ver.)
ISSN 2703-8084 (electronic ver.)

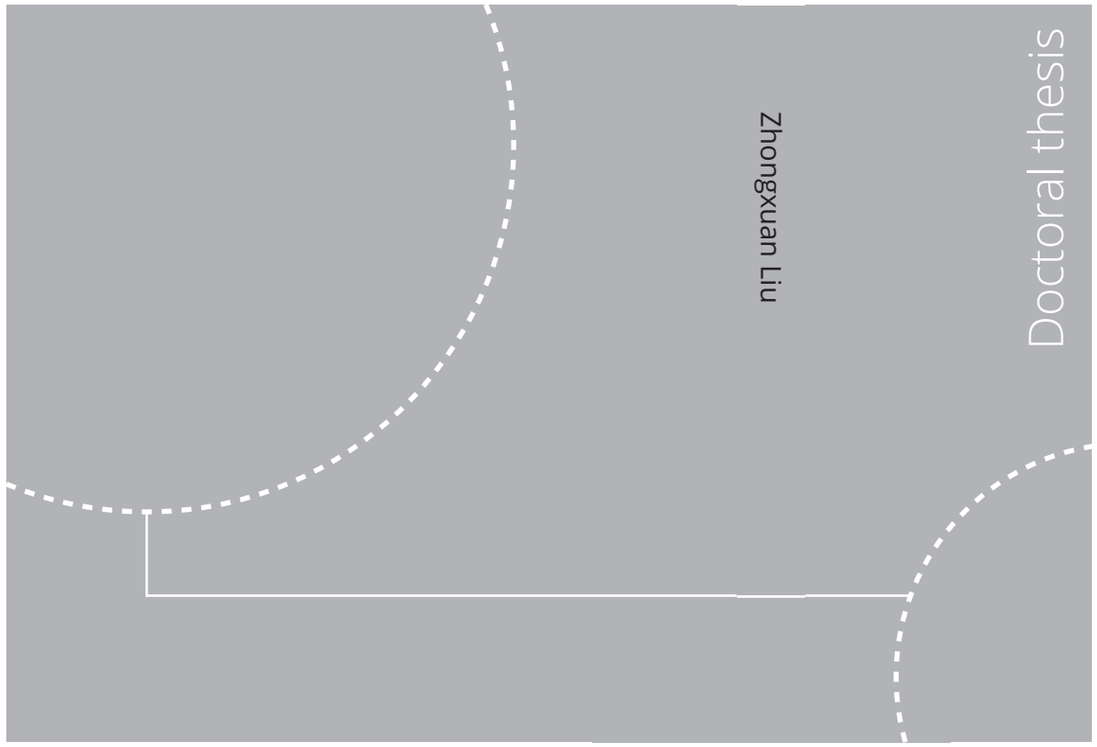

Doctoral theses at NTNU, 2022:375

Zhongxuan Liu

Performance Improvements of Standalone Liquid Air Energy Storage

Doctoral theses at NTNU, 2022:375

NTNU
Norwegian University of
Science and Technology
Thesis for the degree of
Philosophiae Doctor
Faculty of Engineering
Department of Energy and Process Engineering

NTNU
Norwegian University of
Science and Technology

NTNU
Norwegian University of
Science and Technology

Zhongxuan Liu

Performance Improvements of Standalone Liquid Air Energy Storage

Thesis for the degree of Philosophiae Doctor

Trondheim, December 2022

Norwegian University of Science and Technology
Faculty of Engineering
Department of Energy and Process Engineering

NTNU
Norwegian University of
Science and Technology

NTNU
Norwegian University of Science and Technology

Thesis for the degree of Philosophiae Doctor

Faculty of Engineering
Department of Energy and Process Engineering

© Zhongxuan Liu

ISBN 978-82-326-5168-9 (printed ver.)
ISBN 978-82-326-6258-6 (electronic ver.)
ISSN 1503-8181 (printed ver.)
ISSN 2703-8084 (electronic ver.)

Doctoral theses at NTNU, 2022:375

PRINTED IN NORWAY
NO - 1598

NORDIC SWAN ECOLABEL
Printed matter
2041 0731

Printed by Skipnes Kommunikasjon AS

Preface

This doctoral thesis is submitted to the Norwegian University of Science and Technology (NTNU) as a summary of my Ph.D. work. The work was conducted under the supervision of Prof. Truls Gundersen at the Department of Energy and Process Engineering as the main supervisor and Prof. Robin Smith at the University of Manchester as the co-supervisor. This research was performed as part of the FME project HighEFF – Centre for an Energy Efficient and Competitive Industry for the future, which is financially supported by the Research Council of Norway and user partners of HighEFF.

Abstract

Due to the threat of climate change, our energy systems tend to adopt lower-carbon energy sources, such as renewables. In addition, our energy systems are likely to follow another trend from very large centralized industrial energy systems to decentralized energy hubs serving both industry and the domestic sector in the coming years. With time variations (daily and seasonal) both on the supply side (intermittency of renewables) and the demand side, energy storage technologies will play a very important role. Liquid air energy storage (LAES) is a promising electricity storage technology that has certain advantages, such as being geographically unconstrained, having high energy density and low maintenance and operational costs. The investigation of the LAES system is in the initial stages of development, thus, a proper evaluation and improvement of the system are important to enhance the competitiveness of this technology. In this thesis, the optimization of various LAES systems is performed by a stochastic search optimization method (Particle Swarm Optimization) to improve their thermodynamic performance, and an economic evaluation of the proposed systems is carried out to test their feasibility.

In a stand-alone LAES system, the cold energy from liquid air regasification is insufficient to liquefy air in the charging part. Thus, the heat transfer efficiency of cold thermal energy recovery cycles is important for the performance of the overall system. In order to explore the improvement potentials for the LAES, different working fluids and configurations are proposed and compared as promising cold thermal energy recovery cycles. The results prove that a dual multi-component fluid cycle has the best performance in terms of exergy efficiency and round-trip efficiency (RTE). The system with only one cold energy recovery cycle has lower RTE due to the large exergy destructions in low-temperature heat exchangers caused by the large temperature differences between the working fluid and air. Organic Rankine Cycles (ORCs) have also been tested as cold thermal energy recovery cycles. However, optimization results

indicate that ORCs used in the cold thermal energy recovery system are not producing any work, and only phase change of the working fluid takes place, thus they should not be used.

The compression and expansion sections directly affect the power consumption and production and are therefore critical to the RTE of the system. To improve the performance of the LAES, systems with different number of compression and expansion stages are studied. It is found that the best performance of the LAES is achieved in a process where hot and cold streams have close to parallel temperature profiles in the preheaters of the expansion section. The optimal results show that the highest RTE of 66.7% is obtained when there is a 2-stage compressor and a 3-stage expander in the LAES system.

The incomplete utilization of compression heat from the charging part is another factor that limits the RTE of the LAES system in some configurations. Organic Rankine Cycle (ORC), Absorption Refrigeration Cycle (ARC) and High Temperature Heat Pump (HTHP) are considered to utilize the surplus compression heat in the LAES system. Optimal results indicate that the ORC, the ARC and the HTHP can effectively improve the performance of the LAES system with the available surplus compression heat. The RTE of the LAES-ORC system is increased by 4% with R600a as working fluid. For the optimized LAES-ARC system, the RTE reaches 63.5% with an increased liquid yield of air of 89.6%. In the LAES-HTHP system, the RTE is increased by 7% when the HTHP uses R1233zd as working fluid.

To study the feasibility of the proposed LAES system, an economic comparison of four LAES configurations with a storage capacity of 10 MW / 80 MWh is carried out. The results show that the LAES system with a 3-stage compressor and a 4-stage expander has a lower Levelized Cost of Storage (LCOS) compared to other LAES configurations. However, the system with a 2-stage compressor and 3-stage expander is the most profitable layout for the LAES when the income of the LAES is considered. The comparison between the LAES and other energy storage technologies indicate that the LAES system has a better economic performance than Li-ion and Pb batteries, but LAES cannot compete with Pumped Hydroelectric Energy Storage (PHES) and Compressed Air Energy Storage (CAES).

Acknowledgements

In the past four years, the way to pursuing a doctorate degree has been challenging and rewarding. I would like to thank the people for helping me to achieve this.

I would like to express my sincere gratitude to my main supervisor Professor Truls Gundersen for giving me this opportunity to carry out my PhD project. For a new research field, he could always provide excellent guidance and enlightening suggestions. Discussions during weekly meetings have laid a solid foundation for my academic research. His valuable suggestions and positive support for the development of my work have truly been inspiring.

I would like to thank my co-supervisor Prof. Robin Smith at the University of Manchester (UOM). The early discussions and meetings with him were greatly helpful for the initial stage of my PhD work. His critical scientific inputs and academic guidance played a key role and brought me inspiration for the PhD project. I would also like to thank Dr. Julia Jimenez Romero and other lab members at the UOM for the warm welcome during my participation in the PIRC conference in Manchester.

My colleagues in our Process Integration (PI) group have been very helpful and supportive. Many thanks to Dr Donghoi Kim for introducing me into the MACH-2 project, which brought me into a new research field of hydrogen production. Furthermore, he has spent time contributing great ideas in my papers and discussing research results with me. He is acknowledged here for his contributions. Many thanks to Prof. Haoshui Yu for his valuable suggestions when I encountered scientific problems. Many thanks to Miss He Ting for her excellent cooperation. Thanks to Rahul, Chao, Bjørn, Matias, Avinash, and Ruiqi for the nice presentations and discussions within our PI group during our lunch meetings. Thanks to all the

Chinese and Norwegian friends and colleagues at the Department of Energy and Process Engineering for making this PhD journey a fun and pleasant experience. Many thanks to Xinru Wang at the department of marine technology for her support in my hour of need. Furthermore, I greatly appreciate the support received from the administration staff.

Finally, I would like to express my deepest gratitude to my parents, Xiuxia and Guangqi, for their unlimited love, support and understanding. Thanks to my boyfriend, Yuhang, who has enlightened my present and future.

Trondheim, October 2022

Zhongxuan Liu

Table of Contents

List of Figures

List of Tables

Nomenclature

Abbreviations

ARC	Absorption Refrigeration Cycle
CAES	Compressed Air Energy Storage
COP	Coefficient of Performance
CS	Carbon Steel
DES	Distributed Energy System
EES	Electrical Energy Storage
ETE	Exergy Transfer Effectiveness
GWP	Global Warming Potential
HTHP	High Temperature Heat Pump
KC	Kalina Cycle
KPI	Key Performance Indicator
LAES	Liquid Air Energy Storage
LCOS	Levelized Cost Of Storage
LMTD	Logarithmic Mean Temperature Difference
LNG	Liquefied Natural Gas
MCFC	Multi-component Fluid Cycle
MTD	Minimum temperature difference
NPP	Nuclear Power Plant
NPV	Net Present Value
ODP	Ozone Depletion Potential
ORC	Organic Rankine Cycle
PHES	Pump Hydroelectrical Energy Storage
PSO	Particle Swarm Optimization
PTES	Pump Thermal Energy Storage

RTE	Round-Trip Efficiency
SS	Stainless Steel
VCRC	Vapor Compression Refrigeration Cycle

Roman symbols

A	Heat exchanger area (m^2)
C	Cost ($)
$\dot{E}$	Exergy (kW)
f	Factor (-)
$\dot{H}$	Enthalpy rate (kW)
i	Interest rate (%)
$\dot{m}$	Mass flow rate (kg/s)
N	Number of years (-)
p	Pressure (bar)
$\dot{Q}$	Heat rate (kW)
$\dot{S}$	Entropy rate (kW/°C)
T	Temperature (°C)
t	Service life (year)
U	Overall heat exchanger coefficient (kW/°C·m^2)
V	Volume (m^3)
VF	Vapor fraction
$\dot{W}$	Power (kW)
w	Specific power (kJ/kg)
x	Set of decision variables

Greek symbols

β	Residual value rate (%)
η	Efficiency (%) or Conversion rate (%)
ΔT	Minimum heat transfer approach temperature (°C)

Subscripts and superscripts

ac	Aftercoolers
AI	Annual Income
air	Air
an	Annual
AOC	Annual Operating Cost
APC	Annualized Post-production Cost
ARC	Absorption Refrigeration Cycle
BM	Bare-Module
c	Cold fluids (working fluids in cold storage cycles) or Cost
C	Compressors
CC	Contingency and Contractor
ch	Charging process
coldbox	Cold box
Con	Condensation
comp	Compression/Compressor
cr	Critical
cryotur	Cryo-turbine
CT	Cryo-turbine
D	Depreciation of capital investment
dc	Discharging process
dir	Direct expansion in the discharging part
eva	Evaporation/Evaporator
exp	Expansion part or expander
F	Fluid
fa	Air feed
feed	Feed stream
h	Thermal oil (working fluid in the hot storage cycle)
hd	High demand
HTHP	High Temperature Heat Pump
in	Inlet
int	Intercooler
LA	Land Acquisition
LC	Labor Cost
liq	Liquid air
LMTD	Logarithmic mean temperature difference
LY	Liquid yield

m	Material
M	Number of expansion stages
MC	Maintenance Cost
MSHX	Multistream heat exchanger
N	Number of compression stages
nb	Normal boiling point
net	Net power output
ORC	Organic Rankine Cycle
out	Outlet
p	Pressure
P	Pump
pre	Preheaters
pump	Pump
rec	Cold energy recovery part
reh	Reheater
RT	Round-trip efficiency
RTE	Round-trip efficiency
TCI	Total Capital Investment
trans	Heat transfer part
tur	Turbine
UC	Utility Cost
WC	Working capital

Chapter 1 Introduction

1.1 Motivation

With the increase in global energy demand and the growing environmental issues associated with CO_2 emissions, a transition from fossil fuels to renewable energy for energy systems is observed [1, 2]. Another trend for the energy market is that the traditional centralized power plants will be shifted towards smaller decentralized utility systems, where local sources, especially renewables, can be utilized [3]. These two changes motivate the development of energy storage technologies. The employment of energy storage can not only handle the instability of energy systems caused by the intermittent renewables, but provide ancillary services to electricity markets (e.g., peak shaving and valley filling) [4].

Energy storage technologies are mainly categorized into thermal energy storage (TES) and electrical energy storage (EES), depending on the form of released energy (thermal energy or power) [5]. Although TES is important, EES is the major topic of our work since electricity is one of the most convenient forms of energy. Currently, pumped hydroelectric energy storage (PHES) [6], compressed air energy storage (CAES) [7], and batteries [5] are the most mature EES technologies. However, the application of these technologies is limited by their drawbacks.

Among various proposals, liquid air energy storage (LAES) has been suggested to have outstanding performance compared with the above-mentioned energy storage technologies. Energy is stored in the form of liquid air with a higher energy density, so the volume of storage tanks is considerably reduced. The use of LAES also avoids the geographical constraints of

PHES and CAES. In addition, the LAES can be integrated with other energy conversion processes, and it can be located near these processes to avoid additional pipelines and corresponding costs. Thus, the LAES is a promising alternative for large-scale energy storage. However, the main drawback for the LAES is the relatively low round-trip efficiency (RTE). Thus, various studies have been conducted to improve the performance of the cold energy storage cycles, the compression and expansion parts, and the hot storage cycle in the LAES system.

Briefly, the LAES works as follows: When there is excess electricity, air is compressed, cooled and liquefied before storage. When there is a demand for electricity, liquid air is pumped, vaporized and expanded to produce power.

Most published work use two pure working fluids (i.e., methanol and propane) in the cold energy recovery cycles to transfer cold energy from liquid air regasification to the air liquefaction part. There is a lack of research on studying alternative fluids and configurations for cold energy storage cycles in the LAES system, such as multi-component fluid cycles (MCFCs) and Organic Rankine Cycles (ORCs). Moreover, in the existing literature, development of novel LAES configurations has been performed without optimization. Therefore, thorough optimization is required for an objective comparison between the LAES with different cold energy recovery cycles.

A large number of variations for the LAES can be generated by varying the number of compression and expansion stages. The expansion section is strongly influenced by the compression section since there is a heat recovery cycle between these two parts of the LAES.There is a lack of studies related to the complex effect of different number of compression and expansion stages on the performance of the LAES system. Thus, a comparison of different layouts for the LAES has to be carried out to identify the optimal configuration for the process.

A part of the compression heat is not efficiently used in the expansion part of certain LAES configurations. ORCs and absorption refrigeration cycles (ARC) have been adopted to utilize

the surplus compression heat to improve the RTE of the LAES. However, the research on the utilization of surplus compression heat is far from complete. High temperature heat pumps (HTHPs) are also promising technologies to utilize waste heat. Therefore, development of various technologies for the utilization of compression heat and working fluid selection for the ORC and the HTHP are needed for objective evaluation and comparison of the LAES with additional thermodynamic cycles.

Although there have been various suggestions for the improvement of the LAES based on energy analysis, a real-life application of the LAES depends not only on energy efficiency but also on the economic viability of the system. Therefore, an economic analysis of various LAES configurations is required to achieve a comprehensive evaluation of the process.

1.2 Objectives

The main objective of this work is to improve the system performance of a standalone LAES. To achieve this, it is attempted to develop novel concepts for the system and use mathematical optimization. Another objective of this thesis is to evaluate the feasibility of the LAES based on economic analysis.

The specific targets of this work include:

1. To explore possible ways to improve the performance of the cold energy recovery cycles in the LAES.
2. To study the complex relationship between the compression and the expansion parts, and to identify the optimal LAES configuration.
3. To achieve a performance improvement for the LAES by utilizing the unused compression heat in the system.
4. To test the economic viability of the LAES and compare the results with other energy storage technologies.

1.3 Scope

This study is limited to electrical energy storage (EES) technologies. Liquid air energy storage is one of the most promising EESs due to its characteristics of being geographically unconstrained and having high energy density. The major focus of this thesis is a standalone LAES system. Integration between the LAES and other energy conversion processes with waste heat and cooling has the potential of significant improvements in energy efficiency, however, this is beyond the scope of the thesis and therefore only briefly discussed. This study is also limited to the main components of the LAES, such as the compression and expansion parts, the heat recovery cycle, the cold energy recovery cycles and possible additional thermodynamic cycles (ORC, ARC and HTHP). Thus, the gas pre-treating steps are not included in our simulation and optimization studies. The ORC, ARC and HTHP are only used to utilize surplus compression heat to produce power. Optimal heat integration between the LAES and these cycles is not the scope of this work. In the simulation models of the LAES with varying number of compression and expansion stages, a thermodynamic analysis is conducted to explore the potential for system efficiency improvements. Mechanical limitations and cost issues related to large pressure ratios and outlet temperatures of compressors and expanders are important topics, but these will not be considered.

The scope of this work is to develop steady state models of the LAES system for the design, optimization and analysis of the process. Thermodynamic properties of process streams are evaluated by cubic equations of state (Peng-Robinson). The LAES system is optimized by using a population-based stochastic optimization method to maximize the RTE. Development of optimization algorithms is not part of this work.

1.4 Contributions

The main contributions of this PhD project can be listed as follows:

- For the first time, multi-component fluid cycles (MCFCs) were proposed to replace the conventional cold energy recovery cycles (the methanol cycle and the propane cycle) in the LAES. Rigorous process models were developed to be optimized with a stochastic search algorithm (particle swarm optimization). Optimal compositions and operating conditions for the MCFCs used in the LAES were determined.
- Organic Rankine Cycles (ORCs) were proposed as a promising alternative for the cold energy recovery cycles in the LAES. These ORCs can transfer the cold duty as well as produce electricity by utilizing the temperature difference between the air regasification and liquefaction. Unfortunately, the power output from the ORCs comes at the expense of a less perfect match for the heat transfer between air and the cold energy recovery fluids in the evaporator and the cold boxes. As a result, energy performance is deteriorated rather than improved.
- The complex effect of different number of compression and expansion stages on the performance of the LAES system was investigated for the first time. Because of the hot storage cycle, the amount and temperature of thermal oil change with different number of compressor stages, directly affecting the inlet air temperature to expanders and the power output. The best layout for the LAES was identified as the process with enough amount of thermal oil to obtain parallel temperature profiles in the preheaters of the LAES.
- Additional technologies (ORC, ARC and HTHP) for the utilization of compression heat in the LAES were explored. The system performance can be improved, but only marginally, by recovering the unused compression heat using such thermodynamic cycles. The most suitable working fluid and the operation of the cycles that utilize surplus heat in the system were determined.

- An economic comparison was performed among four layouts of a 10 MW / 80 MWh LAES system. A sensitivity analysis on the cost of using unconventional compressors with higher pressure ratios than conventional units were conducted to cope with the uncertain cost data for such equipment. A comparison between the studied LAES and other energy storage technologies was also carried out to reveal the economic feasibility of this energy storage technology.

1.5 Thesis structure

This thesis consists of eight chapters. Chapters 4 to 6 discuss performance improvement approaches for a standalone LAES based on energy efficiency, while Chapter 7 performs economic evaluation of selected LAES configurations.

- **Chapter 1** is an introductory chapter, showing the motivation, objectives, scope of work, and contributions of this thesis.
- **Chapter 2** gives a brief overview of the literature related to electrical energy storage technologies, emphasizing the state-of-the-art LAES technologies.
- **Chapter 3** introduces the key performance indicators used in this study. The simulation tools and optimization methods for the LAES are also presented.
- **Chapter 4** suggests six new cold energy recovery cycles in the LAES to improve the RTE. Optimization is also performed for a fair comparison between the new cycles and the conventional methanol and propane cycles.
- **Chapter 5** evaluates different configurations for the LAES to find the most energy efficient layout. The effect of varying the number of compression and expansion stages is analyzed.
- **Chapter 6** proposes three methods (ORC, ARC and HTHP) for the utilization of surplus compression heat in the LAES. Furthermore, the most suitable working fluids for the ORC and the HTHP are identified.

- **Chapter 7** is a natural continuation of the previous chapters, where economic analysis of some LAES configurations is conducted. A comparison is also made with other mature energy storage technologies.
- **Chapter 8** summarizes the main conclusions in this thesis and provides recommendations for future work.

1.6 Publications

Journal papers:

- Liu Z, Kim D, Gundersen T. Optimal recovery of thermal energy in liquid air energy storage. Energy. 2022;240:122810.
- Liu Z, Kim D, Gundersen T. Optimization and analysis of different liquid air energy storage configurations. Computers & Chemical Engineering (under review).
- Liu Z, He T, Kim D, Gundersen T. Optimal utilization of compression heat in liquid air energy storage. Submitted to Industrial & Engineering Chemistry Research.
- Liu Z, Kim D, Gundersen T. Performance analysis of the optimal integration between liquid air energy storage and LNG regasification process. To be submitted.

Conference publications:

- Liu Z, Kim D, Gundersen T. Techno-economic analysis of different liquid air energy storage configurations. Chemical Engineering Transactions. 2022;94:241-246.
- Liu Z, Yu H, Gundersen T. Optimization of Liquid Air Energy Storage (LAES) using a Genetic Algorithm (GA). Computer Aided Chemical Engineering. 2020;48:967-972.
- Liu Z, Kim D, Gundersen T. Multi-component fluid cycles in liquid air energy storage. Chemical Engineering Transactions. 2020;81:55-60.

Presentations:

- Liu Z, Kim D, Gundersen T, Techno-economic Analysis of Different Liquid Air Energy Storage Configurations, 25th Conference on Process Integration for Energy Saving and Pollution Reduction (PRES 2022), 5-8 September 2022, Bol, Croatia. Oral presentation.
- Liu Z, Gundersen T, Liquid Air Energy Storage - Integration Opportunities, AIChE Annual Meeting, 7-19 November 2021, Boston and Virtual, USA. Oral presentation.
- Liu Z, Yu H, Gundersen T, Optimization of Liquid Air Energy Storage (LAES) using a Genetic Algorithm (GA), 30th European Symposium on Computer Aided Process Engineering (ESCAPE 2020), 31 August - 2 September 2020, Milano, Italy (moved online). Oral presentation.
- Liu Z, Kim D, Gundersen T, Multi-component Fluid Cycles in Liquid Air Energy Storage, 23rd Conference on Process Integration for Energy Saving and Pollution Reduction (PRES 2020), 17-21 August 2020, Xi'an, China (moved online). Oral presentation. (Won 2nd place Best Young Speaker Award)

Chapter 2 Electrical energy storage overview

Energy storage (ES) technologies are developed on the basis of collecting and storing available energy, and then providing it in different forms (thermal energy or power) when energy is demanded. ES technologies can be classified as thermal energy storage (TES) and electrical energy storage (EES) according to the form of energy recovered [5]. Although thermal energy storage technologies have been widely applied, this thesis focuses on electrical energy storage, mainly liquid air energy storage (LAES).

2.1 Electrical energy storage

Electricity is regarded as one of the most convenient forms of energy. However, electricity cannot be easily stored in large quantities. Typically, electricity is transformed into a form of energy that is stable and low-cost (e.g., mechanical energy, electrochemical energy, chemical energy, electrical energy, and thermal energy), and the stored energy is then converted back to electricity when demanded [8]. Based on the forms of stored energy, EES can be further classified as follows:

- Mechanical energy storage (Flywheels, Pumped hydroelectric energy storage, Compressed air energy storage, Gravity)
- Electrochemical energy storage (Supercapacitors, Batteries)
- Superconducting magnetic energy storage
- Chemical energy storage (Fuel cells)
- Thermal energy storage (Liquid air energy storage)

Table 2.1 lists technical characteristics of some selected electrical energy storage technologies. It can be observed that the most mature technologies that are suitable for large-scale electricity storage are pumped hydroelectric energy storage (PHES) [6] and compressed air energy storage (CAES) [7]. There is a trend towards developing high capacity batteries, but it is not comparable to PHES and CAES in terms of cost [5]. According to the 2020 report from the U.S. Department of Energy, PHES makes up 96% of the global electricity storage capacity, while CAES with 0.44% represents a relatively small share of world storage capacity [10]. IRENA has predicted that the storage capacity of PHES will double from 152 GW in 2020 to 325 GW in 2050 [11].

However, the drawbacks of PHES and CAES should also be considered when investing in such energy storage projects. Since energy densities for PHES and CAES are relatively low, a large storage space is required for these two technologies. Two reservoirs at different levels and considerable sizes are needed for PHES, and suitable sites for PHES are at locations with adequate fresh water supply. Above ground tanks and underground caverns are used to store compressed air in CAES systems, and caverns are commonly adopted for economic reasons. This means that CAES tends to be located in remote areas far away from other energy conversion processes. The geographical constraints for PHES and CAES increase the operating complexity and require extra cost for energy transmission.

Table 2.1 Technical characteristics of some selected electrical energy storage systems [9].

Technologies	Energy Density (Wh/kg)	Energy Density (kWh/m^3)	Discharge time	Rated Power (MW)	Round-trip Efficiency (%)
Pumped hydro	0.5-1.5	0.5-1.5	1-24h+	100-1000	65-87
Compressed air	30-60	2-6	1-24h+	5-300	41-75
Liquid air	97	98.6	1-24h+	0.35-50	50-70
Na-S	150-240	150-250	Seconds-hours	0.05-8	70-90
Li-ion	75-200	200-500	Minutes-hours	0-0.1	65-90
Lead acid	30-50	25-90	Seconds-hours	0-40	75-90
Thermal	80-250	80-500	Minutes-months	50-250	30-60

2.2 Liquid air energy storage (LAES)

LAES has attracted more focus in recent years due to its characteristics of being geographically unconstrained, having high energy density, and low maintenance and operational costs [12]. In addition, the LAES can be integrated with other energy conversion processes, and it can be located near these processes to avoid additional pipelines and corresponding costs. Thus, the LAES is a promising alternative for large-scale energy storage with hourly to daily output duration.

2.2.1 Concept

A block flow diagram of an LAES system is illustrated in Figure 2.1. Air from the environment is first sent to pre-purification units (PPUs) for the removal of CO_2, H_2O and other trace components to avoid solid formation in the low-temperature process. The pre-treated air is then sent to the LAES system. Although the gas pre-treating steps are important for the operation of LAES systems, they are not included in our simulation and optimization studies, since the main focus is the LAES configuration schemes. The LAES system consists of three parts: charging, storage, and discharging. In the charging part, the air feed is pressurized in a multi-stage compressor with aftercooling before it is fully liquefied in the cold box. The charging process is essentially a liquefaction process, where air is liquefied by using surplus electricity. In other words, energy (or power) is stored in the form of liquid air. In the storage part, liquid air is kept in atmospheric cryogenic tanks. In the discharging part, liquid air is pumped and regasified by other heat sources. Then, the high pressure air enters a multi-stage expander to generate power. The main sub-systems in the LAES will be discussed in detail in the following sections.

2.2.1.1 Air liquefaction process (charging process)

One of the advantages for the LAES is that the working fluid (air) is stored in liquid phase, so the size of storage tanks is smaller compared to PHES and CAES. The air liquefaction process is crucial for the performance of the LAES system, as its energy consumption is mainly due tto

compression work in the charging process. In addition, the temperature difference between hot (air) and cold (working fluids in the cold energy recovery cycles) composite curves in the low-temperature heat exchangers also affects the process efficiency. Commonly used liquefaction processes for air are Linde-Hampson [13], Claude [14], and Kapitza cycles [15]. Mixed refrigerants and cascade systems are commonly used in natural gas liquefaction processes, which of course also represent possible technologies to liquefy air [16-18]. A detailed introduction to the mentioned liquefaction methods will be provided in the following.

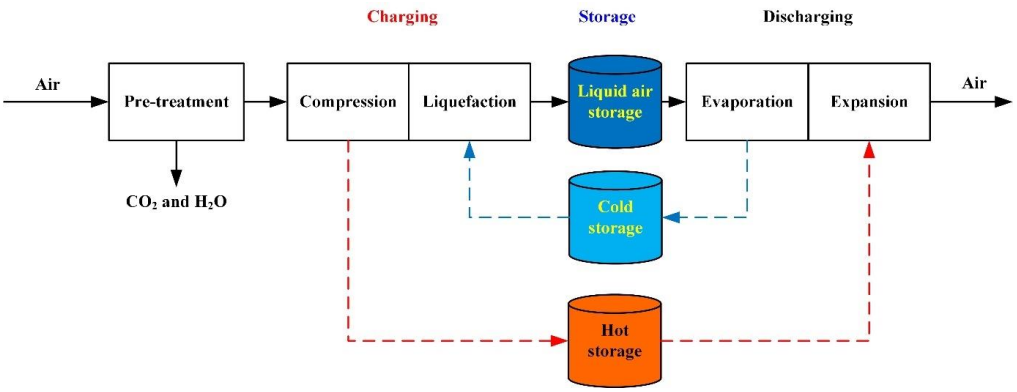

Figure 2.1 Block flow diagram of an LAES plant.

Recuperative systems

Linde–Hampson, Claude, and Kapitza cycles have a similar basic configuration, including a compressor, a heat exchanger, a Joule-Thompson (J-T) valve and a phase separator. These cycles are categorized as recuperative systems.

Linde-Hampson cycle. The simplest cycle for air liquefaction was proposed and patended by William Hampson and Carl von Linde in 1895. The process flow diagram of the Linde-Hampson cycle is shown in Figure 2.2. The purified air is pressurized in a multi-stage

compressor with aftercoolers before it is sent to the cold box, where the compressed air is further cooled by vapor from the separator. Then air enters a Joule-Thompson (J-T) valve to be expanded. A mixture of gas and liquid obtained at the outlet of the J-T valve, is subsequently separated. The liquid air is stored in cryogenic tanks.

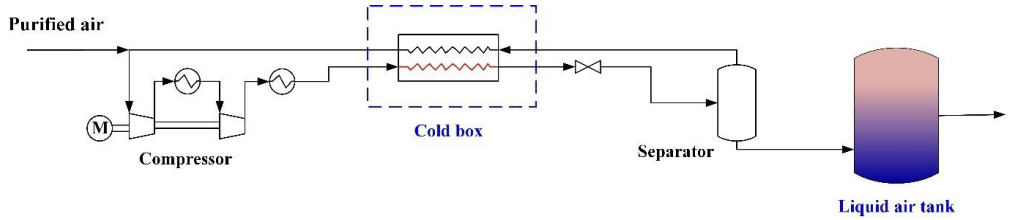

Figure 2.2 Process flow diagram of the Linda-Hampson cycle.

Claude cycle. The Claude cycle is based on the Linde-Hampson cycle and is illustrated in Figure 2.3. The difference between the two cycles is the heat exchanger part. Unlike the Linde-Hampson cycle, air is split into two branches after the first heat exchanger. One of the branches is cooled in the following heat exchangers and then throttled in the valve to be liquefied. The other branch is sent to an expander to produce refrigeration and power. The expanded branch is mixed with the recirculating vapor from the separator to provide cold duty to heat exchangers in the cold box.

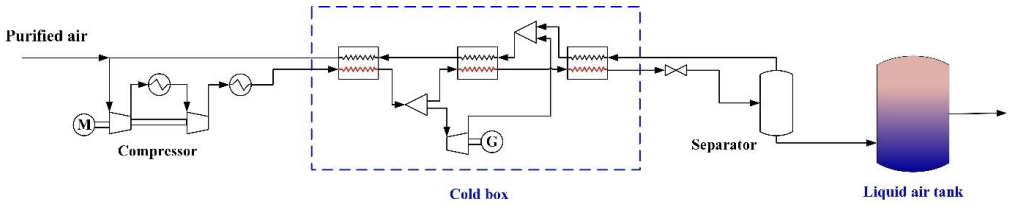

Figure 2.3 Process flow diagram of the Claude cycle.

Kapitza cycle. The Kapitza cycle is also a variant of the Linde-Hampson and Claude cycles. Compared to the Claude cycle, the third heat exchanger in the cold box is removed, as shown in Figure 2.4. Vapor from the separator is mixed directly with the expanded branch.

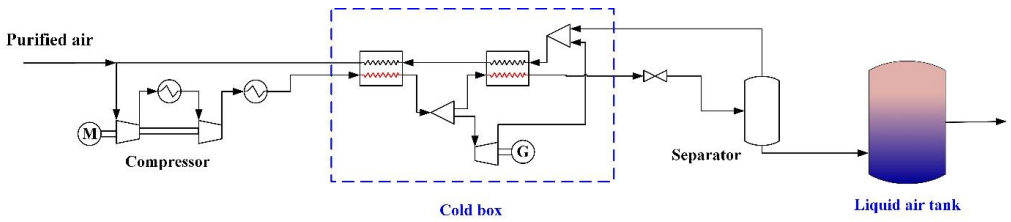

Figure 2.4 Process flow diagram of the Kapitza cycle.

Cascade and mixed refrigerant systems

The cascade system has more than one refrigeration cycle for the liquefaction of the gaseous stream. Figure 2.5 shows one example of the cascade system for liquefaction of natural gas. The advantage of using multiple refrigeration cycles is that the temperature difference in cryogenic heat exchangers can be reduced by selecting the most suitable working fluids for the cycles. With the cascade system, mixed refrigerants (multi-component working fluids) can also be considered for each cycle to improve the system performance. Multi-component fluids, unlike pure components, can customize the composition and thereby make the operating temperature range wider while considering the freezing and boiling points of the components. A good match between the temperature profiles of hot and cold streams can be obtained while keeping the configuration simple when using multi-component fluids. Common combinations of working fluids for natural gas liquefaction processes are listed in Table 2.2.

2.2.1.2 Discharging process

The discharging process is associated with the process that converts the energy stored in liquid air to electricity. This process is also referred to the power recovery cycle. The evaluation of the discharging process is not only dependent on the amount of power generation, but also the exergy efficiency in the LAES. In this section, four power recovery configurations have been considered in order to achieve a higher exergy efficiency: direct expansion cycle, Rankine cycle, Brayton cycle and Combined cycle.

Table 2.2 Some cascade and mixed refrigerant systems for natural gas liquefaction processes.

Cycles	Refrigerants	
	Pure	Mixed
2	CO_2-N_2 [19]	2 hydrocarbon mixtures [21-25]
	CH_4-N_2 [20]	C_3H_8-hydrocarbon mixture [26]
3	C_3H_8-C_2H_6-CH_4 [18]	3 hydrocarbon mixtures [27]
		2 hydrocarbon mixtures-N_2 [28]
		(N_2+CH_4+C_2H_6)-(N_2+CH_4+C_2H_6)-N_2 [29]

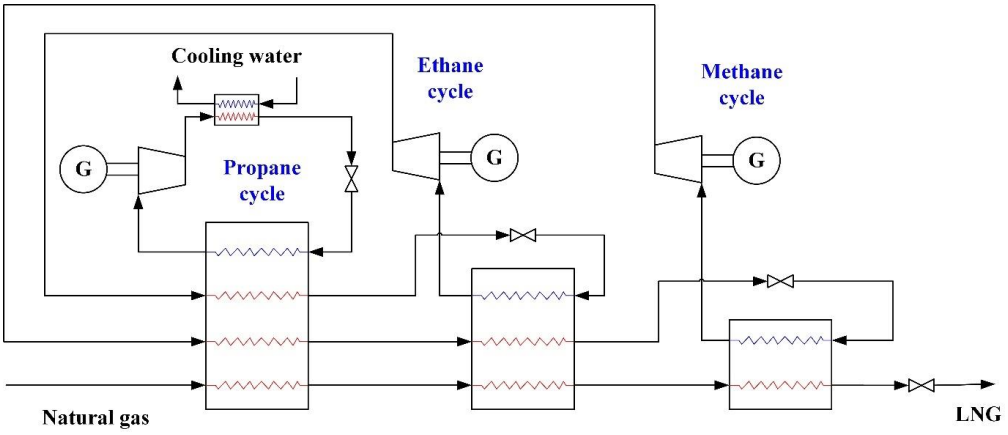

Figure 2.5 Process flow diagram of cascade refrigeration cycles for natural gas liquefaction.

Direct expansion cycle

One example of a direct expansion cycle is the regasification of nitorgen. The working fluid (e.g. LNG) of the cycle is pressurized, regasified, and superheated by other heat sources before it is sent to a turbine train to be expanded. The other heat sources can be ambient heat, combustion heat, and industrial waste heat. A concept of converting the cold energy from cryogen to power has been proposed by Knowlen et al. [30-32]. A schematic of the direct expansion cycle is shown in Figure 2.6.

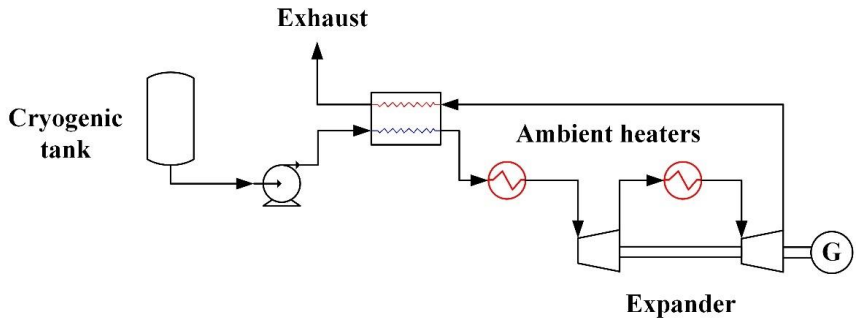

Figure 2.6 Schematic of the direct expansion cycle for power generation.

Rankine cycle

The Rankine cycle is another possible approach to convert the cryogenic energy to electricity. This method is often adopted to recover the cold energy in LNG regasification processes [33-38]. Figure 2.7 shows an example layout of the Organic Ranking Cycle (ORC) for power generation in LNG regasification processes. Organic working fluids are usually used as the working medium for the cycle, driven by the temperature difference between the heat source (ambient temperature) and the heat sink (LNG) to produce power. In addition to the single

Rankine cycle, cascade cycles have also been suggested to improve the performance of the process.

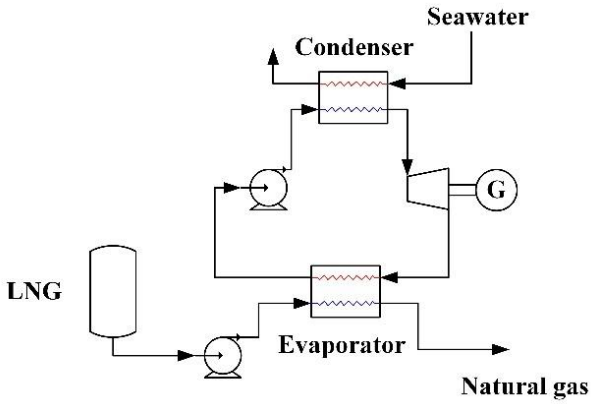

Figure 2.7 Configuration of an ORC for power generation in LNG regasification processes.

Brayton cycle

The working fluid in the Brayton cycle is in gas phase, thus, a gas compressor replaces the pump used to pressurize the fluid [39-42], as illustrated in Figure 2.8. Cold energy from the cryogenic fluid is provided to cool down the inlet stream to the compressor. It is also worth noting that only sensible heat of the working fluid is involved, which contributes to the reduction in exergy losses in the heat exchanger.

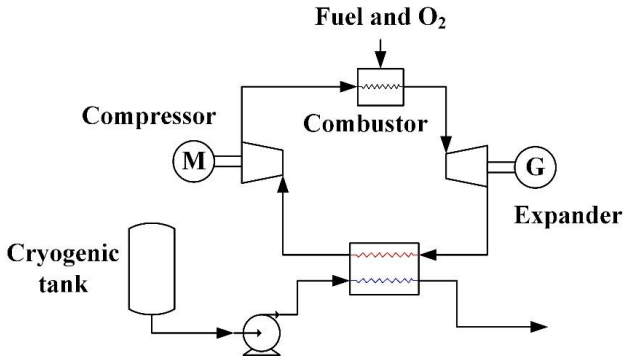

Figure 2.8 Schematic of the Brayton Cycle for power generation.

Combined cycle

A combination of the aforementioned cycles has also been applied in LNG regasification processes [43-47]. This is which is a more efficient method to collect the cold energy from the cryogen. A typical combined cycle for the LNG regasification process is provided in Figure 2.9.

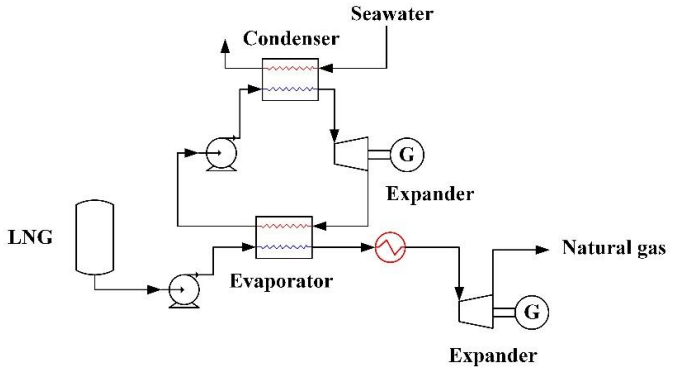

Figure 2.9 Schematic of combined cycle for power generation.

2.2.1.3 Thermal energy storage

In the LAES, both the compression heat and the cold energy from liquid air regasification can be recovered to improve the performance of the overall system.

Figure 2.1 presented a typical approach to collect the available energy in the system by using hot and cold thermal energy storage cycles. The suggested configurations and working fluids for the hot and cold thermal energy storage cycles in existing literature are listed in Table 2.3.

Table 2.3 Configurations and working fluids for the hot and cold thermal energy storage cycles.

	Working fluids	Configurations	Reference
Heat storage	Diathermic oil	One storage cycle with two tanks	[48]
	Water	One storage cycle with two tanks	[49-51]
	Solar salts	One storage cycle with two tanks	[52]
Cold storage	Methanol-propane	Two storage cycles with four tanks	[48]
	Methanol-R218	Two storage cycles with four tanks	[50]
	R123-Propane	Two storage cycles with four tanks	[53]
	Quartzite	Packed bed regenerator	[54]

2.2.2 Improvements in the performance of LAES systems

The advantages of LAES are related to the properties of not being geographically constrained and having high energy density, which make the LAES stand out among many energy storage technologies [55, 56]. However, the drawback for the LAES is that the round-trip efficiency (RTE) is lower compared to PHES, CAES and batteries. A considerable amount of research related to liquid air energy storage has been conducted to analyze the thermodynamic performance and improve the technical feasibility of this technology.

2.2.2.1 Stand-alone LAES system

A stand-alone system is defined as being independent of external hot or cold thermal energy sources and additional thermodynamic cycles. Guizzi et al. [48] studied a stand-alone LAES system that utilizes storage of compression heat and cold duty from regasification. An RTE of 54.4% was obtained with effective hot and cold thermal energy recirculation between the charging and discharging processes. Morgan et al. [57] tried to improve the efficiency of the LAES system by adding a Claude cycle to the low-temperature heat exchanger. The air was further cooled down before entering the separator. As a result, the RTE was improved to 57%. Borri et al. [58] simulated and compared three microgrid scale LAES systems with different liquefaction cycles, i.e. the Linde, Claude and Kapitza cycles. The optimal configuration of the liquefaction part was found to be the Kapitza cycle with two-stage compression where the specific energy consumption can be reduced by up to 25% by optimizing the operating conditions (recirculation ratio and flash pressure). Chen et al. [59] considered phase change materials (PCMs) for the cold thermal energy storage between the charging and discharging processes in the LAES system. It was found that the optimal design of the cold storage process consists of 12 stages with 12 different PCMs, which means that one type of PCM is used at each stage that is operated at a certain temperature. The RTE of the LAES system with the optimal cold storage process is 54.2%.

For a standalone system, the RTE of the LAES is increased considerably with the use of hot and cold thermal energy storages. However, the methanol and propane cycles are typically used as cold energy recovery cycles, which contribute to considerable exergy losses in the LAES related to irreversibilities caused by large temperature differences in the heat exchangers. Thus, this thesis will propose new configurations and working fluids for the cold thermal energy recovery cycles in the LAES to improve the system performance.

Modification of the configuration of the LAES has frequently been a subject of research in the past. A large number of variants for the LAES can be obtained by varying the number of compression and expansion stages. However, the expansion section is strongly influenced by the compression section since there is a hot thermal energy storage between these two sections

in the LAES. This important issue has been ignored by most of the papers. Therefore, this thesis will explore the potential of system efficiency improvements for different configurations of the LAES system (different number of compression and expansion stages).

2.2.2.2 LAES with additional thermodynamic cycles

In addition to studies on the configuration of a stand-alone LAES system, there are some publications focusing on the utilization of waste heat in the LAES system with additional thermodynamic cycles. Peng et al. [60] analyzed the LAES system with a 4-stage compressor and a 4-stage expander. It is reported that 20-45% of compression heat is wasted in the discharging process under different operating conditions of the LAES system. One method to handle the unused compression heat is to use an ORC to convert this heat to power. An alternative method is to let 31% of the unused compression heat be used to drive an ORC and the remaining unused heat is supplied to an Absorption Refrigeration Cycle (ARC) to generate a cold stream below ambient temperature. The cold stream is used as the heat sink for the ORC. It is observed that the performance of the LAES system with an ORC (62.7%) is better than the combined system with an ORC and an ARC (61.3%). She et al. [61] utilized the unused compression heat in the LAES system to drive an ORC. The heat sink for the ORC is provided by the refrigeration capacity generated by a Vapor Compression Refrigeration Cycle (VCRC). It is observed that the RTE of the LAES system with ORC-VCRC can be improved to 55.5% compared to the baseline LAES system (50.3%). Zhang et al. [62] tried to use cascade storage of compression heat to reduce temperature differences in compression heat exchangers and thereby increase the temperature of compression heat. In the LAES system with a 2-stage compressor and a 2-stage expander, there is a part of compression heat that is not efficiently utilized in the discharging part. The surplus compression heat is supplied as a heat source to an ORC and a Kalina Cycle (KC) to produce extra power. The results suggest that the LAES system with an ORC has a higher RTE of 56.9% compared to the system with a KC (RTE of 56.1%). Tafone et al. [63] tested and compared different methods to utilize the surplus compression heat in the LAES system. The excess compression heat is used to drive an ORC and a water-LiBr Absorption Chiller (AC). It is indicated that the RTE of the LAES with an

ORC can be increased to 52.9%, while the performance of an LAES with an AC is not improved due to the poor performance of the AC. Cui et al. [64] proposed a novel multi-functional LAES system, where electricity, heat, and cold energy are generated. The electricity is generated by the conventional discharging process in the LAES system. After delivering heat to expanders in the discharging part, the waste low-temperature heat of thermal oil (58°C) is used for heating. The cold energy is provided by an absorption refrigerator that utilizes the heat from the unused part of high-temperature thermal oil. The cycle efficiency of the system is 75.4% when taking all outputs into account. Xue et al. [65] also studied the multi-functionality of an LAES system. The electricity is produced by both the direct expansion process and an ORC. The heat of thermal oil at the outlet of the expansion heat exchangers is recovered to provide heat to an absorption refrigeration cycle to generate cold energy, and the remaining heat of thermal oil is used for heating. A round-trip efficiency of 69.6% for the LAES system is obtained. Nabat et al. [66] investigated an integrated system, which consists of an LAES system, a heat storage tank embedded with a thermoelectric generator, and an organic Rankine cycle. With the thermoelectric generator, the air is heated up to 1027°C before it is sent to expanders to generate power. The results show that the RTE of the LAES system reaches 61.1%. Based on the reviewed papers [60-66], ORCs and ARCs are widely studied to utilize the unused part of compression heat to produce power, and thereby improving the performance of the system. Thus, this thesis will study three technologies (ORC, ARC and HTHP) for the utilization of compression heat in different LAES configurations to increase the RTE of the LAES system.

2.2.2.3 Integrated LAES systems

The aforementioned studies focus on the improvement of the LAES system without external thermal energy sources. In addition, the integration of the LAES system with other processes to enhance the performance of the LAES has also been considered. Li et al. [67] studied the integration of an LAES with a nuclear power plant (NPP) to utilize the excess reaction heat. This further increased the inlet air temperature to expanders, and an RTE of 71.3% could be reached. Cetin et al. [68] tried to use a geothermal power plant to drive an LAES system. The

power generated from the geothermal plant supports air liquefaction in the LAES, and the waste geothermal heat was used to increase the inlet air temperature to expanders in the discharging process. The RTE of the LAES was 46.7%, and the thermal efficiency of the combined system, where the geothermal heat is supplied at 180°C, was increased from 6.6 to 24.4%. The thermal efficiency of the overall system is relatively low since a large amount of geothermal heat is the input, while the power generated is the output. Lee et al. [69] integrated the LAES with a terminal for liquefied natural gas (LNG). Cold energy from LNG regasification is collected and used to liquefy air in the LAES, and power is generated from the expansion of both natural gas and air. The performance of the charging and discharging parts has been improved, and the corresponding exergy efficiencies are 94.2% and 61.1%. Lee and You [70] performed a similar study, where air was liquified by utilizing the cold thermal energy from LNG regasification. In this case, direct expansion was used for the power generation from LNG and liquid air, and an Organic Rankine Cycle (ORC) with a multi-component working fluid was applied to produce additional power in LNG regasification before the NG expansion part. The exergy efficiency of the combined process was 70.3%. Qi et al. [71] further improved the combined system with the LAES and an LNG regasification process. During discharging, both the LAES discharging process and the LNG regasification process are used to produce power. During charging, the LNG is first used to cool the charging process in LAES, and then it is fed to an ORC to utilize the remaining cold energy. The RTE of the combined system reaches 129.2%, since the cold energy from LNG is regarded as "free" and would otherwise be lost. Antonelli et al. [72] analyzed and compared different configurations of the discharging process in the LAES: direct expansion, direct expansion combined with additional combustion heat, and direct expansion combined with both additional combustion heat and an ORC or a Brayton Cycle. Results demonstrated that the LAES with additional combustion heat and a Brayton Cycle (the last case) has the highest RTE of 90%. It is observed from the above mentioned references that the performance can be significantly improved by integrating the LAES system with external hot or cold thermal energy sources.

A possible integration system between the LAES and an LNG regasification process and external waste heat sources has been presented at the AIChE Annual Meeting (2021) [73].

When surplus power is available, the LAES charging process is started. LNG is first pumped to a high pressure, and then sent to the LAES system, where its cold energy is utilized in two distinct places. LNG cold regasification energy is first utilized in the cold box and thereafter used to precool air in the compression part. During these steps, LNG is heated and becomes gaseous high-pressure NG. The high-pressure NG is next sent to the direct expansion part to generate power. The air is compressed and cooled by the cold regasification energy from both LNG and liquid air. When power is demanded, the power production of the integrated system comes from both the liquid air and LNG. The liquid air is pumped, regasified and depressurized through expanders to produce power. To further improve the system, the regasified air can be heated by an Organic Rankine Cycle (ORC), where the temperature difference between the ambient air and regasified air is used to generate power, before the heated air is being sent to the expansion part. In discharging mode (without the need for external cold energy), pumped LNG is regasified by an ORC and then sent to the direct expansion part to produce power. The RTE of the LAES-LNG process reaches 106.2%. With an available external waste heat source at 300°C supplied to the integrated LAES-LNG, the RTE can be finally improved to 188.9%. The round-trip efficiency has been greatly improved since extra power is generated from the "free LNG cold energy". Of course, having an RTE above 100% must be seen as an effect of utilizing an external cold resource that otherwise would be wasted to the environment. A more objective measure of the performance of the integrated system is to use exergy analysis, which is based on physical (or thermomechanical) exergies of the inlet and outlet streams as well as power consumption/production in the integrated system.

2.2.3 Economic analysis of LAES

Most of the research on the LAES focuses on the improvement of energy aspects for the LAES. However, an economic analysis of the LAES should also be conducted to comprehensively evaluate the technology. There are a few publications investigating the economic feasibility of the system. Wang et al. [74] proposed a novel system consisting of an air separation unit and a liquid nitrogen energy storage process. The profitability of the system comes not only from the electricity price arbitrage, but also from the sale of pure oxygen and heat. The multi-functional

LAES system with a storage capacity of 10 MW / 80 MWh has a relatively short payback period of 5.7 years. Cui et al. [75] compared the economic feasibility of a conventional LAES and a multi-generation LAES (1.5 MW / 12 MWh). The results show that the multi-generation LAES has a better economic performance than the conventional system. The net present value is increased from 1.5 M$ to 2.3 M$ and the payback period is reduced from 6.3 years to 4.1 years. Park et al. [76] performed a techno-economic study of a 300 MW / 2.4 GWh integrated system between a nuclear power plant and an LAES. The results indicate that the levelized cost of electricity of the integrated system (182.6 $/MWh) is less than for a standalone LAES (219.8 $/MWh), which means that the integrated system has a better economy than the standalone process. Xie et al. [77] tested the economic feasibility of an LAES system, which is used to provide ancillary services to the grid and make profits through electricity price arbitrage. It is found that the payback period is reduced from 25.7 years to 5.6 years for a 200 MW LAES system as the external heat from the power plant increases from 0 °C to 250 °C. Lin et al. [78] evaluated the economic viability of the LAES in the UK real-time electricity market. It is suggested that a high NPV of 43.8 M£ can be achieved for a 200 MW LAES system. With a waste heat source at 150 °C, the payback period for the LAES system can be reduced from 39.4 years to 9.8 years. Tafone et al. [79] conducted an economic comparison between a standalone LAES and the LAES with an additional Organic Rankine Cycle (ORC) to utilize the unused compression heat. The results show that the integrated LAES-ORC system (100 MW / 400 MWh) has a slightly lower levelized cost of storage of 0.44 €/kWh compared to the standalone process at 0.48 €/kWh, which justifies the economic viability of the additional ORC in the LAES.

Hamdy et al. [80] proposed seven integrated systems between the LAES and an LNG regasification process, the combustion of natural gas, and external waste heat. The results indicate that the specific cost is decreased from 1400 €/kW to 1100 €/kW when a 300 MW / 1.2 GWh LAES is integrated with external waste heat at 450 °C. The lowest levelized cost of electricity of 171 €/MWh is obtained when the LAES is integrated with the combustion of natural gas. Georgiou et al. [81] compared the economics of pumped thermal energy storage

(PTES) and LAES systems. The commercial scales for the two energy storage technologies are at different levels, which is why the system sizes for the PTES and LAES are not the same in their study, i.e. 2 MW / 11.5 MWh and 12MW / 50MWh, respectively. It is pointed out that LAES has a lower capital cost and lower levelized cost of storage than the PTES. Kim et al. [82] analyzed the economic feasibility of an integrated system, which is composed of renewable power sources, an LAES, and natural gas combustion. The integrated system purchases renewable electricity during off-peak periods, while electricity generated from both liquid air and LNG regasification and expansion is sold at on-peak times. It is found that the levelized cost of energy for the novel integrated system with a storage capacity of 33 MW / 264 MWh is 163.5 $/MWh, which is lower than that of 209.5 $/MWh for the CAES with a storage capacity of 50 MW / 400 MWh.

The economic analysis of the LAES can reveal the feasibility of this energy storage technology. Thus, this thesis also investigates economics of different LAES configurations to identify the most economic layout for a standalone LAES system.

Chapter 3 Analysis methods for the LAES

Abstract

This chapter explains the methodology of the thesis. The main key performance indicators to evaluate the energetic, exergetic, and economic performance of different LAES configurations are presented, followed by an introduction to the simulation tools and settings to support the assessment of the proposed systems. Finally, the optimization procedure used to obtain optimal operating conditions and comparing different candidate processes is reported.

3.1 Energy, exergy and economic analysis

Energy conversion processes consist of energy inputs and energy outputs. Energy is required to transform the inputs to output products in a step-by-step process. Evaluating the transformation steps and energy inputs provides information about how to save energy. Several Key Performance Indicators (KPIs) that are based on thermodynamic and economic performance can be used for a comprehensive evaluation of the LAES system. In this thesis, the evaluation of thermodynamic performance for the LAES is conducted by using liquid yield, round-trip efficiency, specific power consumption and exergy efficiency. The economic performance of the process is evaluated by net present value (NPV), payback period and levelized cost of storage (LCOS).

Liquid yield, which is an important parameter for processes involving air liquefaction, is related to the liquid air fed to the discharging process and the part of air recycled to the charging process. A higher liquid yield leads to less compression work, since the recirculation ratio is reduced, and less air is re-compressed. The liquid yield of air is calculated by Equation (3.1(3.1).

$$\eta_{\mathrm{LY}} = \frac{\dot{m}_{\mathrm{liq}}}{\dot{m}_{\mathrm{comp}}} \tag{3.1}$$

Here, $\dot{m}_{\mathrm{liq}}$ and $\dot{m}_{\mathrm{comp}}$ represent the mass flow rates of liquid air and air entering the compressors, respectively.

Round-trip efficiency is a commonly used parameter in energy storage systems, including EES, to evaluate different technologies. It quantifies the amount of power that is recovered relative to the amount of power used to store the energy for different energy storage technologies. The round-trip efficiency is defined as the work produced ($\dot{W}_{\mathrm{out}}$) in the discharging process divided by the work consumed ($\dot{W}_{\mathrm{in}}$) in the charging process, see Equation (3.2).

$$\eta_{\mathrm{RT}} = \frac{\dot{W}_{\mathrm{out}}}{\dot{W}_{\mathrm{in}}} = \frac{\dot{m}_{\mathrm{liq}} w_{\mathrm{tur}}}{\dot{m}_{\mathrm{comp}} w_{\mathrm{comp}}} = \eta_{\mathrm{LY}} \cdot \frac{w_{\mathrm{tur}}}{w_{\mathrm{comp}}} \tag{3.2}$$

Here, w_{comp} and w_{tur} denote the specific work of compressors in the charging process and turbines in the discharging process, respectively.

Specific power consumption (*SPC*) is widely used to assess liquefaction systems [83-92], thus, this parameter can indicate the efficiency of the charging process in the LAES. The definition of *SPC* is given by Equation (3.3) as the net work consumed per mass of liquid air produced.

$$SPC = \frac{\dot{W}_{\mathrm{net}}}{\dot{m}_{\mathrm{liq}}} \tag{3.3}$$

The net work ($\dot{W}_{\mathrm{net}}$) required is calculated by Equation (3.4).

$$\dot{W}_{\mathrm{net}} = \sum \dot{W}_{\mathrm{comp}} - \sum \dot{W}_{\mathrm{tur}} \tag{3.4}$$

Here, $\dot{W}_{\mathrm{comp}}$ and $\dot{W}_{\mathrm{tur}}$ are the work of the compressors and turbines respectively. The above-mentioned performance parameters evaluate the system in terms of energy efficiency.

However, changes in temperatures, pressures, and compositions of process streams also have significant effects on the performance of the system. This information cannot be revealed by energy performance parameters. Exergy analysis is a comprehensive method to include both the 1st and 2nd laws of thermodynamics [93-103]. All variations in process streams, work and thermal energy in the system are considered in the concept of exergy, which represents the maximum available work obtained by varying the stream temperature, pressure and composition to equilibrium with its environmental conditions. Without considering kinetic, potential, electrical, and nuclear exergies, the exergy of material streams includes physical (or thermo-mechanical) exergy ($\dot{E}^{\mathrm{TM}}$) and chemical exergy ($\dot{E}^{\mathrm{Ch}}$) [104], see Equation (3.5).

$$\dot{E} = \dot{E}^{\mathrm{TM}} + \dot{E}^{\mathrm{Ch}} \tag{3.5}$$

Physical exergy is the maximum work obtained when the stream temperature and pressure is changed from its original state to environment conditions by ideal (reversible) processes, as is given by Equation (3.6).

$$\dot{E}^{\mathrm{TM}} = \dot{H}(T,p) - \dot{H}(T_0,p_0) - T_0[\dot{S}(T,p) - \dot{S}(T_0,p_0)] \tag{3.6}$$

Chemical exergy is the maximum work obtained when the stream is taken to a state that has the same composition as its natural surroundings, again by ideal (reversible) processes. Since no chemical reactions are present in the LAES system, chemical exergy has relatively small effects related to separation and mixing. As a consequence, only the physical exergy of streams is considered in this work.

In this thesis, Exergy Transfer Effectiveness (*ETE*) is applied to measure the exergy efficiency of the LAES system. The *ETE* is defined as the exergy sinks (produced exergy) divided by the exergy sources (consumed exergy) in a process. The *ETE* considering only thermo-mechanical exergy was proposed by Marmolejo-Correa and Gundersen [105] and has been further developed by Kim and Gundersen [106] to include chemical exergy. The ETE with chemical exergy was successfully used as an objective function by Kim and Gundersen [107] to optimize LNG processes with NGL extraction. In those processes, similar to the LAES, there are no chemical reactions, but mixing and separation are more important, thus chemical exergy was also included.

The exergy efficiency can be expressed by using the definition of ETE as shown in Equation (3.7).

$$\eta_{\dot{E}} = ETE = \frac{\sum \text{Exergy Sinks}}{\sum \text{Exergy Sources}} \tag{3.7}$$

The physical exergy of streams, which can be calculated by Equation (3.6), is obtained by applying Visual Basic codes in Aspen HYSYS simulations as proposed in the work of Abdollahi-Demneh et al. [108].

In Chapters 4-6, where configuration modifications for performance improvement are the main topic, only energy and exergy performance indicators are used for the thermodynamic evaluation of the LAES system. The round-trip efficiency (RTE) is selected as the objective function when performing the optimization of different LAES configurations. For energy storage technologies, the charging process and the discharging process typically do not operate at the same time. Thus, the exergy efficiencies of these processes are considered separately, and detailed definitions of exergy efficiency for the two subprocesses in the LAES are addressed from Chapter 4 to Chapter 6.

An economic evaluation is important for the marketing of a complex system [109-114]. It is essential to perform an economic assessment of the process, which is the topic in Chapter 7. However, it is difficult to get accurate cost data for equipment and maintenance costs as some information is not easily available. The economics of the LAES is calculated with net present value (NPV), payback period and levelized cost of storage (LCOS).

The net present value (NPV) is a widely used parameter to evaluate the profitability of a project, and it represents the difference between the present worth of net annual income and the present worth of initial cost, as is shown in Equation (3.8). A positive NPV means that the project is economically feasible, while a negative NPV means that the project is not recommended.

$$NPV = -C_{\mathrm{TCI}} + (C_{\mathrm{AI}} - C_{\mathrm{AOC}} + C_{\mathrm{D}}) \cdot \frac{(1+i)^t - 1}{i \cdot (1+i)^t} \tag{3.8}$$

Here, C_{TCI}, C_{AI}, C_{AOC}, and C_{D} represent the total capital investment cost, the annual income, the annual operating cost and the depreciation of capital investment for the LAES plant, respectively; i is the annual interest rate (%) and t is the service life of the LAES system (year).

Payback period is another parameter selected to estimate the time required to completely recover the capital investment of a project, see Equation (3.9).

$$Payback\ period = \frac{\text{Total investment cost}}{\text{Annualized cash flow}} = \frac{C_{\mathrm{TCI}}}{(C_{\mathrm{AI}} - C_{\mathrm{AOC}} + C_{\mathrm{D}}) \cdot \dfrac{(1+i)^t - 1}{i \cdot (1+i)^t}} \tag{3.9}$$

Levelized cost of storage (*LCOS*) is also a commonly used factor for evaluation of the cost of various power generation technologies and the cost of the different energy storage technologies. *LCOS* of the LAES can be calculated as the ratio between the sum of cost in the entire lifetime and the total produced electricity over the lifetime, as provided in Equation (3.10).

$$LCOS = \frac{C_{\mathrm{TCI}} + C_{\mathrm{APC}} \cdot \dfrac{(1+i)^t - 1}{i \cdot (1+i)^t}}{\dot{W} \cdot h_{\mathrm{an}} \cdot \dfrac{(1+i)^t - 1}{i \cdot (1+i)^t}} \tag{3.10}$$

Here, $\dot{W}$ denotes the power production in the discharging process (kW); h_{an} represents the annual number of hours for power generation (h/year).

3.2 Simulation tools and settings

The LAES processes in Chapters 4-6 are simulated with Aspen HYSYS Version 10.0 [115]. The Peng-Robinson equation of state is adopted to calculate physical properties of the streams. It is assumed that the air feed consists of 78.82 mole% nitrogen, 21.14 mole% oxygen and 0.04 mole% argon. The mass flow rate of air feed is 2000 kg/h at 20°C and 1 bar, which is considered as feed to the LAES system in Chapter 4. In Chapters 5-6, the feed condition is adjusted to a larger scale plant with an approximate storage capacity of 10 MW power output. The mass flow rate of feed for the 10 MW LAES plant is 61520 kg/h, and air is supplied at 20°C and 1 bar.

In order to simplify the system analysis, several assumptions are made. Simulation assumptions are shown in Table 3.1. In addition, pressure drops and heat losses in heat exchangers, storage tanks and the flash tank are neglected in this work.

Table 3.1 Simulation conditions and assumptions.

Parameter	Value	Unit
Ambient temperature	20	°C
Ambient pressure	1	bar
Isentropic efficiency of compressors	85	%
Isentropic efficiency of expanders	90	%
Isentropic efficiency of cryo-turbines	75	%
Isentropic efficiency of pumps	80	%

3.3 Optimization algorithm

As introduced in Section 2.2, the LAES consists of the air liquefaction process (charging), the power recovery process (discharging), and the hot and cold thermal energy storage cycles. Due to the thermal energy storage cycles, the charging and discharging parts are closely connected. The power recovery ratio is crucial for an energy storage technology, and measures to increase the RTE of the system are strongly required. This can be solved by using optimization algorithms in combination with thermodynamic analysis to improve the process performance. In order to have an objective comparison between different alternatives for the LAES, it is also significant to have uniform evaluation and comparison metrics. Thus, rigorous optimization is required for developing novel LAES concepts.

The optimization of the LAES involves highly nonlinear and nonconvex equations, which is challenging for deterministic optimization algorithms due to the complex thermodynamic property calculations. Surrogate models or simplified models can be considered as alternatives for the replacement of rigorous thermodynamic models when performing the optimization. However, accurate thermodynamic models are prerequisite for reliable results. It is also quite important to decide the correct decision variables, which form a multi-dimensional space during optimization. Thus, it is computationally intensive to find global optimal solutions. The

built-in optimizer in HYSYS is too weak to get satisfactory results. To deal with such challenges, stochastic algorithms have been suggested to be used in energy intensive systems like liquefaction processes and LNG regasification processes [116-119]. The Particle Swarm Optimization (PSO) algorithm is applied to optimize the LAES system in this study. PSO is a population-based sampling optimization technique, and no global optimum can be guaranteed due to its stochastic nature. However, the advantage of using this algorithm is that no derivatives of mathematical equations are needed, thus it can be easily used in complex models such as for the LAES [120]. The framework for the optimization is shown in Figure 3.1. Moreover, the parameters for the PSO are listed in Table 3.2. The PSO algorithm is coded in Matlab (version R2018a [121]) and connected to Aspen HYSYS through the "actxserver" command.

Table 3.2 Parameters of the PSO algorithm.

Parameters	Value
Number of particles	150
Global acceleration factor	1
Personal acceleration factor	1
Minimum inertia weight	0.5
Maximum inertia weight	1

The implementation of the optimization is associated with the variables, objective function, and constraints. In Chapters 4-6 of this thesis, the optimization objective is to maximize the round-trip efficiency of the LAES, as shown in Equation (3.11).

$$\min_{x} \quad -\eta_{\mathrm{RT}} = -f(x) = -\frac{\dot{m}_{\mathrm{liq}} w_{\mathrm{tur}}}{\dot{m}_{\mathrm{comp}} w_{\mathrm{comp}}} \tag{3.11}$$

Since the decision variables and constraints are varying for different LAES concepts, a detailed selection of variables and constraints are provided in Chapters 4-6.

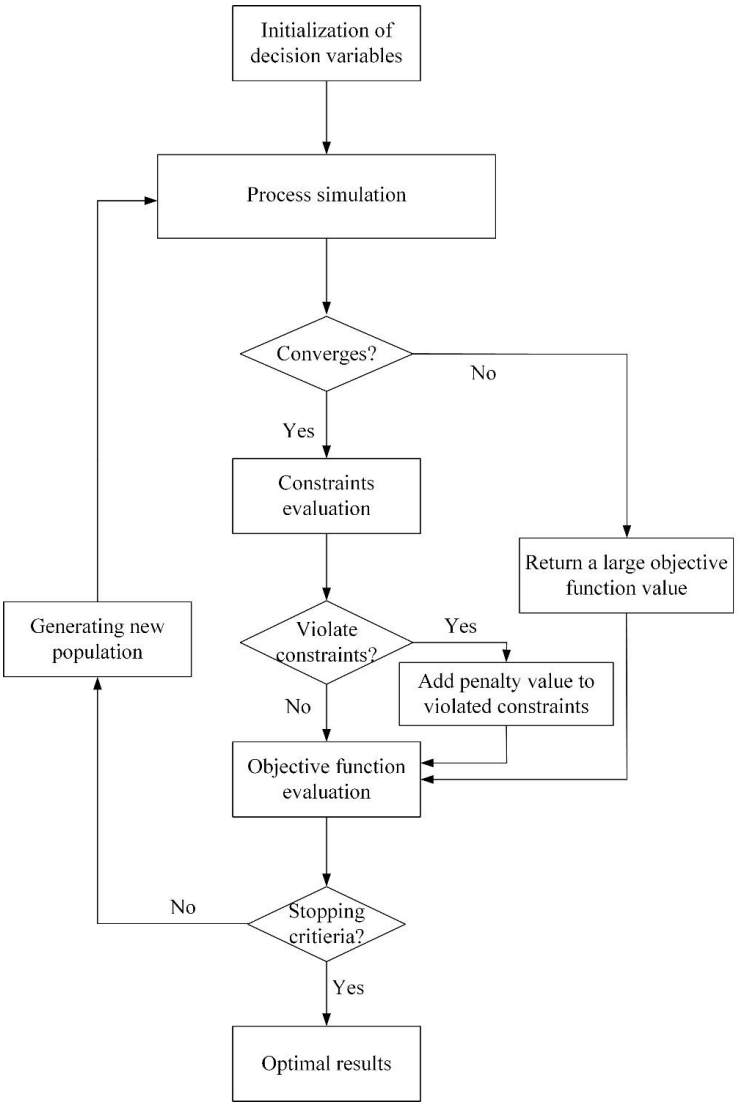

Figure 3.1 Simulation-based framework for the optimization procedure.

Chapter 4 Improvements for the Cold Thermal Energy Recovery in LAES

Abstract

In order to improve the performance of the LAES, in this chapter, seven cases related to different cold thermal energy recovery cycles are simulated, optimized and compared. Multi-component fluid cycles (MCFCs) and Organic Rankine Cycles (ORCs) are considered for the first time to be used as cold thermal energy recovery cycles in the LAES. The optimal results show that the LAES system with dual MCFC has the best performance with an RTE of 62.4%. This RTE can be further increased to 64.7% by reducing the minimum temperature difference of high-temperature heat exchangers from 10°C to 5°C. Optimization results also indicate that ORCs are not suitable as cold energy recovery cycles, since any power produced in the ORC cannot compensate for the reduced power production in the expansion section.

This chapter is based on the publications:

- Liu Z, Kim D, Gundersen T. Optimal recovery of thermal energy in liquid air energy storage. Energy. 2022;240:122810.
- Liu Z, Kim D, Gundersen T. Multi-component fluid cycles in liquid air energy storage. Chemical Engineering Transactions. 2020;81:55-60.

As introduced in Section 2.2, a stand-alone LAES system is composed of the charging part, discharging part, and hot and cold thermal energy storages. According to literature review [48, 57], the RTE of the LAES is increased considerably with the use of hot and cold energy storages. In the hot storage cycle, the common working fluid is thermal oil that is first used to collect compression heat from the charging process, and then used to release this heat to the expansion part of the discharging process. The temperature difference between the thermal oil (cold stream) and the compressed air (hot stream) is evenly distributed within the temperature range of the compression heat exchanger, since no phase change takes place. For cold energy recovery and storage systems that consist of two pure working fluid cycles (i.e. methanol and propane), the situation is different. The cold storage cycles are used to transfer the cold thermal energy from liquid air regasification in the discharging process to the air liquefaction part in the charging process. The operating pressure for air liquefaction is usually larger than the critical pressure of air (37.8 bar) to avoid phase change at constant temperature (a horizontal line in the composite curves for the heat exchanger), so that a smooth liquefaction curve is obtained with decreasing temperature. This makes it easier to find a working fluid to match with the liquefaction curve of air. The methanol and propane cycles in the system have acceptable performances (they both operate in liquid form, so only sensible heat is involved), but they still contribute to considerable exergy losses in the LAES related to irreversibilities caused by large temperature differences in the heat exchangers.

Based on the observations above, it is clear that the research on standalone LAES systems is far from complete. There is a lack of research on studying alternative fluids for cold storage cycles in the LAES system, such as multi-component fluid cycles (MCFCs). The MCFC can provide a wider range of temperature profiles than single-component fluid cycles, and a better match between hot and cold composite curves is obtained. Organic Rankine Cycles offer another solution for cold storage cycles. ORCs can produce electricity by utilizing the temperature difference between air regasification and liquefaction. At the same time, it is used to transfer the cold duty from air regasification to liquefaction. The working fluid for the ORC is multi-component, so the heating and cooling curves of the working fluid are closer to the

temperature profile of the air, and the performance of the LAES will be improved with reduced exergy losses in the cold box.

Thus, in this chapter, multi-component fluid cycles and Organic Rankine Cycles are used for the first time to transfer the cold thermal energy of liquid air regasification to the liquefaction of air in the LAES system. A particle swarm optimization (PSO) method is adopted to find the optimal composition of the multi-component fluids [120]. Cases related to LAES systems with different storage cycles for cold thermal energy recovery are simulated, optimized and compared in Section 4.3.

4.1 System description

The flowsheet of the liquid air energy storage with hot and cold energy storage cycles is shown in Figure 4.1. The three subprocesses in the LAES system are charging, storage, and discharging. In the charging part, air is first compressed in a four-stage compressor with inter/after-coolers (air is cooled to 30°C after each compression stage), then it is cooled by heat exchangers in the cold box, before being expanded to atmospheric pressure in a cryo-turbine, which is used to generate refrigeration capacity and power. The liquid fraction is sent to storage, while the vapor fraction is recirculated to the compression section. The charging process is essentially a liquefaction process, where air is liquefied in periods with excess electric power. In other words, energy (or power) is stored in the form of liquid air. In the storage part, liquid air is kept in atmospheric cryogenic tanks. In the discharging part, liquid air is pumped to a higher pressure before being regasified in evaporators by receiving heat from the cold storage fluids. High-pressure air is then fed to a 4-stage turbine to generate electricity. In order to improve the performance of the LAES system, hot and cold energy storages are employed. The compression heat is used to increase the temperature of inlet air to the expansion stages and thereby produce more electricity in the discharging process. Thermal oil is used as working fluid in the hot storage cycle. The cold thermal energy from air regasification is stored in cold intermediate fluids and will be released to the air liquefaction part.

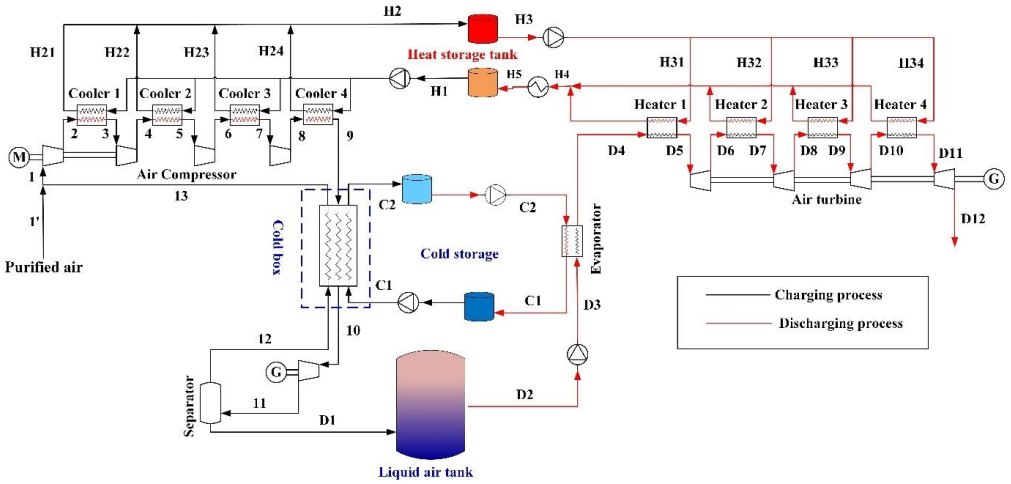

Figure 4.1 Flow diagram for the liquid air energy storage (LAES).

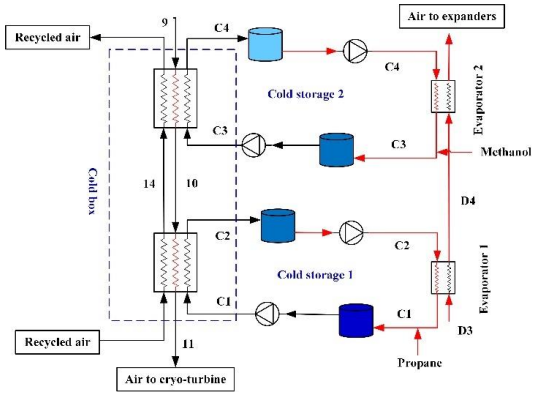

Figure 4.2 Methanol and propane cycles [48] for cold thermal energy recovery in the LAES – Base Case.

In this study, the LAES system with methanol and propane cycles for cold thermal energy recovery is regarded as the Base Case (see Figure 4.2). Other cases related to different cold

thermal energy recovery cycles for the LAES system are considered. To simplify the system, one multi-component fluid cycle (Case 1) is considered to replace the two single-component cycles in the Base Case. Two multi-component fluid cycles are also evaluated for the cold thermal energy recovery system (Case 2). As mentioned before, ORCs could provide extra power while transferring the cold duty from the discharging to the charging process. A single ORC is considered as the cold thermal energy recovery cycle in Case 3. Different combinations of an ORC and a single component fluid cycle are considered as the cold thermal energy recovery system as well. An ORC and a propane cycle are considered in Case 4, while a methanol cycle and an ORC are used in Case 5. Two ORCs are also evaluated as cold thermal energy recovery cycles in Case 6. The components in the working fluids for cold thermal energy recovery cycles are nitrogen, methane, methanol, ethane, propane and n-butane. Although somewhat arbitrarily, the reason for selecting these components is that they can cover the temperature ranges of air liquefaction and regasification (the boiling points and freezing points of these components are considered). In addition, the isobaric specific heat capacities of these six components are close to the specific heat capacity of air for relevant pressure conditions.

4.1.1 Multi-component fluid cycles for cold thermal energy recovery

The purpose of the fluids in the cold energy storage is to transfer cold thermal energy from liquid air regasification to the air liquefaction part. Actually, in LAES systems, the charging and discharging processes typically do not operate at the same time. When energy is demanded, the discharging process is in operation and provides cold regasification energy to fluids from the high-temperature storage tanks. The fluids cooled by the discharging process are then stored in low-temperature storage tanks. When excess electricity is available, the fluids that carry the cold regasification energy are made available for the charging process to provide refrigeration capacity to liquefy air. After receiving heat from the air, the fluids are stored in high-temperature storage tanks to complete the cycle.

A major limitation with single component working fluids is that their operating range for temperature cannot meet the requirements of the entire temperature span in the system. Thus, if the cooling task of hot streams is to be carried out along a wider temperature range, either the fluid needs to go through a phase change, or additional fluid cycles must be used to avoid phase changes. In the former case, a single component cold fluid experiences a constant temperature during phase change, which results in considerable exergy losses and thereby poor thermodynamic performance. In the latter case, extra cycles in the LAES will increase the complexity and cost. Multi-component fluids, unlike pure components, can customize the composition and thereby make the operating temperature range wider while considering the freezing and boiling points of the components. A good match between the temperature profiles of hot and cold streams can be obtained while keeping the configuration simple when using multi-component fluids.

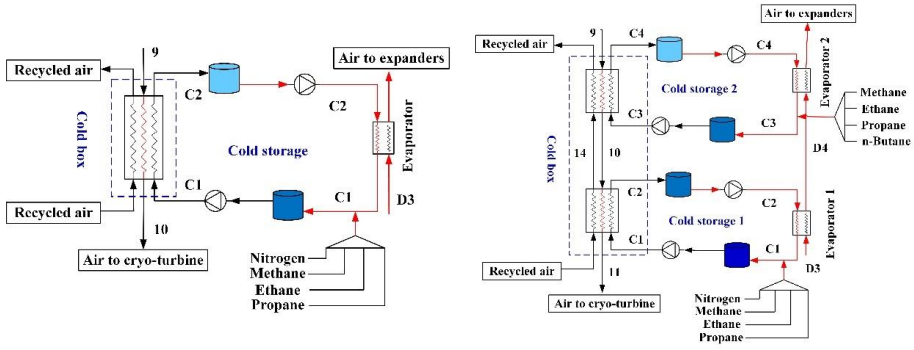

Figure 4.3 Different layouts for cold storage cycles in the LAES system. a) Case 1 (Single multi-component fluid cycle); b) Case 2 (Dual multi-component fluid cycle).

Generally, liquids always have better performance than gases in terms of transferring heat, so the cold storage fluids should remain in liquid phase throughout the LAES system. In this

section, two different configurations of cold storage cycles that use different components are illustrated in Figure 4.3. Figure 4.3a shows a single multi-component cycle (Case 1) that contains nitrogen, methane, ethane and propane. Figure 4.3b shows a dual multi-component fluid cycle (Case 2). Methane, ethane, propane and n-butane are used in the first cycle that is operating at higher temperature. In the second cycle, n-butane is changed to nitrogen since the freezing point of n-butane is -138°C, which is much higher than the boiling point of air (-194°C). Therefore, nitrogen, methane, ethane and propane are considered for the second cycle.

4.1.2 Organic Rankine Cycles for cold thermal energy recovery

Organic Rankine Cycles are also considered for cold thermal energy recovery. They can not only be used to transfer cold duty from the discharging to the charging process, but also to generate additional power due to the temperature difference between air liquefaction and regasification. Any power produced by the cold thermal energy recovery cycles is expected to improve the RTE. However, the specific enthalpy of the working fluid is reduced after being expanded through the gas turbine of the ORC (both temperature and pressure of the fluid are reduced), so the cold regasification energy collected by the same amount of working fluid decreases. This reduces the efficiency of the LAES system, since the temperature of the regasified air is decreased before air is entering the expansion section, resulting in reduced expansion work. In addition, the reduced cold thermal energy from working fluids will lead to a larger compression work to make up for the reduced heat duty in the cold box. These two effects have negative influences on the RTE of the system. The trade-off between the ORC power output and the two negative effects on the RTE means there is an optimal operating condition for the ORC, which will be discussed in Section 4.3.2.

When electricity is required, the ORC working fluid from high-temperature tanks is sent to the liquid air evaporator to collect the cold regasification energy from air during the phase change. After exchanging heat with evaporating air, the working fluid is stored in low-temperature tanks. When the charging process is in operation, the working fluid is first pumped to high pressure before being sent to the cold box, where the working fluid is completely evaporated,

and the high-pressure air is partly liquefied. To produce more electricity, the ORC working fluid enters a gas turbine, before being stored in high-temperature tanks to complete the cycle.

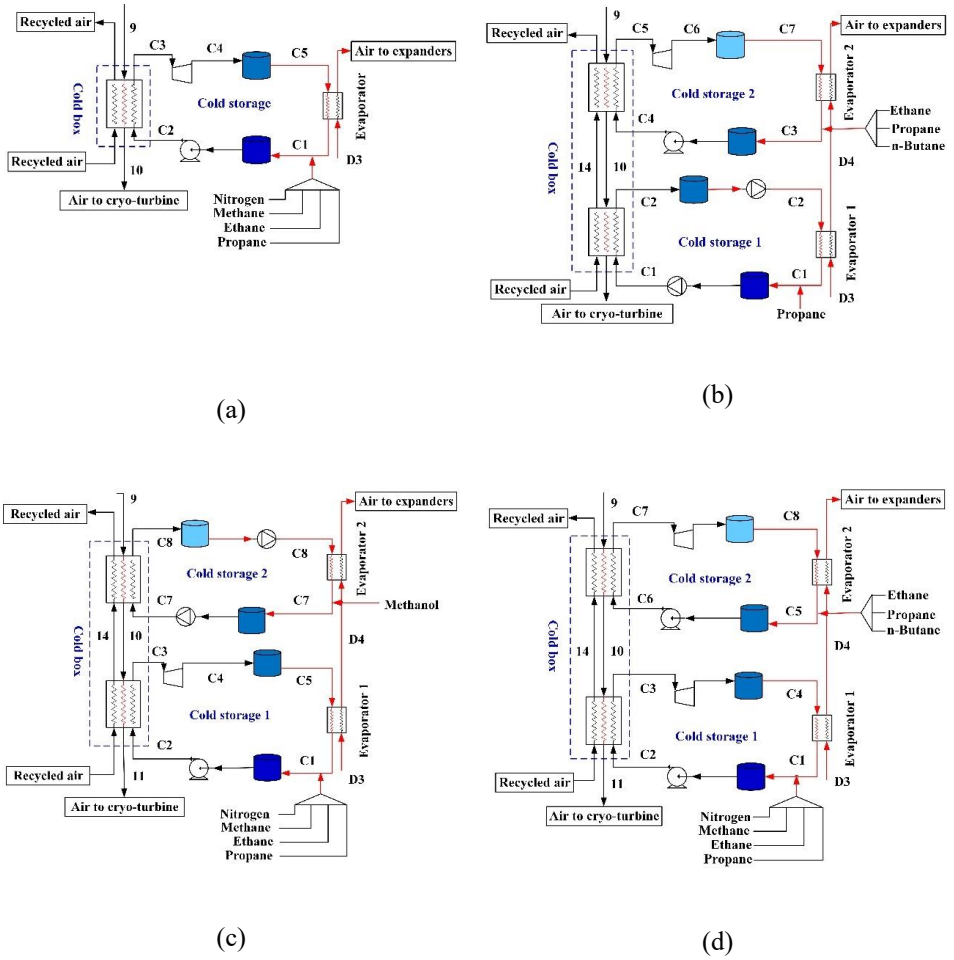

Figure 4.4 Different configurations for cold storage cycles in the LAES: a) Case 3 (Single ORC); b) Case 4 (ORC + Propane cycle); c) Case 5 (Methanol cycle + ORC); d) Case 6 (Dual ORC).

Four cases related to different combinations of ORCs and a single component fluid cycle are illustrated in Figure 4.4. Figure 4.4a shows a single ORC (Case 3) with a working fluid that contains nitrogen, methane, ethane and propane. Figure 4.4b illustrates an ORC operating at higher temperature and a propane cycle operating at lower temperature (Case 4). The components of the ORC working fluid are ethane, propane and n-butane. Figure 4.4c presents the combination of a methanol cycle operating at higher temperature and an ORC operating at lower temperature (Case 5). The components of the ORC working fluid are nitrogen, methane, ethane, and propane. Finally, Figure 4.4d illustrates a dual ORC (Case 6). The components of the working fluid in the 1st ORC that is operated at a higher temperature are ethane, propane and n-butane, while the components of the working fluid in the 2nd ORC that is operated at a lower temperature are nitrogen, methane, ethane, and propane.

4.2 Process evaluation, validation and optimization

This chapter starts by introducing the key performance indicators (KPIs) used for the evaluation of the proposed LAES configurations. Next, the validation of the model is provided, followed by a detailed presentation of the optimization procedure for the LAES system.

4.2.1 Process evaluation

The seven cases are evaluated by using energetic and exergetic indicators. The energetic indicators include liquid yield of air, round-trip efficiency (RTE), and specific power consumption (SPC), which have been introduced in Section 3.1. In addition, exergy efficiency is another important performance indicator that measures the quality of work and heat in a consistent way, considering both the first and second laws of thermodynamics. While the LAES as a total system primarily deals with power, the charging and discharging parts, that operate at different times, handle both power and thermal energy (heating/cooling). Thus, the exergy efficiencies of these processes are considered separately to reveal the exergy transfer

effectiveness within each process. The exergy efficiency of the charging process $\eta_{\dot{E}_{\mathrm{ch}}}$ is calculated by Equation (4.1).

$$\eta_{\dot{E}_{\mathrm{ch}}} = \frac{\dot{W}_{\mathrm{cryotur,ch}} + \dot{E}_{\mathrm{liq}} + \dot{E}_{\mathrm{h}}}{\dot{W}_{\mathrm{comp,ch}} + \dot{E}_{\mathrm{c}} + \dot{E}_{\mathrm{fa}}} \tag{4.1}$$

Here, $\dot{W}_{\mathrm{cryotur,ch}}$ and $\dot{W}_{\mathrm{comp,ch}}$ denote the expansion work produced by the cryo-turbine and the compression work consumed by compressors in the charging process. $\dot{E}_{\mathrm{liq}}$, $\dot{E}_{\mathrm{h}}$, $\dot{E}_{\mathrm{c}}$ and $\dot{E}_{\mathrm{fa}}$ represent the physical exergy of liquid air, working fluid in the hot storage cycle (thermal oil), working fluids in the cold storage cycles, and the air feed. The calculation method for the exergy of streams can be found in Section 3.1. Similar to exergy efficiency for the charging process, the exergy efficiency of the discharging process $\eta_{\dot{E}_{\mathrm{dc}}}$ is given by Equation (4.2).

$$\eta_{\dot{E}_{\mathrm{dc}}} = \frac{\dot{W}_{\mathrm{tur,dc}} + \dot{E}_{\mathrm{c}}}{\dot{W}_{\mathrm{pump,dc}} + \dot{E}_{\mathrm{liq}} + \dot{E}_{\mathrm{h}}} \tag{4.2}$$

Here, $\dot{W}_{\mathrm{tur,dc}}$ and $\dot{W}_{\mathrm{pump,dc}}$ are the expansion work produced by turbines and the work consumed by the pump in the discharging process, respectively.

4.2.2 Process validation

The Aspen HYSYS model of the LAES has been validated against available data in the literature. Figure 4.5 presents a comparison between this study and Guizzi et al. [48] of the LAES system performance. It is found that the differences between the values obtained using the simulation model in this study and the values in Guizzi's work are within 1.4%. Thus, a sufficient accuracy of the system model is confirmed, and the model is found to be acceptable for our research.

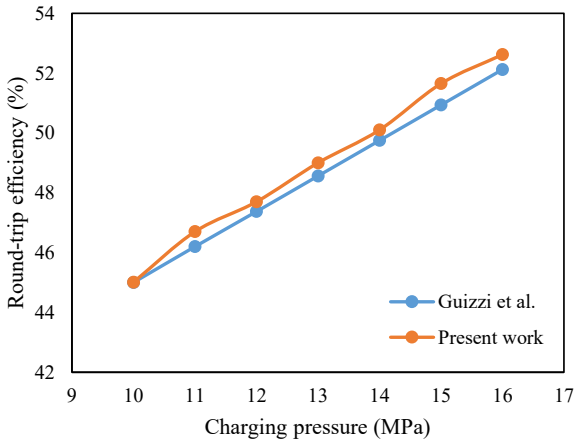

Figure 4.5 Model validation by comparing RTE with numbers from Guizzi et al. [48].

4.2.3 System optimization

Optimization using Particle Swarm Optimization (PSO) algorithm is performed to evaluate the different LAES configurations. The parameter settings and optimization framework for this algorithm are provided in Section 3.3. The motivation for the use of optimization is to make a fair comparison between the LAES systems with different configurations and to find optimal compositions for multi-component working fluids for the corresponding cold thermal energy recovery cycles. The objective is to maximize the round-trip efficiency of the LAES, as shown in Equation (4.3).

$$\min_{x} \quad -\eta_{\mathrm{RT}} = -f(x) = -\frac{\dot{m}_{\mathrm{liq}} w_{\mathrm{tur}}}{\dot{m}_{\mathrm{comp}} w_{\mathrm{comp}}} \tag{4.3}$$

The selection of decision variables, listed in Table 4.1 with their bounds and here represented by x, can be made by analyzing the degrees of freedom in the system. In this study, all pressure ratios for compressors and expanders are selected as variables. The outlet temperature of

thermal oil from compression heat exchangers, the outlet air temperature from the cold box, and the outlet temperature of recycled air from the cold box are also selected as decision variables. In addition, operating temperatures, pressures and molar flowrates of working fluids are considered as variables. Variables for the LAES system with one or two cold thermal energy recovery cycles are listed separately in Table 4.1, since the operating conditions of the two cycles are different.

Table 4.1 Decision variables with lower and upper bounds.

Variables	Lower Bounds	Upper Bounds
Pressure ratio for compressors [a, b]	1	5
Pressure ratio for expanders [a, b]	1	10
Thermal oil temperature ($T_{H21\text{-}H24}$) (°C) [a, b]	150	230
Cold box outlet air temperature (°C) [a, b]	-188	-165
Cold box outlet recycled air temperature (°C) [a, b]	-10	29
Working fluid operating temperature (higher) (°C) [a, b]	-10	29
Working fluid operating pressure (bar) [a, b]	1	120
Working fluid molar flowrate (kmol/h) [a, b]	0	60
Working fluid operating temperature (lower) (°C) [b]	-100	-20

[a] variable bounds for the LAES with single cold cycle
[b] variable bounds for the LAES with dual cold cycle

The constraints for the LAES system are discussed in the following: The minimum temperature difference (ΔT_{min}) of intercoolers and reheaters is assumed to be 10°C (see Equations (4.4) and (4.5)), while ΔT_{min} of the cold box and evaporators is assumed to be 1°C (see Equations (4.6) and (4.7)), which is commonly used in low-temperature processes [122].

$$\Delta T_{\text{int,ch}} \geq 10 \tag{4.4}$$

$$\Delta T_{\text{reh,dc}} \geq 10 \tag{4.5}$$

$$\Delta T_{\text{coldbox}} \geq 1 \tag{4.6}$$

$$\Delta T_{\text{eva}} \geq 1 \tag{4.7}$$

In addition, for multi-component fluid cycles, the vapor fraction should be less than 0.005 to essentially assure liquid phase in the entire cycle, as shown in Equation (4.8). For ORCs, the vapor fraction of the working fluid at the inlet of the pump should be zero, indicating the phase to be totally liquid (see Equation (4.9)), and the vapor fraction of the working fluid at the outlet of the cold box (inlet stream to the turbine) should be one, indicating the phase to be totally gas (see Equation (4.10)).

$$VF_{\text{MCFC}} \leq 0.005 \tag{4.8}$$

$$VF_{\text{ORC,pump,in}} = 0 \tag{4.9}$$

$$VF_{\text{ORC,tur,in}} = 1 \tag{4.10}$$

4.3 Results and discussions

The optimal results of the seven cases are discussed here. The compression and expansion parts have the same configuration in all cases, i.e. four compressor stages and four expander stages. The difference between the seven cases is the cold thermal energy recovery and storage parts. Since optimization, however, is performed for the entire system, the compression and expansion parts are also included. As a result, the optimal operating conditions of the compression and expansion parts can be different for different cold thermal energy recovery cycles. One example is that more compression work is needed to ensure sufficient refrigeration capacity for air liquefaction when the cold thermal energy recovery ratio is low.

4.3.1 Round-trip efficiencies for the seven cases

Figure 4.6 illustrates the RTE for the LAES system with different cold thermal energy recovery cycles. It shows that LAES configurations with two cold thermal energy recovery cycles to transfer the cold regasification energy (Base Case and Cases 2, 4, 5 and 6) have better performance than the systems with only one cold thermal energy recovery cycle (Cases 1 and 3). The reason is that the temperature range for air is very large (from 30°C to -180°C) and the specific heat capacity of air changes significantly during the liquefaction and evaporation processes. Thus, better temperature match in the cold box can be obtained when two cold recovery fluids with different specific heat capacities are used. Among the five LAES configurations with two cold storage cycles, the LAES system with dual multi-component fluid cycle (MCFC) for cold thermal energy recovery has the highest RTE of 62.4%.

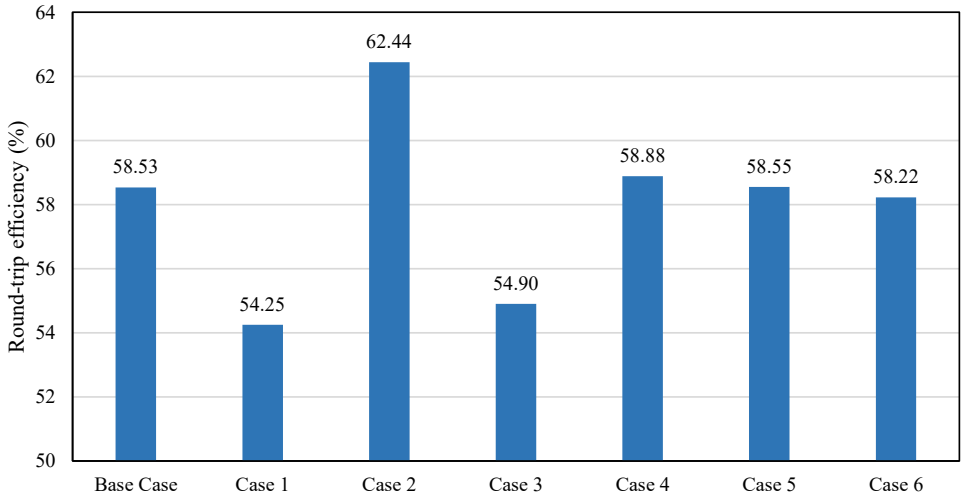

Figure 4.6 Round-trip efficiency for the LAES system with different cold thermal energy recovery cycles.

4.3.2 Optimal operating conditions for cold cycles

Optimal operating variables, such as temperatures, pressures and compositions for the working fluids are listed in Table 4.2 for the seven cases, while the optimal results (heat duty and logarithmic mean temperature difference (LMTD) of cold boxes) for different cold thermal energy recovery cycles are shown in Table 4.3. In both tables, the terms 1st cycle and 2nd cycle refer to the cycle operating at higher and lower temperatures respectively.

Table 4.2 Optimal operating variables for different cold thermal energy recovery cycles in the LAES system.

Cases	Cycle	Composition [mole%]						p [bar]	T_{lowest} [°C]	$p_{tur,in}$ [bar]	$p_{tur,out}$ [bar]
		CH_3OH	N_2	CH_4	C_2H_6	C_3H_8	nC_4H_{10}				
Base Case	1st	100.00	-	-	-	-	-	1.00	-46.71	-	-
	2nd	-	-	-	-	100.00	-	1.00	-186.33	-	-
Case 1	1st	-	0.08	10.81	7.50	81.61	-	85.80	-184.92	-	-
Case 2	1st	-	-	0.26	4.06	47.43	48.25	32.15	-70.24	-	-
	2nd	-	3.01	2.82	18.56	75.61	-	27.38	-186.34	-	-
Case 3	1st	-	31.34	32.23	16.08	20.35	-	-	-186.51	4.87	4.87
Case 4	1st	-	-	-	53.52	24.32	22.16	-	-43.65	6.89	6.83
	2nd	-	-	-	-	100.00	-	1.00	-184.11	-	-
Case 5	1st	100.00	-	-	-	-	-	1.00	-48.07	-	-
	2nd	-	20.99	39.78	18.31	20.92	-	-	-182.82	3.17	3.17
Case 6	1st	-	-	-	43.60	30.52	25.88	-	-40.20	4.47	4.47
	2nd	-	24.33	40.70	23.30	11.67	-	-	-188.02	3.15	3.15

Case 1, where only one MCFC is used rather than two single fluid cycles (methanol and propane cycles), is proposed to simplify the configuration of the LAES system. In Case 2, the LMTDs for the cold box and evaporator are on average the smallest among the seven cases, indicating that the dual MCFC has the smallest entropy generation in the cold thermal energy recovery part and thereby the highest thermodynamic efficiency. The operating pressures of

the two MCFCs (p = 32.2 and 27.4 bar) in Case 2 are considerably reduced compared to the pressure of the single MCFC (p = 85.8 bar) in Case 1. This is due to the fact that working fluids experience a smaller temperature range in the cold boxes in Case 2 compared with Case 1, thus avoiding high pressure to keep the working fluids in liquid form.

Table 4.3 Optimal results for different cold thermal energy recovery cycles in the LAES system.

Cases	Cycle	$Q_{coldbox}$ [kW]	$LMTD_{coldbox}$ [°C]	$LMTD_{eva}$ [°C]	$\dot{m}_{ORC}$ [kg/h]	$\dot{m}_{F}$ [kg/h]
Base Case	1st	221.54	2.74	4.31	-	824.10
	2nd		2.79	3.92	-	2280.42
Case 1	1st	199.04	3.02	8.13	-	1733.48
Case 2	1st	219.33	2.06	4.89	-	1221.25
	2nd		2.31	2.67	-	2402.89
Case 3	1st	203.46	4.43	6.72	968.60	-
Case 4	1st	210.04	5.19	5.42	329.69	-
	2nd		2.07	5.77	-	2142.01
Case 5	1st	202.45	4.15	6.69	-	1022.14
	2nd		2.44	3.19	882.76	-
Case 6	1st	212.90	10.09	6.34	295.89	-
	2nd		3.29	4.42	859.40	-

It is worth noting that the operating pressures of the working fluids in Case 2 are considerably higher than the operating pressures in the Base Case (1 bar for both cycles). This, of course, increases the CAPEX of the system; however, the higher RTE of the LAES system with multi-component fluids will reduce OPEX. A trade-off analysis between CAPEX and OPEX will determine the economic feasibility of the system. In Case 2, the optimal composition of MCFC-1 is 0.3 mole% methane, 4.1 mole% ethane, 47.4 mole% propane and 48.2 mole% n-butane, while the optimal composition of MCFC-2 is 3.0 mole% nitrogen, 2.8 mole% methane, 18.6 mole% ethane and 75.6 mole% propane. The results show large fractions of propane and n-

butane in the MCFCs, reflecting that these components have specific heat capacities closer to air. Methane and ethane are used to modify the composite curve of the working fluid for a better match with the air liquefaction curve. The amount of nitrogen is very small to keep the MCFC-2 working fluid in liquid form without the need for high pressure.

4.3.3 Using ORCs as cold thermal energy recovery cycles

In Case 3, one ORC is used as the cold thermal energy recovery cycle in the LAES system. The optimal results in Table 4.2 show that no power is produced in the ORC, because this single ORC operates without pressure change (the pump and turbine are inactive), which results in similar performance for Case 3 (single ORC) and Case 1 (single MCFC). The other four configurations (Base Case and Cases 4, 5 and 6) have similar RTEs, however, the optimal operating conditions are quite different. In the Base Case, methanol and propane cycles are used for cold thermal energy recovery, and this configuration is discussed by many researchers. The advantage of this configuration with an acceptable RTE of 58.5% is that the operating pressure of the two cold storage cycles is atmospheric, so that capital costs for cold storage tanks are reduced. For Case 4, the LAES with an ORC and a propane cycle has an RTE of 58.9%. The RTE of the LAES using methanol and an ORC as cold thermal energy recovery cycles (Case 5) is 58.6%. It can be seen from Table 4.3 that the LMTDs for the cold boxes and evaporators in Cases 4 and 5 are similar, which is why the two cases have almost the same performance. In addition, the pressure ratios for turbines in the ORC in these cases are 1 ($p_{tur,in} = p_{tur,out}$), which indicates that running the ORC with power production is not optimal.

For the multi-component working fluid in the ORC, both the sensible and latent heat are used to collect the regasification energy of air. Since the ORC is able to collect more heat than the MCFC with sensible heat only, considerably less working fluid is needed for the ORC (see Table 4.3). The optimal composition of the working fluids can be found in Table 4.2, where ethane has the largest fraction in Case 4, accounting for 53.5 mole%, while the methane fraction (39.8 mole%) is the largest in Case 5. This is due to the fact that components with higher specific heat capacity, such as methane and ethane, are preferred when the mass flow rate of

the working fluid is reduced. In Case 6, two ORCs act as heat transfer cycles, and both the sensible and latent heat of the working fluids are used to collect the cold thermal energy. The LMTDs of the cold boxes and evaporators are larger than the LMTDs in the Base Case and Cases 2, 4 and 5. As a result, the RTE of the LAES configuration with dual ORC is lower (58.2%) but still better than the RTEs of Cases 1 and 3. One conclusion from the optimal results of the different cases is that the operating pressure of the working fluid in the cold thermal energy recovery cycles should be kept unchanged. This is because it is more efficient to use the cold thermal energy collected from the regasification to liquefy air than producing work in the ORCs.

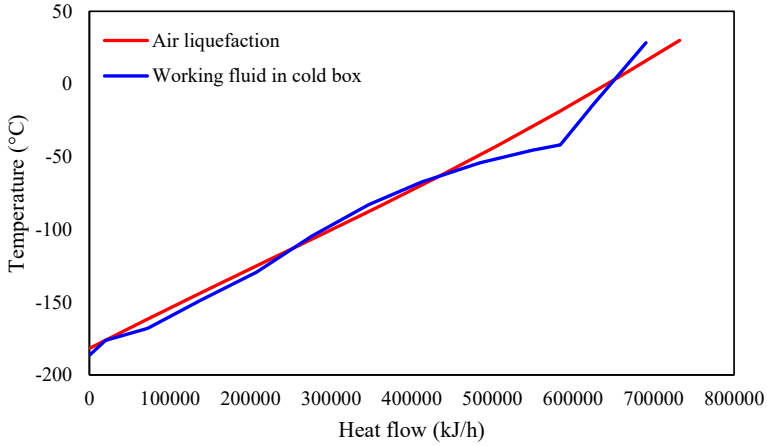

(a)

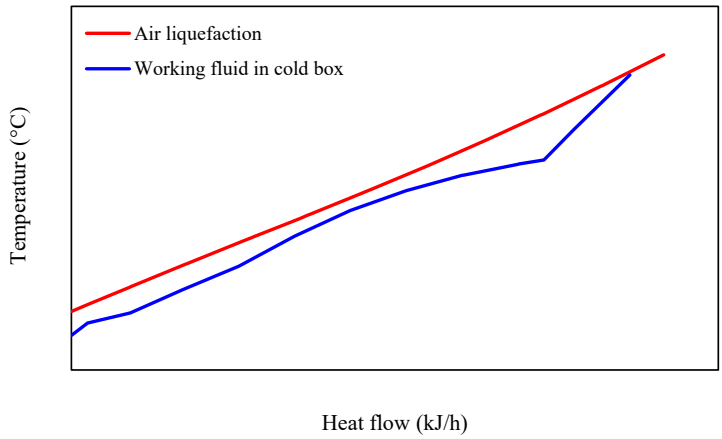
Air liquefaction
Working fluid in cold box
Temperature (°C)
Heat flow (kJ/h)

(b)

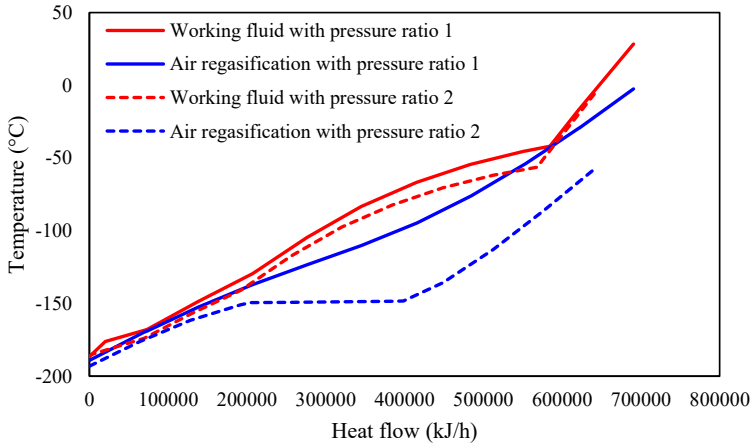
Working fluid with pressure ratio 1
Air regasification with pressure ratio 1
Working fluid with pressure ratio 2
Air regasification with pressure ratio 2
Temperature (°C)
50
0
-50
-100
-150
-200
0
100000
200000
300000
400000
500000
600000
700000
800000
Heat flow (kJ/h)

(c)

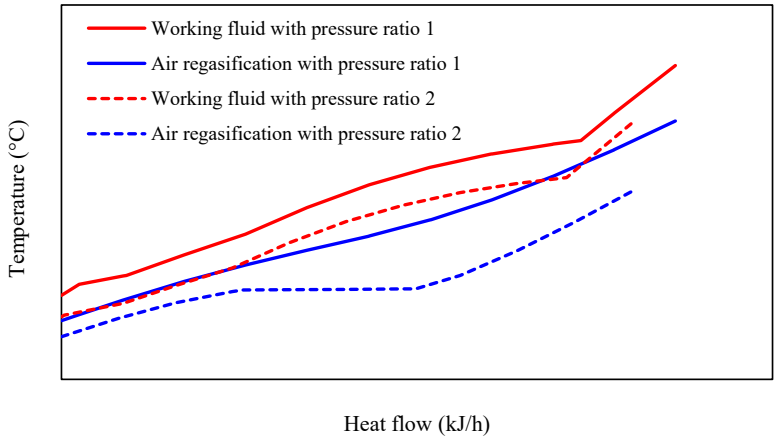

(d)

Figure 4.7 T-H diagram for the cold box and the evaporator in Case 3: a) Real data from Aspen HYSYS for the cold box in the charging part; b) Hand drawn figure to better explain the cold box in the charging part; c) Real data from Aspen HYSYS for the evaporator in the discharging part; d) Hand drawn figure for the evaporator in the discharging part.

The driving forces between the liquefaction (charging) and regasification (discharging) curves for air in the T-H diagram are small. As shown in Figure 4.7a and 4.7c, which is based on simulation results from Aspen HYSYS, the temperature of the working fluid is sometimes higher than the temperature of air in the cold box. However, this is not an indication of temperature cross-over in the heat exchanger. Recirculation air is also a cold fluid and contributes to the total heat capacity flowrate of the cold composite curve, and thereby avoids temperature cross-over in the cold box. Figure 4.7b and 4.7d are an enlarged hand-drawn illustration of Figure 4.7a and 4.7c. The gap between the air liquefaction or air regasification curves on one side and the evaporation or condensation curves of the working fluid in the ORC on the other side is artificially increased, i.e. drawn out of scale.

Results from the optimization indicate that the pressure ratio for the turbine and the pump in the ORC is 1, which means that the turbine and the pump are not active, and the ORC works like a multi-component fluid cycle (MCFC) with phase change. This also means that the composite curves in a T-H diagram for the working fluid in the cold box and the evaporator should coincide. However, with normal operation of the ORC (e.g. if the pressure ratio of the pump is 2), the specific enthalpy of the working fluid would be reduced, as the red dotted line shows in Figure 4.7d. The match with the temperature profile of air would be less perfect in the evaporator, and the work produced by the ORC would not compensate for the lost work in the discharging part. The cold composite curve of air in the evaporator, i.e. the blue dotted line in Figure 4.7d, is shifted down (the discharging pressure of liquid air is reduced to avoid temperature cross-over in the heat exchanger, since air at lower pressure has a higher heat of evaporation). Due to the work produced in the ORC when the pressure ratio is 2, the duty in the evaporator is reduced. This results in a lower air temperature after the evaporator and therefore less work produced in the discharging part.

For Case 1, the sensible heat of the MCFC is used to transfer the cold duty from air regasification, and the change in the slope of the MCFC in the T-H diagram is relatively small compared to the change in the slope of air during the heat transfer process. Thus, poor performance (RTE = 54.3%) is the result due to the mismatch between the air and the single MCFC temperature profiles. The optimal composition of the single MCFC is shown in Table 4.2, where more than 80% is propane. Moreover, the operating pressure of the single MCFC is quite high (p = 85.8 bar), which leads to high capital costs. However, the situation is different for Case 3. An ORC with a multi-component working fluid is used for cold thermal energy recovery. It can be seen from Table 4.2 that the pump and turbine are not active in this single ORC case, and the operating pressure (p = 4.9 bar) of the working fluid is considerably reduced compared to Case 1. However, with the gradual evaporation and liquefaction of the working fluid, the temperature profiles between the air and the working fluid do not have a good match, which can be confirmed by the large LMTDs of the cold box and the evaporator ($LMTD_{coldbox}$ = 4.4°C and $LMTD_{eva}$ = 6.7°C). In this case, the optimal composition of the working fluid is 31.3 mole% nitrogen, 32.2 mole% methane, 16.1 mole% ethane and 20.4 mole% propane.

4.3.4 KPIs for the optimized cases

Table 4.4 shows optimal pressure values for charging and discharging together with key performance indicators (liquid yield, specific power consumption, exergy efficiencies of the charging and discharging processes, and round-trip efficiency) for the different cases. It can be seen that Case 2 has a superior performance compared to the other cases. Case 2 obtains the highest liquid yield (93.8%), highest exergy efficiencies of the charging (86.1%) and discharging (86.0%) processes, the smallest specific power consumption (188.66 kWh/t, which is consistent with the lowest charging pressure among the seven cases), and a superior round-trip efficiency (62.4%). These good results are primarily related to the best heat transfer efficiency of the dual MCFC. The difference in round-trip efficiency, exergy efficiency, liquid yield and specific power consumption is marginal for the Base Case and Cases 4, 5 and 6, except for the fact that the Base Case has a considerably lower liquid yield. The LAES with one cycle for cold recovery (Case 1) has the lowest RTE, which results from the mismatch between the air and working fluid temperature profiles. In Cases 1 and 3, higher charging pressures are needed to compensate for the reduced cold air regasification energy.

Table 4.4 Optimal results for some variables and key performance indicators.

	Base Case	Case 1	Case 2	Case 3	Case 4	Case 5	Case 6
p_{ch} (bar)	191.36	458.18	147.38	335.72	257.08	349.05	215.30
p_{dc} (bar)	145.38	175.94	100.62	109.26	150.02	186.30	108.59
η_{LY} (%)	86.65	88.54	93.79	91.55	91.09	91.61	92.42
SPC (kWh/t)	218.07	256.6	188.66	232.34	223.10	234.7	212.89
$\eta_{\dot{E}_{ch}}$ (%)	83.45	70.73	86.13	82.49	84.1	83.73	83.69
$\eta_{\dot{E}_{dc}}$ (%)	83.17	70.05	86.00	80.23	82.38	82.00	83.35
η_{RT} (%)	58.53	54.25	62.44	54.90	58.88	58.55	58.22

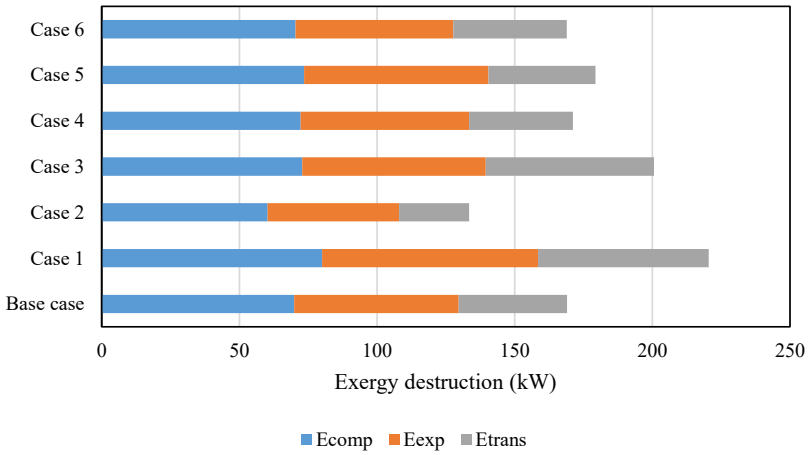

Figure 4.8 Exergy destruction for the compression, expansion and heat transfer parts in the seven cases.

Figure 4.8 illustrates exergy destruction for the compression, expansion and heat transfer parts in the seven cases. It can be noticed that Case 2 has the lowest exergy destruction in all three parts, while Cases 1 and 3 have the largest exergy destructions. The Base Case and Cases 4, 5 and 6 have medium exergy destructions. This is consistent with the previous discussion: Case 2 has the highest RTE, followed by the Base Case and Cases 4, 5 and 6, while Cases 1 and 3 have the lowest RTE. By comparing Cases 5 and 6, it is found that the total exergy destruction in Case 5 is higher. However, this mainly comes from the expansion part and is associated with larger work production, which improves the RTE. In addition, exergy losses due to heat transfer are slightly smaller in Case 5. This reveals that the cold thermal energy transfer part, which is related to LMTDs of cold boxes and evaporators, and the liquid yield have decisive effects on the RTE of the system. Thus, higher efficiency of cold thermal energy recovery cycles leads to a higher RTE.

4.3.5 Sensitivity analysis

The cryo-turbine efficiency and the ΔT_{min} of heat exchangers (high-temperature and low-temperature) have important influences on the system performance. As the LAES system with dual multi-component fluid cycles (Case 2) has the best performance according to Section 4.3.1, this process configuration is selected as the design basis for a sensitivity analysis. In Case 2, the isentropic efficiency of the cryo-turbine is 75%, and the ΔT_{min} of high-temperature and low-temperature heat exchangers are 10°C and 1°C, respectively. In this section, the cryo-turbine efficiencies of 65% and 85% are assumed and discussed. In addition, the ΔT_{min} of high-temperature heat exchangers are varied from 5°C to 15°C, and the ΔT_{min} of low-temperature heat exchangers is varied from 1°C to 2°C. The optimal results with different cryo-turbine efficiencies are listed in Table 4.5. For obvious reasons, the round-trip efficiency increases as the cryo-turbine efficiency is increased from 65 to 85%. It is worth noting that the optimal charging pressure is reduced with increasing cryo-turbine efficiency. Increased cryo-turbine efficiency results in a higher exergy efficiency of the equipment and a larger refrigeration capacity.

Table 4.5 Influence of cryo-turbine efficiency on system performance.

Cryo-turbine efficiency (%)	Optimal		η_{RT} (%)
	p_{ch} (bar)	p_{dc} (bar)	
65	149.23	95.71	61.29
75	147.38	100.62	62.44
85	143.71	101.55	63.12

The influence of ΔT_{min} for heat exchangers is listed in Table 4.6. As the ΔT_{min} of high-temperature heat exchangers increases, exergy destructions for the compression and expansion parts are increased, while the exergy destruction for the heat transfer part remains almost the same. It should be emphasized that the compression part consists of compressors and intercoolers, the expansion part consists of expanders and reheaters, while the heat transfer part

consists of the cold box, the evaporators, the cryo-turbine and the separator. Due to this decomposition, the heat transfer part is only affected by the ΔT_{min} for the low-temperature heat exchangers. Heat transfer in the high-temperature heat exchangers is accounted for in the compression and expansion parts. It is pointed out that the RTE is increased to 64.72% when the ΔT_{min} of high-temperature exchangers is reduced to 5°C. However, the reduction of ΔT_{min} will result in a larger heat exchanger area and CAPEX, which is verified by the average *UA* values of high-temperature and low-temperature heat exchangers in Table 4.6. The *UA* value is the product of the overall heat transfer coefficient and heat transfer area and therefore indicates the size of the heat exchanger. Thus, an economic analysis will be required to identify the cost optimal conditions for practical applications. In addition, the ΔT_{min} of the low-temperature heat exchangers affect the system performance significantly, since the liquid yield and the exergy destruction for the heat transfer part are related to this parameter. As the ΔT_{min} is increased to 2°C in the low-temperature heat exchangers, a drop of 1.2% points for the RTE is observed. This mainly results from the increase in exergy destruction in the heat transfer part, as seen in Table 4.6.

Table 4.6 Influence of minimum approach temperature for heat exchangers on system performance.

Parameters	ΔT_{min} (°C)	$UA_{int/reh}$ (kW/°C)	$UA_{coldbox/eva}$ (kW/°C)	$\dot{E}_{comp}$ (kW)	$\dot{E}_{exp}$ (kW)	$\dot{E}_{trans}$ (kW)	η_{RT} (%)
High-temperature heat exchangers	5	11.51	44.87	56.89	32.91	24.39	64.72
	10	6.59	41.49	60.28	36.02	25.46	62.44
	15	4.03	40.16	68.66	41.66	25.32	58.56
Low-temperature heat exchangers	1	6.59	41.49	60.28	36.02	25.46	62.44
	2	6.58	29.35	61.50	36.63	30.00	61.22

4.3.6 Performance with additional heat recovery

For the heat recovery between the charging and discharging parts, there is an imbalance caused by different charging and discharging pressures and the recirculation of air. Some of the compression heat carried by the hot oil cycle is not efficiently used in reheaters of the discharging part in the seven cases, as listed in Table 4.7. In this section, in order to further improve the performance of the LAES, an ORC is used as an additional heat recovery cycle for power production to utilize the heat that is wasted in the discharging process. Figure 4.9 illustrates the additional heat recovery cycle in the LAES. For the seven cases, the working fluid is assumed to be cooled to 20°C by sea water, which is regarded as a constant temperature heat sink. The heat source is stream H35 in the LAES system. For the additional heat recovery cycle, R600 (n-butane with critical temperature 151.9°C and critical pressure 37.9 bar) is chosen as the working fluid. Thus, an additional ORC is included and added to the optimized seven cases to analyze the effect of the waste heat recovery. Since the only change in the system is to replace sea water cooling of stream H35 with an ORC utilizing the waste heat in stream H35, the rest of the system is not affected.

Table 4.7 Stream data for the surplus hot oil.

Case study	$T_{\text{surplus ho}}$ (°C)	$mf_{\text{surplus ho}}$ (kmol/h)
Base case	177.58	2.03
Case 1	206.09	5.50
Case 2	167.29	1.89
Case 3	194.41	4.70
Case 4	187.83	1.70
Case 5	195.94	1.74
Case 6	183.30	1.53

Figure 4.10 shows the round-trip efficiencies for the seven cases when an ORC is used to further utilize the waste compression heat. The blue columns represent the RTE of the system for different configurations of the cold thermal energy recovery cycles, while the orange columns show the increment in RTE when using the additional ORC as heat recovery cycle. Case 2 still has the best performance and the RTE is improved from 62.4% to 64.7%. The RTE of the Base Case and Cases 4 and 5 are all above 61% after additional heat recovery. The LAES with two ORCs in Case 6 has an RTE of 60.1%. The RTE of Cases 1 and 3 are also improved to around 58%. It can also be noticed that the increment in RTE is largest for Cases 1 and 3. This is because more compression work is needed to compensate for the poor performance of the cold thermal energy recovery cycles in these two cases. Increased compression means more compression heat with higher temperature and increased flow rate of the hot oil. This means that the ORC utilizing waste heat can produce more work in these two cases.

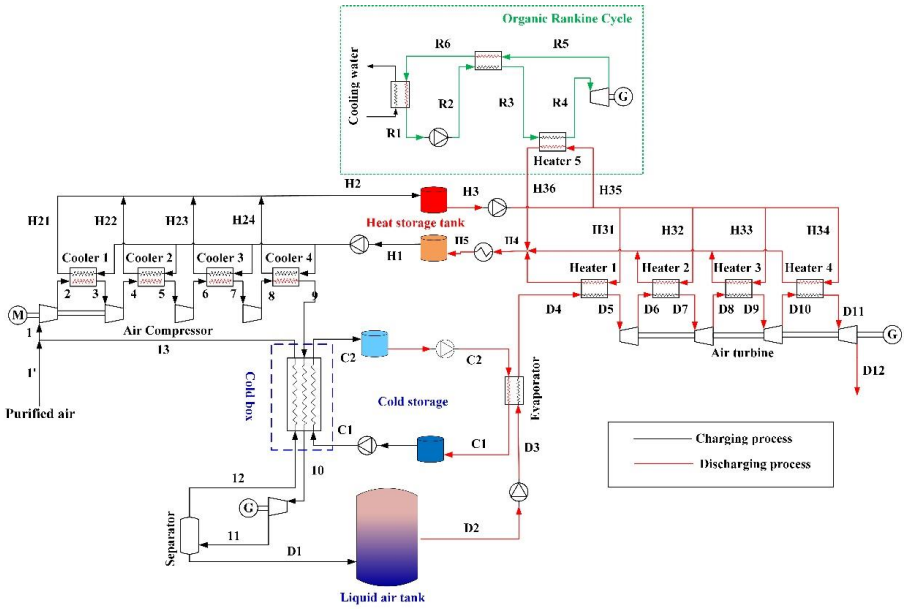

Figure 4.9 Heat recovery cycle in the LAES system.

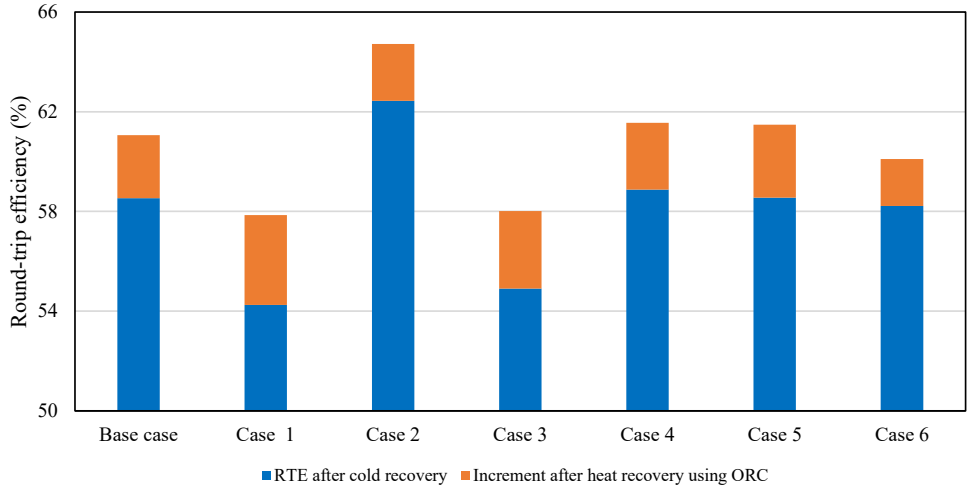

Figure 4.10 Round-trip efficiency for LAES configurations with an additional heat recovery cycle

The detailed results after optimization of using an additional heat recovery cycle in the seven cases are listed in Table 4.8. The flow rate and temperature of the surplus hot oil are relatively high in these cases, and more net work (18.5 kW and 14.4 kW in Cases 1 and 3, respectively) is generated. The work produced by the other cases are also listed in Table 4.8.

Figure 4.11 illustrates the exergy destruction for the expansion part in the seven cases after utilizing the additional ORC to recover waste compression heat. The reduction in exergy destruction for the seven cases with an additional heat recovery cycle is also shown by gray bars in the figure. It is clear that the largest reduction in exergy destruction is obtained in Cases 1 and 3, which is related to the net work produced by the additional heat recovery cycle in these two cases. The reduction in exergy destruction for the Base Case and Cases 2, 4, 5 and 6 can also be found in Figure 4.11.

Table 4.8 Performance of the additional heat recovery cycle in the seven cases.

Case study	Working fluids	$\dot{W}_{net}$ (kW)	$P_{orc,con}$ (bar)	$P_{orc,eva}$ (bar)	mf (kmol/h)	$T_{orc,eva}$ (°C)	$\dot{W}_{orc,tur}$ (kW)	$\dot{W}_{orc,pump}$ (kW)
Base case	R600	11.06	2.08	34.10	7.47	145.20	11.89	0.83
Case 1	R600	18.53	2.08	30.44	11.84	138.20	19.70	1.17
Case 2	R600	8.59	2.08	17.81	7.05	105.51	8.96	0.37
Case 3	R600	14.44	2.08	34.12	9.75	145.20	15.53	1.09
Case 4	R600	11.92	2.08	34.11	8.06	145.20	12.82	0.90
Case 5	R600	13.73	2.08	34.15	9.29	145.30	14.77	1.04
Case 6	R600	8.00	2.08	34.11	6.59	145.20	8.74	0.74

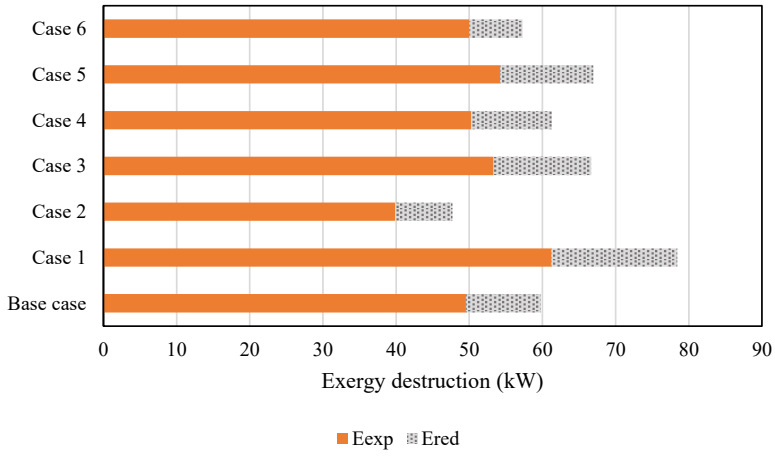

Figure 4.11 Exergy destruction for the expansion part in the seven cases with the additional heat recovery cycle.

4.4 Conclusions

The standalone liquid air energy storage (LAES) system with different cold thermal energy recovery cycles is discussed, optimized and compared in this study. Multi-component fluid cycles (MCFCs) and Organic Rankine Cycles (ORCs) are considered for the first time to transfer the cold thermal energy from air regasification to air liquefaction in the LAES. Seven cases are optimized by using a particle swarm optimization (PSO) algorithm. For the different cold thermal energy recovery cycles, the following conclusions are drawn:

- The dual MCFC has the best performance in terms of liquid yield, specific power consumption, exergy efficiency and round-trip efficiency (RTE). The RTE of the standalone LAES with dual MCFC in Case 2 is 62.4%. This RTE can, however, be improved to 64.7% when the ΔT_{min} of high-temperature heat exchangers is reduced from 10°C to 5°C. This performance is higher than standalone LAES systems in the literature with RTEs below 63%.

- Cases 1 and 3 with only one cold thermal energy recovery cycle has lower RTE, since the specific heat capacity of the air is different before and after its phase change, and large exergy destructions are caused by the large temperature differences between the working fluid and air.

- Organic Rankine Cycles are not suitable for transferring the cold duty between the charging and discharging processes. The optimal results show that both the sensible and latent heat of the working fluid are used, however, the pump and turbine are not active. The purpose of using an ORC (i.e. to produce additional work) is therefore not achieved. The actual heat transfer is between the air regasification and air liquefaction, and a better match can be obtained in both cold boxes and evaporators when the operating temperature and pressure of the working fluid is kept the same on both sides.

For heat recovery cycles, the following conclusions are drawn:

- The additional heat recovery cycle results in a larger improvement in performance for Cases 1 and 3 than for the other cases. With lower efficiency of the cold thermal energy recovery cycles for Cases 1 and 3, more compression work is needed to compensate for this poor performance, and more compression heat can be utilized to produce work in the additional heat recovery cycle that uses an ORC. The RTE of Cases 1 and 3 can be improved to around 58%.

- After integrating an additional heat recovery cycle (i.e. ORC) in the discharging process, the RTE is improved to 64.7% for Case 2, which has the best performance in terms of the RTE. For the other cases, the RTEs are between 60.0 and 61.6%.

Although the dual MCFC has a larger operating pressure than the typical methanol cycle and propane cycle, leading to a larger CAPEX, this novel cycle still provides a possible approach to improve the performance of cold thermal energy recovery cycles. A slightly simpler set of working fluids can be used in order to reduce the computational efforts with a marginal decrease in RTE. In the following chapters, a methanol and a multi-component fluid cycle, which consists of propane, ethane and n-butane, are used as the cold thermal energy recovery cycles that are operated at different temperatures.

Chapter 5 Optimization and Analysis of LAES with Different Number of Compression and Expansion Stages

Abstract

As discussed in Section 2.2, one drawback of a standalone LAES is the relatively low round-trip efficiency (RTE). In this chapter, the performance of a standalone LAES system with different number of compression and expansion stages is studied. All cases are optimized by using a particle swarm optimization (PSO) algorithm. The optimal results show that the highest RTE of 66.7% is obtained when there is a 2-stage compressor and a 3-stage expander in the LAES system. When the number of compression stages is fixed, the highest RTE is obtained when hot and cold streams have close to parallel temperature profiles in the preheaters of the expansion section.

This chapter is based on the following publications.

- Liu Z, Kim D, Gundersen T. Optimization and analysis of different liquid air energy storage configurations. In review for Computers & Chemical Engineering, 2022.
- Liu Z, Yu H, Gundersen T. Optimization of Liquid Air Energy Storage (LAES) using a Genetic Algorithm (GA). Computer Aided Chemical Engineering. 2020;48:967-972.

The LAES is commonly divided into charging, storage and discharging processes based on its operating mode. However, for a standalone LAES, the overall system can also be decomposed into three parts, which are the compression, the hot and cold energy storage and exchange, and the expansion sections, according to the function of each part. In the previous chapter, different cold energy recovery cycles are proposed and compared to identify the most suitable cold cycles for the LAES. The compression and expansion sections, as main subsections in the LAES, directly affect the power consumption and production, and are therefore critical to the RTE of the system. It is important to notice that the expansion section is strongly influenced by the operation of the compression section since compression heat is transferred between the two sections by a thermal oil system with storage.

Adiabatic operation will result in maximum power consumption and considerable amounts of high temperature compression heat that is carried by the thermal oil. The inlet air temperature to expanders is increased and the power generation in the discharging process is increased. The near isothermal operation of compression with a large number of stages and aftercoolers approaches minimum power consumption. However, when the number of compression stages is increased in the LAES system, the amount of compression heat and its temperature are reduced. As a result, the temperature of the thermal oil used to collect the compression heat is reduced. The reduced thermal oil temperature will reduce the power production in the expansion part. However, the flow rate of thermal oil is increased due to the repeated cooling in aftercoolers. This counteracts the negative effects in the expansion section of reduced duty and temperature for the thermal oil carrying the reduced compression heat, since the heat transfer pinch is moved to the hot end of the preheaters before the expanders. In summary, while less heat is transferred from charging to discharging, resulting in less power produced in the expansion process, the compression heat is better utilized with a larger thermal oil flowrate. Since less power is consumed in compression with increased number of stages, there is a trade-off where the number of compression and expansion stages plays a significant role.

Most of the existing literature discuss the expansion section and compression section separately for the LAES system. There is a lack of studies related to the complex relations of different number of compression and expansion stages and how this affects the performance of the LAES system. The challenge is to deal with the interacting temperature changes and pressure changes of process streams. This paper focuses on the potential for system efficiency improvements for different configurations of the LAES system, where the term configuration relates to having different number of compression and expansion stages, as well as potential use of Organic Rankine Cycles (ORCs) [123-125].

To have a fair comparison between these different configurations of the LAES system, all cases have been optimized to maximize their RTE by using a particle swarm optimization (PSO) method [120]. Different configurations of the LAES system are optimized and analyzed in Section 5.3. It is worth noting that the corresponding pressure ratios of compressors and expanders are changing with different number of compression and expansion stages. The pressure ratio will be relatively high when the number of compression (or expansion) stages is small, which may affect the efficiencies of compressors (or expanders). However, this work emphasizes purely on a thermodynamic analysis, which is why mechanical limitations and cost issues related to pressure ratios and outlet temperatures of compressors and expanders will not be considered.

5.1 System description

Flowsheets of the liquid air energy storage system are illustrated in Figure 5.1 and 5.2. The liquid air energy storage is commonly divided into charging, storage and discharging processes based on its operating mode. However, for a standalone LAES, the overall system can also be decomposed into three parts, which are the compression, the hot and cold thermal energy recovery cycles, and the expansion sections, according to the function of each part. In the compression section, air is compressed in stages by using available electricity. Air is cooled to 30°C after each compressor stage and the compression heat is collected and stored by the hot

thermal energy recovery cycle. The high-pressure air is then sent to the cold thermal energy recovery part. It is precooled in the cold box by working fluids in cold thermal energy recovery cycles before it is expanded in the cryo-turbine to atmospheric pressure. The name of this turbine refers to the very low (i.e. cryogenic) temperature, and the unit is operating with a liquid inlet stream and a two-phase outlet stream. The cryo-turbine can produce additional refrigeration capacity and power, and thereby improve the efficiency of the system. The partially evaporated stream is then separated into a vapor stream, which is sent back to the compression part, and a liquid stream that is sent to storage. When there is a need for power, liquid air is first pumped to a high pressure before it is sent to evaporators, where liquid air is heated to be regasified by working fluids in cold thermal energy recovery cycles. After delivering the cold regasification energy, air is sent to the expansion part, where air is expanded through a series of turbine stages to generate power. There is a preheater before each expander (Heater 1-M) to increase the power generation.

The hot thermal energy storage between the compression and expansion parts is used to collect the compression heat and release it to increase the inlet air temperature to the turbine stages. The working fluid for the hot energy recovery cycle is Therminol 66 with a wide operating temperature range from -3 to 350°C. This fluid is widely used in the hot storage cycle for LAES systems [63]. Two cold thermal energy recovery cycles are used to transfer the cold regasification energy of liquid air to the compressed air. In Chapter 5, different cold thermal energy recovery cycles are proposed and compared to identify the most suitable cold cycles for the LAES when the configurations of the compression and expansion parts are fixed. It was found that two multi-component fluid cycles gave the highest performance (RTE) among six studied cases. Since the focus here is on configurations of the compression and expansion parts rather than working fluids, a slightly simpler set of working fluids with a marginal decrease in RTE was used in order to reduce the computational efforts. The cold thermal energy recovery cycles are therefore using a single-component cycle with methanol and a multi-component fluid cycle, which consists of 70 mol% propane, 20 mol% ethane and 10 mol% n-butane. These working fluids are operated at different temperatures. For different LAES processes in this

work, the configuration and the components of cold thermal energy recovery cycles are the same, while the compression and expansion parts are changed by varying the number of compression and expansion stages.

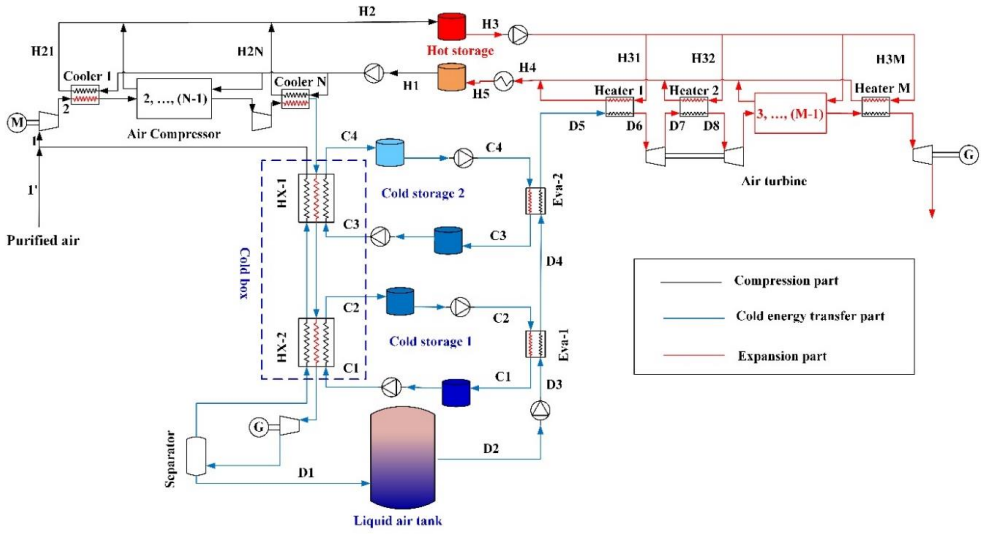

Figure 5.1 Process flowsheet of the liquid air energy storage (LAES) system.

The process flowsheet of the LAES system with N compression stages ($2 \leq N \leq 6$) and M expansion stages ($3 \leq M \leq 5$) is shown in Figure 5.1. When the number of compression stages N is greater than or equal to the number of expansion stages M, there will always be a part of the compression heat that cannot be utilized in the expansion part. This is due to the fact that the amount of compression heat and the temperature of the air are reduced when the number of compression stages is increased. As a result, the temperature of the thermal oil is reduced. Despite the fact that the compressor duty is decreased with increasing number of stages, the repeated cooling of air will increase the flowrate of thermal oil since it must be split into more branches. In order to improve the performance of the system, ORCs are considered to utilize the unused part of compression heat. For the additional ORC, R152a ($C_2H_4F_2$ with critical temperature 113.3°C and critical pressure 45.2 bar) is chosen as the working fluid. The reason for selecting R152a as the working fluid in the ORC is that it is environment-friendly and non-

toxic to humans, and it is also reported to be more efficient than several other working fluids, such as R134a, R143a, and R32 [126]. In addition, the critical temperature of R152a is within the temperature range of the compression heat in different LAES configurations. The critical pressure of R152a is relatively large and the saturation pressure at ambient temperature is only 3.7 bar, therefore, we can take advantage of the large pressure drop during expansion. Figure 3 illustrates the LAES system with an additional ORC, where the working fluid of the ORC is assumed to be cooled to 20°C by cooling water.

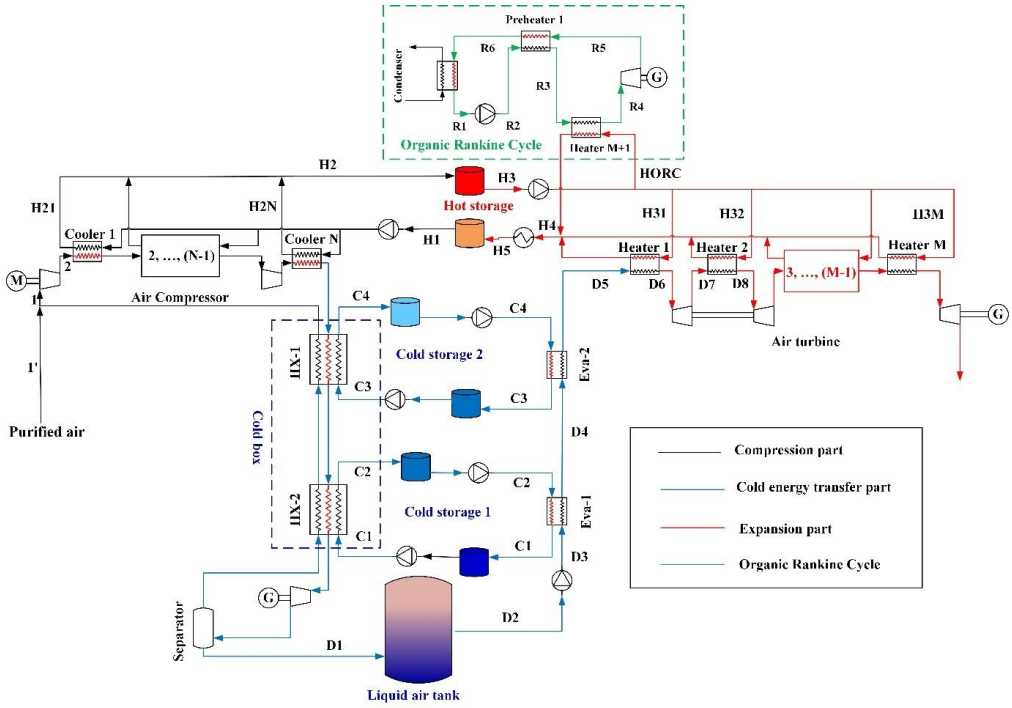

Figure 5.2 Process flowsheet of the LAES system with an additional ORC.

5.2 Process evaluation and optimization

This section introduces the key performance indicators (KPIs) that are used to evaluate the different process configurations, followed by a presentation of the optimization formulation for the LAES.

5.2.1 Process evaluation

As mentioned in Section 3.1, the most widely used parameter for energy storage technologies is the round-trip efficiency, which is commonly used for comparison with other technologies in the literature. The specific power consumption is a performance parameter to indicate the efficiency of liquefaction process in the LAES system. In addition, exergy efficiency (such as the Exergy Transfer Effectiveness - ETE) is also considered as a performance indicator for the LAES system. Since the system is decomposed into three parts: compression, hot and cold energy recovery, and expansion sections, exergy efficiencies of the three parts are evaluated to reveal the performance of each part. The exergy efficiency of the compression part $\eta_{\dot{E}_{\text{comp}}}$ is calculated by Equation (5.1).

$$\eta_{\dot{E}_{\text{comp}}} = \frac{\dot{E}_{\text{out,air,comp}} + \dot{E}_{\text{h}}}{\dot{W}_{\text{comp}} + \dot{E}_{\text{feed,air}}} \tag{5.1}$$

Here, $\dot{W}_{\text{comp}}$ denotes the work consumed by compressors, $\dot{E}_{\text{out,air,comp}}$ and $\dot{E}_{\text{feed,air}}$ represent the thermo-mechanical exergy of outlet air from the compression part and the air feed, and $\dot{E}_{\text{h}}$ is the thermo-mechanical exergy of hot oil. Similar to exergy efficiency for the compression section, exergy efficiencies of the cold energy recovery $\eta_{\dot{E}_{\text{rec}}}$ and expansion sections $\eta_{\dot{E}_{\text{exp,dir}}}$ or $\eta_{\dot{E}_{\text{exp,dir+ORC}}}$ are given by Equations (5.2) - (5.4). $\eta_{\dot{E}_{\text{exp,dir}}}$ represents the exergy efficiency of

the expansion part that only considers the multistage turbine, while $\eta_{\dot{E}\,\mathrm{exp,dir+ORC}}$ is the exergy efficiency of the expansion section when an additional ORC is part of the LAES system.

$$\eta_{\dot{E}\,\mathrm{rec}} = \frac{\dot{E}_{\mathrm{out,air,rec}} + \dot{W}_{\mathrm{cryotur,rec}}}{\dot{E}_{\mathrm{out,air,comp}} + \dot{W}_{\mathrm{pump}}} \tag{5.2}$$

$$\eta_{\dot{E}\,\mathrm{exp,dir}} = \frac{\dot{W}_{\mathrm{tur,exp}}}{\dot{E}_{\mathrm{out,air,rec}} + \dot{E}_{\mathrm{h}}} \tag{5.3}$$

$$\eta_{\dot{E}\,\mathrm{exp,dir+ORC}} = \frac{\dot{W}_{\mathrm{tur,exp}} + \dot{W}_{\mathrm{tur,ORC}}}{\dot{E}_{\mathrm{out,air,rec}} + \dot{E}_{\mathrm{h}} + \dot{W}_{\mathrm{pump,ORC}}} \tag{5.4}$$

Here, $\dot{E}_{\mathrm{out,air,rec}}$ represents the thermo-mechanical exergy of outlet air from the cold energy recovery part and $\dot{W}_{\mathrm{tur,exp}}$ is the work produced by the multistage turbine in the expansion part. $\dot{W}_{\mathrm{tur,ORC}}$ and $\dot{W}_{\mathrm{pump,ORC}}$ are the expansion work and pump work in the additional ORC.

5.2.2 Process optimization

The optimization of different LAES configurations in this work is conducted by using a Particle Swarm Optimization (PSO) algorithm. The PSO algorithm is implemented in Matlab and connected to Aspen HYSYS simulation models. The objective function and the constraints of the optimization formulation are provided in Equation (5.5).

$$\begin{aligned}
&\min_{x} \ -\eta_{\mathrm{RT}} = -f(\boldsymbol{x}) = -\frac{\dot{m}_{\mathrm{liq}} w_{\mathrm{tur}}}{\dot{m}_{\mathrm{comp}} w_{\mathrm{comp}}} \\
&\text{subject to } \Delta T_a \geq 10 \qquad \text{a}=\{\text{intercoolers 1, 2, ..., N, reheaters 1, 2, ..., M}\} \\
&\qquad \Delta T_b \geq 1 \qquad \text{b}=\{\text{HX-1, 2, Eva-1, 2}\} \\
&\qquad VF_{\mathrm{ORC,pump,in}} = 0 \\
&\qquad VF_{\mathrm{ORC,tur,in}} = 1 \\
&\qquad \boldsymbol{x}_{\mathrm{LB}} \leq \boldsymbol{x} \leq \boldsymbol{x}_{\mathrm{UB}}
\end{aligned} \tag{5.5}$$

Here, ΔT_{a} is the minimum temperature difference (MTD) of aftercoolers and preheaters, while ΔT_{b} is the minimum temperature difference (MTD) for heat exchangers and evaporators. $VF_{\mathrm{ORC,pump,in}}$ and $VF_{\mathrm{ORC,tur,in}}$ denote the vapor fraction of inlet streams of the pump and the turbine in the ORC. $\boldsymbol{x}$ represents decision variables in the LAES system, while $\boldsymbol{x}_{\mathrm{LB}}$ and $\boldsymbol{x}_{\mathrm{UB}}$ are the lower and upper bounds of the variables.

The purpose of optimizing the system is to identify the most promising option among different LAES configurations. The decision variables in this work include the pressure ratios of compressors and expanders, the outlet temperature of thermal oil from coolers, the outlet temperature of air and the recycled air stream from the cold box, and the molar flowrates and temperatures of the working fluids in the cold thermal energy recovery cycle. In the system with an additional ORC, the evaporation temperature and pressure and the molar flowrate of the working fluid are also selected as variables. The degrees of freedom for design are different in different cases, since the number of compression and expansion stages are varying in the LAES.

MTDs for heat exchangers are economic parameters trading off investment cost and operating cost. Transferring heat with large temperature differences increases irreversibilities in the plant, and these exergy losses are paid for by increased compressor work. In sub-ambient processes, these exergy losses depend on both the temperature difference and the absolute temperature level, making it more important to reduce temperature driving forces at lower temperatures. As a result, MTDs of aftercoolers and preheaters that are operating above ambient temperature are assumed to be 10°C, while MTDs for HX-1,2 and Eva-1,2 that are operating significantly

below ambient temperature are assumed to be 1°C [122]. This is a simplification, but the focus of this work is not cost minimization, emphasis is on energy efficiency. It is shown in the literature that below ambient, UA_{max} is a better design specification than MTD, where UA is the lumped parameter of heat transfer coefficient and heat transfer area, also referred to as the heat exchanger conductance [127-129]. In the LAES system with an additional ORC to utilize the unused compression heat, the inlet stream to the pump should be totally liquid and the inlet stream to the turbine should be totally vapor. Thus, the vapor fraction of the inlet stream to the pump and the turbine in the ORC should be 0 and 1, respectively. In reality, the outlet temperature of compressors should be considered as constraints during optimization. However, constraints related to the pressure ratio and outlet temperature of compressors and expanders are not considered in this thermodynamic analysis of the LAES system. The decision variables and their lower and upper bounds are listed in Table 5.1.

It is worth noting that the pressure ratios of compressors would be relatively high when the number of compression (or expansion) stages is small in the LAES. In the ADELE and ADELE-ING projects [130, 131], the combination of an axial LP compressor and a radial HP compressor has been suggested to elevate the pressure of air from 1 bar to 100 bar with an outlet temperature of 600°C. Axial and radial compressors have been used in some aerospace applications with a pressure ratio of up to 40 and in some industrial applications with a pressure ratio of up to 30 [132]. The upper bound for the pressure ratio of compressors is arbitrarily set to 20 in this work, which is achievable according to the literature review.

Table 5.1 Decision variables with lower and upper bounds.

Variables	Lower Bounds	Upper Bounds
Pressure ratio for compressors [a, b]	1	20
Pressure ratio for expanders [a, b]	1	10
Thermal oil temperature ($T_{H21\text{-}H2N}$) (°C) [a, b]	100	230
Cold box outlet air temperature (°C) [a, b]	-185	-165
Cold box outlet recycled air temperature (°C) [a, b]	-10	29
Working fluid operating temperature (higher) (°C) [a, b]	-90	-20
Working fluid molar flowrate (kmol/h) [a, b]	0	200
Working fluid operating temperature (lower) (°C) [a, b]	-186	-166
Working fluid molar flowrate in ORC (kmol/h) [b]	0.01	800
Working fluid evaporation pressure in ORC (bar) [b]	1.1	41
Working fluid evaporation temperature in ORC (°C) [b]	10	113.6

[a] variable bounds for the LAES when the number of compression stages is less than the number of expansion stages (N<M)

[b] variable bounds for the LAES with additional ORC when the number of compression stages is greater than or equal to the number of expansion stages (N≥M)

5.3 Results and discussion

In this work, the LAES system with different number of compression and expansion stages is optimized and compared. It is worth noting that an additional ORC is utilized only when the number of compression stages is greater than or equal to the number of expansion stages.

5.3.1 Performance of different LAES configurations

Figure 5.3 shows the round-trip efficiency of the LAES system with different number of compression and expansion stages. It can be seen that when there is a 3-stage turbine in the expansion part, the RTE of the system reduces with increasing number of stages in the

compression part. The trend for an LAES system with a 4-stage turbine is different. The RTE first increases when the number of compression stages is changed from 2 to 3, and then, the RTE decreases when the number of compression stages continues to increase from 3 to 6. For the system with 5 stages expansion, the RTE that has a maximum at 4 compression stages is increased with changing number of compression stages from 2 to 4, and then it is reduced with further increasing number of compression stages from 4 to 6. Optimization results show that there exists an optimal match between the number of compression stages and expansion stages. When the number of expansion stages is 3, 4 and 5, the highest RTE is obtained with 2, 3, and 4 compression stages in the LAES system, respectively. This is due to the fact that the hot storage cycle connects the compression and expansion parts in a standalone LAES system. With varying numbers of compression stages, the temperature and flowrate of thermal oil change, which influences not only the temperature of the air entering expanders but also the location of pinch points in preheaters before each stage of the expander. The overall best performance for the LAES system is with a 2-stage compression and a 3-stage expansion, and the highest RTE is found to be 66.7%. The temperature-entropy diagram for the energy storage and release mode of the three best matches between compression and expansion stages is provided in Figure 5.4.

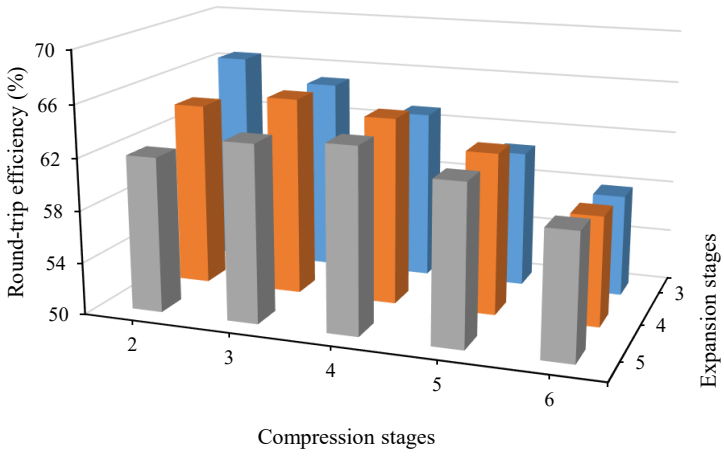

Figure 5.3 Round-trip efficiency of the LAES for different configurations.

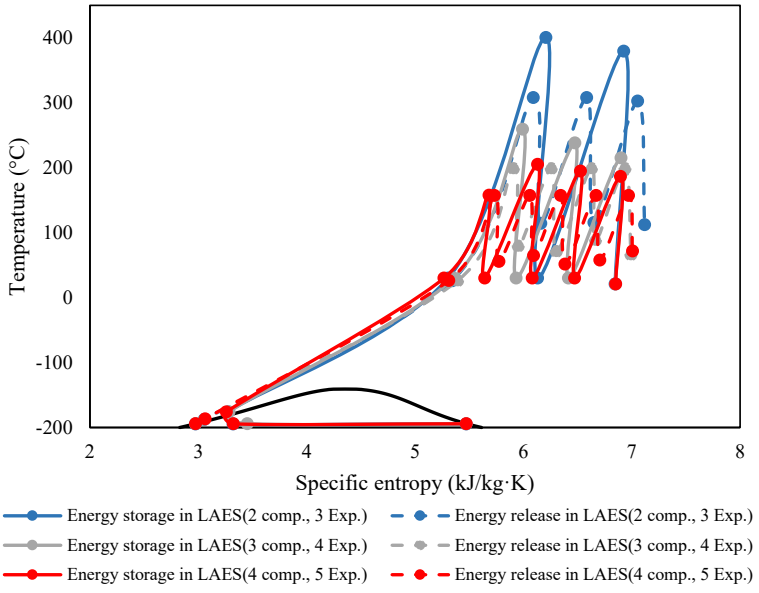

Figure 5.4 Energy storage and release mode in a T-S diagram for the three best matches between compression and expansion stages.

The properties of the thermal oil transferring heat of compression to the expansion section depend only on the configuration of the compression section. With increasing number of compressor stages, both the total compressor duty (and thereby the compression heat, see Table 5.2) and the outlet temperature of air from the compressor stages are reduced. This obviously also reduces the outlet temperature of thermal oil from the aftercoolers, as shown in Figure 5.5. As mentioned in Section 5.1, even though the compressor duty is decreased with increasing number of stages, the repeated cooling of air increases the flowrate of thermal oil since it must be split into more branches. The effect of repeated cooling of air is more important than the reduced compressor duty. As a result, the flowrate of thermal oil increases with the number of compression stages, and this is also shown in Figure 5.5.

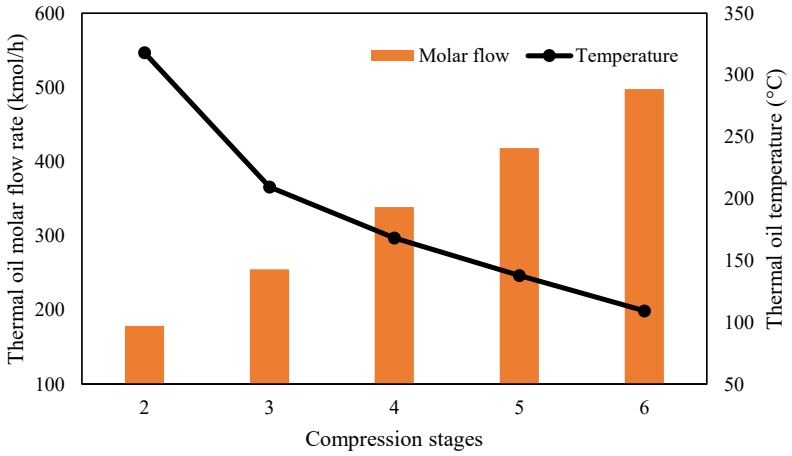

Figure 5.5 Molar flow rate and temperature of thermal oil for configurations with 3 expansion stages and 2-6 compression stages.

Table 5.2 The compression heat recovered by the thermal oil for configurations with 3 expansion stages and 2-6 compression stages.

Compression stages		2	3	4	5	6
Recovered heat duty	GJ/h	56.88	47.78	48.11	46.49	41.37

Focusing on the expansion section, the fact that the flowrate and temperature of thermal oil have opposite trends with respect to the number of compression stages also means that they have opposite effects on the preheating of air in the expansion section, and therefore also on the power generation and round-trip efficiency. Thus, there is a trade-off between mass flowrate and temperature of thermal oil, which is why there exists an optimal match between the number of compression stages and the number of expansion stages. This optimal match has already been presented based on the results in Figure 5.3. For 3, 4 and 5 expansion stages, the optimal number of compression stages is 2, 3 and 4, respectively. The best combination with 2 compression stages and 3 expansion stages has the highest RTE of 66.7%.

The easiest way to explain the trends in Figure 5.3 is to consider a case with a fixed number of expansion stages, such as 5. Then the thermal oil must be split into 5 branches and sent to the air preheaters. With few compression stages, such as 2 or 3, the temperature of thermal oil is relatively high, but the flowrate of thermal oil is too low, causing a pinch in the cold end of the preheaters. This means that the expansion part is not able to take advantage of the high thermal oil temperature, although the situation is somewhat improved from 2 to 3 compression stages. With 4 compression stages, the composite curves in the preheaters are almost parallel, and the RTE reaches its maximum value for the case with 5 expansion stages. Increasing the number of compression stages further to 5 or 6 will result in a too high flowrate of thermal oil, and the pinch will move to the hot end of the preheaters. Air can now be preheated to a temperature that is ΔT_{min} below the thermal oil temperature, however, this temperature is reduced due to the relatively large number of compression stages, and the large flowrate of thermal oil also means that the compression heat cannot be fully utilized.

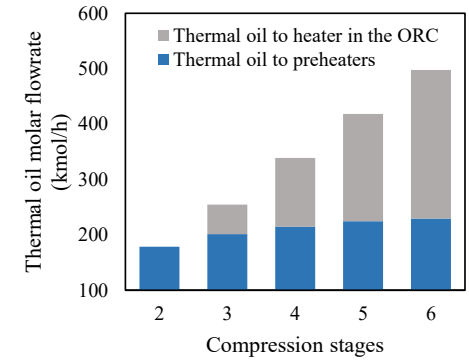

(a)

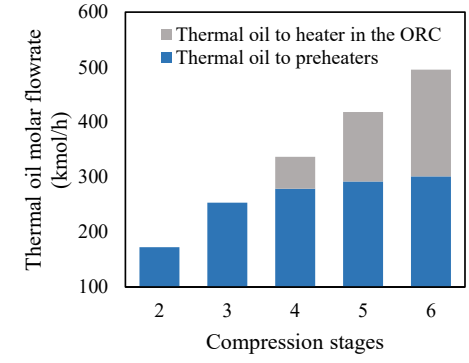

(b)

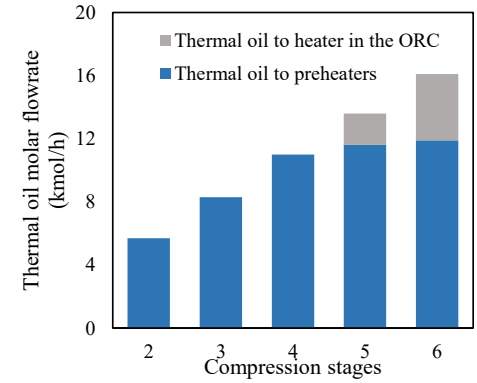

(c)

Figure 5.6 Optimized distribution of thermal oil between the expansion preheaters and the heater in the ORC in different configurations of the LAES: (a) 3-stage turbine; (b) 4-stage turbine; (c) 5-stage turbine.

Figure 5.6 shows the scope for using ORC to produce power from compression heat that is not fully utilized in the expansion section. As already explained, such surplus heat will be available when the number of compression stages is equal to or larger than the number of expansion stages. The split of thermal oil between the preheaters and the additional ORC is shown as a function of number of compression stages for 3 expansion stages (Figure 5.6(a)), 4 expansion stages (Figure 5.6(b)) and 5 expansion stages (Figure 5.6(c)). Unfortunately, the power from the ORC is not enough to compensate for the reduction in power production in the expansion section in these cases, partly caused by reduced thermal oil temperature. As a result, for the entire system (charging and discharging), the RTE will be reduced when the number of compression stages is increased beyond the optimal number for the given number of expanders (the 2-3, the 3-4, and the 4-5 matches). This explains the trends in Figure 5.3.

The logarithmic mean temperature differences (LMTDs) of preheaters in different LAES configurations are listed in Table 5.3. When the LAES system has 3 stages of expansion, a relatively good match between the temperature profiles of thermal oil and air is obtained with 2 stages of compression. The flowrate of thermal oil is slightly less than required to have parallel profiles, and the pinch is in the cold end of the preheaters. As a result, the LMTD is 10.8°C in this case. It is observed that the LMTDs for the cases with surplus thermal oil are 10.3°C. Since $\Delta T_{\min}$ equals 10°C, an LMTD of 10.3°C indicates a case with close to parallel composite curves in preheaters. For the same reason, when the LAES has 4 or 5 stages of expansion, systems with 3 or 4 stages of compression have better performance compared to other combinations. The composite curves for the cases mentioned above are shown in Figure 5.7. In Figure 5.7(a)-(c), the composite curves are close to parallel as indicated by the listed LMTD values, and they have higher RTE values than other cases having the same number of expansion stages. Figure 5.7(d), in contrast, illustrates an example of composite curves for preheaters when the system has insufficient amounts of thermal oil in the expansion part. In this particular case, the LAES system has a 2-stage compressor and a 4-stage turbine, and the LMTD of the preheaters is 29.1°C. As a result, the relatively large temperature difference between hot and cold streams lead to a poor performance and a lower RTE of the system.

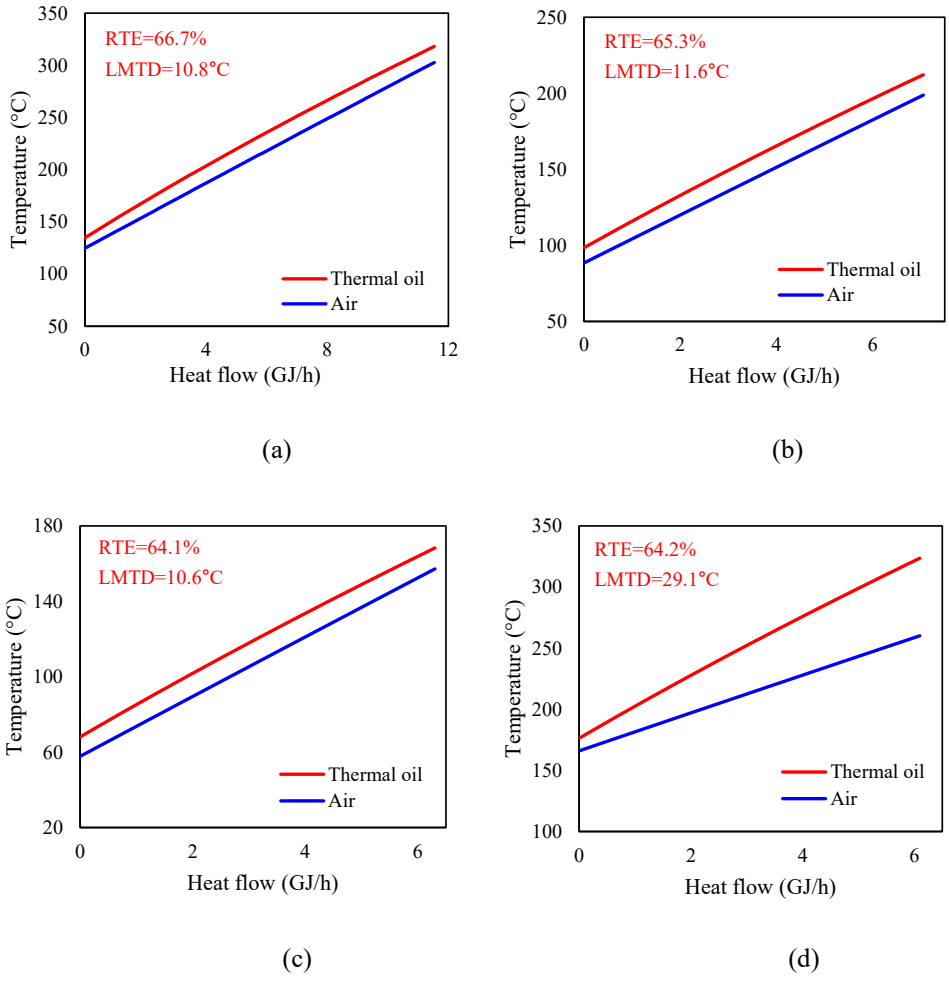

Figure 5.7 Composite curves of preheaters in the LAES system: (a) 2-stage compressor and a 3-stage turbine; (b) 3-stage compressor and a 4-stage turbine; (c) 4-stage compressor and a 5-stage turbine; (d) 2-stage compressor and a 4-stage turbine.

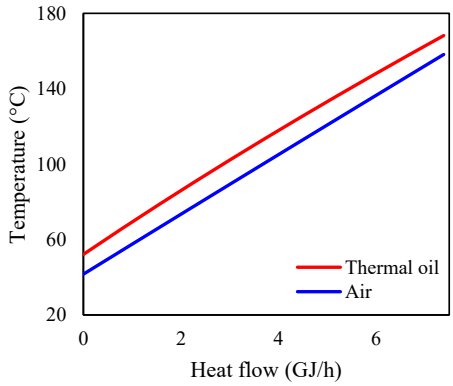

Figure 5.8 Composite curves of preheaters in the LAES system with a 4-stage compressor and a 4-stage turbine.

In addition, when the number of compression stages is greater than or equal to the number of expansion stages, composite curves of preheaters in LAES systems with an additional ORC are similar to and slightly better than Figure 5.7(a)-(c). The reason is that one part of the thermal oil flowrate is sent to the ORC, while the remaining part has a cooling curve that is parallel with the air preheating curve. The composite curves of the LAES system with a 4-stage compressor and a 4-stage turbine are used as an example and shown in Figure 5.8. However, even if there is a good match between the thermal oil and air temperature profiles, the RTE is reduced when the number of compression stages is increased from 3 to 4 and the number of expansion stages is 4. This means that despite the power production in the ORC, there is a larger reduction in the power production in the expansion part compared to the case with 3 compression stages. The thermal oil temperature is reduced when increasing the number of compression stages from 3 to 4, and the RTE is reduced.

Table 5.3 Optimal values for some variables and key performance indicators in different LAES configurations.

Exp. stages	Comp. stages	pr_{comp}	pr_{exp}	$LMTD_{pre}$ (°C)	$LMTD_{heater,ORC}$ (°C)	η_{LY} (%)	SPC (kWh/t)	$\dot{W}_{ch}$ (MW)	$\dot{W}_{dc}$ (MW)	η_{RT} (%)
3	2	13.11	5.29	10.78	-	86.21	243.95	15.01	10.00	66.65
	3	5.24	4.98	10.27	32.85	86.19	204.79	12.60	8.19	64.99
	4	3.70	5.43	10.27	20.46	86.62	203.41	12.51	7.90	63.12
	5	2.86	5.45	10.27	18.11	86.64	195.93	12.05	7.30	60.60
	6	2.25	4.82	10.27	20.17	85.98	176.83	10.88	6.30	57.88
4	2	12.86	3.45	29.11	-	86.34	241.59	14.86	9.55	64.23
	3	5.31	3.37	11.62	-	86.26	207.08	12.74	8.32	65.32
	4	3.70	3.56	10.27	21.50	86.57	203.05	12.49	8.05	64.41
	5	2.86	3.57	10.27	18.24	86.65	195.96	12.06	7.52	62.40
	6	2.23	3.21	10.27	19.26	85.93	175.39	10.79	6.30	58.42
5	2	14.19	2.79	39.95	-	86.68	252.99	15.56	9.64	61.93
	3	5.34	2.65	21.42	-	86.29	207.85	12.79	8.13	63.61
	4	3.72	2.77	10.59	-	86.65	204.07	12.55	8.05	64.10
	5	2.89	2.79	10.27	18.26	86.65	197.88	12.17	7.57	62.22
	6	2.22	2.54	10.27	19.56	85.91	174.70	10.75	6.40	59.53

Optimal results for compression and expansion pressure ratios and key performance indicators (liquid yield, specific power consumption, exergy efficiency and round-trip efficiency) for different LAES configurations are listed in Table 5.3. It can be seen that optimal pressure ratios, the power consumption of compressors and SPCs are reduced with increasing number of compression stages for a given number of expansion stages in the LAES. This is because a near isothermal operation of compression requires near minimum power consumption. Moreover, the power production of the discharging part has the same trend as the power consumption of the charging part. This is because a higher expansion pressure results in more work produced, but the expansion pressure is constrained to be less than the compression pressure due to the

cold thermal energy recovery cycles. The cold regasification energy from liquid air is needed to liquefy compressed air in the LAES system. In order to have driving forces for cold regasification energy transfer, the liquid air must be at a lower temperature than the compressed air. After the cold box, the optimal phase separation temperature is around - 176°C for all cases, since the amount and temperature of cold thermal energy in the cold energy recovery part are insufficient. With almost constant temperature at the outlet of the cold box, compression pressure is the only factor that affects the liquid yield of air. A higher charging pressure increases the pressure drop in the cryo-turbine, with atmospheric pressure at the outlet. This results in a lower outlet temperature and reduced fraction of air in vapor phase, which improves liquid yield of air. For the entire system, the use of the hot thermal recovery cycle has decisive effects on the performance (the inlet temperature of air to expanders and the location of pinch points in preheaters), and the highest energy recovery ratio of the LAES (RTE) is obtained when the composite curves of hot and cold streams in preheaters are close to parallel.

The detailed optimization results for an additional ORC in different LAES configurations are listed in Table 5.4. The heat source is stream HORC (thermal oil, see Figure 5.2) in the LAES system. The condensation pressure of the ORC is 5.30 bar for all the cases, which is the saturation pressure of the working fluid at ambient temperature. When the number of compression stages is less than 6 in the LAES system, the evaporation pressure of the ORC reaches the upper bound, which is set to 41 bar, i.e. 90% of the critical pressure of the working fluid, resulting in the largest power output. When the number of compression stages is 6, the heat source temperature (thermal oil) is less than the saturation temperature of the ORC working fluid at critical pressure. Thus, the pressure and temperature of the working fluid in the ORC are less than for the other cases that have 2-5 compression stages. It is shown that the largest net work output of 605.01 kW is obtained when there is a 4-stage compressor and a 3-stage turbine in the LAES system. It is worth noting that the net power output in the ORC is affected by the physical properties of the working fluid (critical pressure and temperature). Thus, the performance of the ORC may be different for other working fluids.

Table 5.4 Performance of the additional ORC for utilizing wasted compression heat.

Expansion stages	Compression stages	$\dot{W}_{net}$ (kW)	$p_{orc,con}$ (bar)	$p_{orc,eva}$ (bar)	$T_{orc,eva}$ (°C)	$\dot{W}_{orc,tur}$ (kW)	$\dot{W}_{orc,pump}$ (kW)
3	2	-	-	-	-	-	-
	3	363.86	5.30	41.00	112.50	394.96	31.10
	4	605.01	5.30	41.00	112.00	657.02	52.01
	5	576.67	5.30	41.00	110.32	627.33	50.66
	6	361.94	5.30	18.64	69.17	379.90	17.96
4	2	-	-	-	-	-	-
	3	-	-	-	-	-	-
	4	281.80	5.30	41.00	113.03	305.74	23.94
	5	374.21	5.30	41.00	110.44	407.03	32.82
	6	216.20	5.30	21.22	92.48	226.80	10.60
5	2	-	-	-	-	-	-
	3	-	-	-	-	-	-
	4	-	-	-	-	-	-
	5	185.89	5.30	41.00	110.37	202.21	16.32
	6	141.81	5.30	20.82	89.56	148.75	6.94

5.3.2 Exergy analysis of different LAES configurations

Exergy efficiencies of the compression, cold thermal energy recovery and expansion parts in the LAES system with different number of compression and expansion stages are shown in Figure 5.10. From Figure 5.10(a), it can be seen that the exergy efficiency of the compression part is reduced with increasing number of compression stages. This is mainly caused by the

increased exergy losses related to irreversibilities in the aftercoolers. The same trend is observed in Figure 5.10(b) and 11(c). It is worth noting that the exergy efficiencies of the cold thermal energy recovery part are almost the same in the various cases. The number of compression and expansion stages has only marginal effects on the cold thermal energy recovery part. The somewhat obvious reason is that the configuration of this part is the same in all cases. The exergy efficiencies of the expansion part, however, show significant differences. These exergy efficiencies are affected by both the heat transfer efficiency in preheaters and the performance of the ORC.

For the direct expansion part, which means the multistage turbine part, it is observed that when the number of expansion stages is 3, the highest exergy efficiency is obtained with a 2-stage compressor in the system. For the system with a 4-stage or 5-stage turbine, the best performance is obtained when there is a 3-stage or 4-stage compressor. This is in line with the previous discussion and conclusion based on composite curves in the preheaters.

As already established in Section 5.3.1, the best performance measured by the RTE is obtained when the flowrate of thermal oil is large enough to have close to parallel temperature profiles in the preheaters of the expansion part of the LAES. If the flowrate of thermal oil is too small, the pinch in the preheaters is in the cold end, and air preheat cannot take advantage of the thermal oil inlet temperature. If the flowrate of thermal oil is too large, the pinch in the preheaters is in the hot end, which is an advantage for air preheat, but then there is a part of the compression heat transferred by the thermal oil that is not utilized. In such cases, one could envisage that the surplus flowrate of thermal oil could be sent to an ORC to produce additional power while making the composite curves parallel.

The following conclusions can be made based on the results in Table 5.3 and Figure 5.9(a)-(c) and explained by exergy analysis, as well as the observations in Section 5.3.1:

- Increased flowrate of thermal oil is a result of increased number of compression stages, and despite a reduction in compression work, irreversibilities in the aftercoolers are increased. Repeated cooling of air increases with more compression stages, thereby

increasing irreversibilities due to heat transfer with temperature differences larger than zero.

- When the flowrate of thermal oil is larger than required in the expansion section, the use of ORC both makes the temperature profiles in the preheaters parallel (and thereby reduce irreversibilities) and produces additional power by utilizing otherwise wasted compression heat.
- Since the work produced by the ORC is quite small, it cannot compensate for the additional irreversibilities in the compression part by having more stages.

Considering first the cases without ORC, the maximum exergy efficiency of the expansion part coincides with the maximum RTE (i.e., 2 compression stages for 3 expansion stages, 3 compression stages for 4 expansion stages, and 4 compression stages for 5 expansion stages). However, while the RTE is reduced for these cases with increased number of expansion stages (from 66.7% via 65.4% to 64.2%), the expansion section exergy efficiency is increased with increased number of expansion stages (from 84.3% via 85.0% to 85.4%). Contributing to the overall system, exergy efficiency of the compression part is reduced with increasing number of compression stages (from 89.4% via 88.5% to 87.5%). The larger reduction in exergy efficiency of the charging part compared to the discharging part explains why there is a reduction in RTE for the overall system.

As explained before, use of an additional ORC only makes sense when the number of compression stages is greater than or equal to the number of expansion stages. As can be seen in Figure 5.9, the maximum exergy efficiency of the expansion section for LAES systems with an additional ORC is obtained when the number of compression stages is equal to the number of expansion stages. However, Figure 5.9 also indicates that the exergy efficiency with ORC is only marginally better than for the optimal case without ORC. For 3 expansion stages, the exergy efficiency is improved from 84.3% to 84.8%. For 4 expansion stages, a similar improvement from 85.0% to 85.7% is observed. Finally, for 5 expansion stages, the exergy efficiency with the use of an ORC is actually reduced from 85.4% to 84.5%. In summary then,

the power produced by the additional ORC does not justify the investment cost and added complexity.

As for a standalone LAES system without external heat sources, the exergy efficiency of the overall system would be very similar to the definition of the round-trip efficiency, which is why it has not been calculated in this work. The major terms in the exergy efficiency for the overall system are the work produced in the discharging and the work consumed in the charging. The minor terms are the thermo-mechanical exergy of the inlet air (which is constant) and the outlet air, and both terms are negligible. On the other hand, the individual exergy efficiencies of the charging and discharging parts can help explain the change in RTE. However, the economic feasibility of the system should be analyzed for a comprehensive evaluation of the LAES system before any project is implemented, and this is beyond the scope of this work.

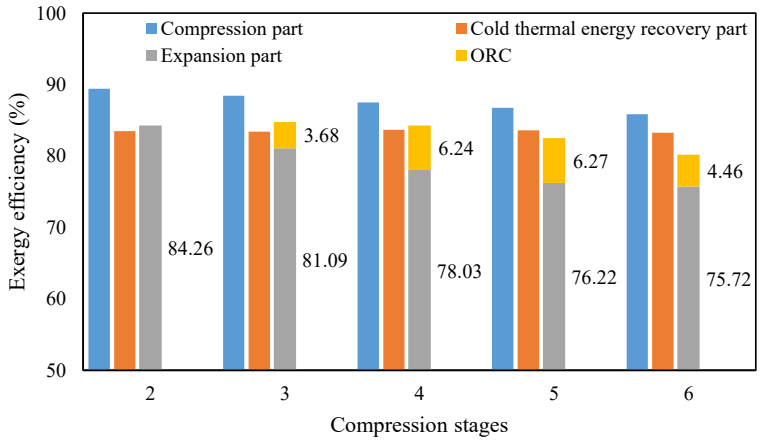

(a)

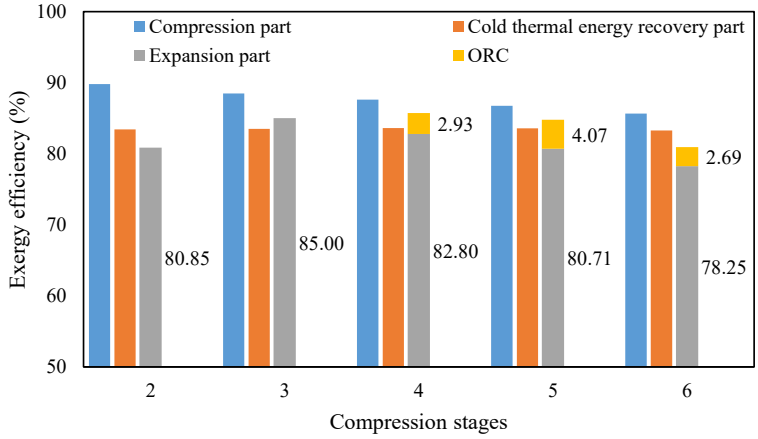

(b)

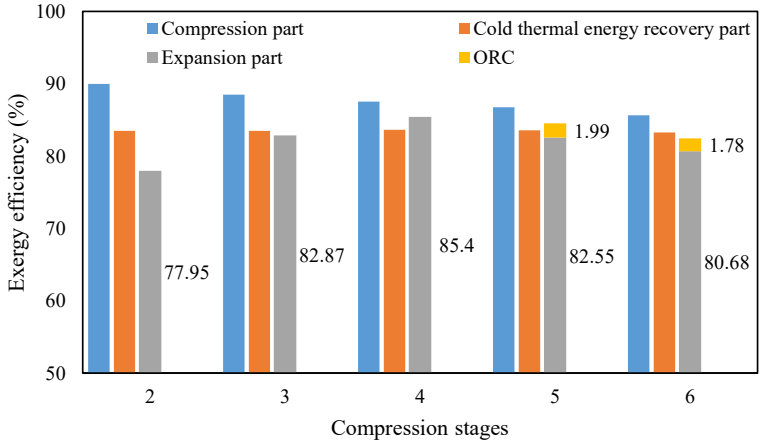

(c)

Figure 5.9 Exergy efficiencies of the compression, cold energy transfer and expansion parts in different LAES configurations: (a) 3-stage turbine; (b) 4-stage turbine; (c) 5-stage turbine.

5.3.3 Effects of additional ORCs

In addition to the ORC for the unutilized part of compression heat, an ORC can also be used to collect the heat carried by the exhaust air from the last stage expander for further improvement of the LAES. In this study, we used the same working fluid (R152a, as discussed in Section 5.1) as for the ORCs for unutilized compression heat. As mentioned in Section 5.3.1, the LAES system with a 2-stage compressor and a 3-stage expander has the best performance, and this process configuration is selected as the design basis. The process flow diagram of this configuration is shown in Figure 5.10. In this process, the temperature of exhaust air (stream D11) is 103.6°C. Optimization results indicate that only 78.2 kW power is produced by the ORC, and this added power does not justify the investment in an ORC. The RTE of the LAES system can only be improved from 66.7% to 67.2% with this additional ORC. The improvement by producing power from the heat of exhaust air is marginal compared to the system where wasted compression heat is utilized by ORCs.

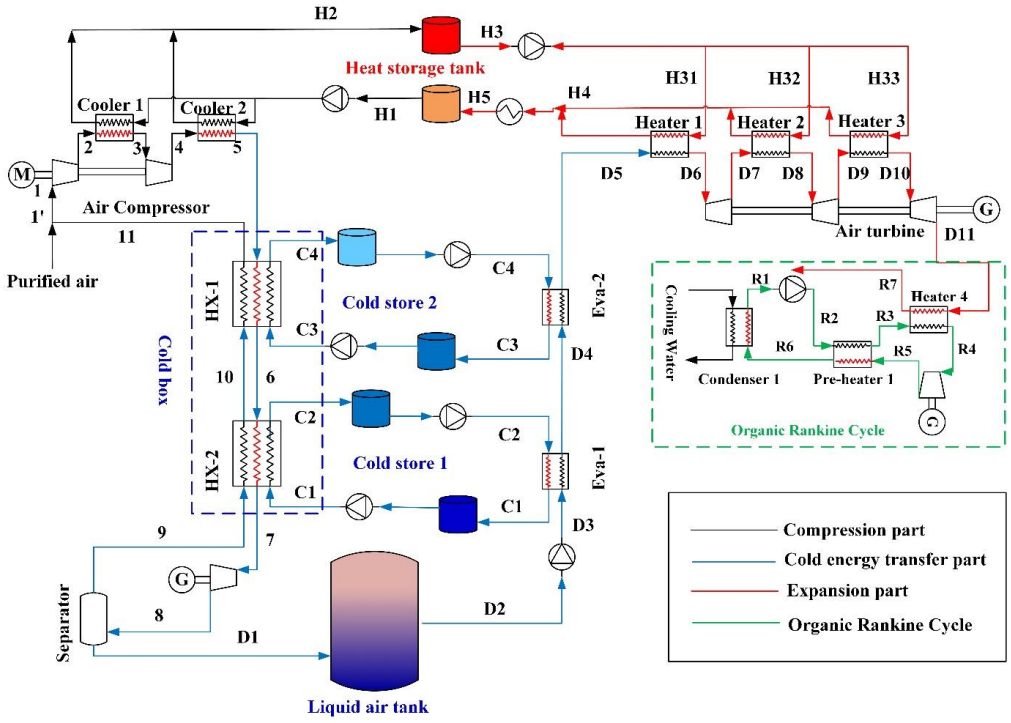

Figure 5.10 Flow diagram of the liquid air energy storage with an additional ORC for exhaust air.

5.4 Conclusions

The scope of this work has been to investigate opportunities for improving the energy performance of Liquid Air Energy Storage (LAES) systems. While previous work in our group considered improving the cold thermal energy recovery cycles, this work has focused on the different configurations of the compression and expansion sections, meaning the number of compressor and expander stages as well as the hot thermal energy recovery cycle.

The main assumptions in this work are:

- Constant isentropic efficiencies for varying compressor and expander duties and number of stages.
- Fixed ΔT_{min} for heat exchangers, however, adjusted values for above (10°C) and below (1°C) ambient temperature.
- Fixed set and composition of the two cold thermal energy recovery cycles.
- R152a has been selected as the working fluid for all cases involving ORC.
- Pressure ratios have been allowed to vary between 1 and 20.
- No heat losses to the surroundings or pressure drops in piping and equipment.

One important observation from this work is that when the number of compression stages is greater than or equal to the number of expansion stages, the expansion section is not able to fully utilize the compression heat that is carried by the thermal oil in the hot energy recovery cycle. This can easily be explained by relative slopes of the temperature profiles in the air preheaters. An Organic Rankine Cycle (ORC) has been used to turn this unused compression heat into power. The LAES configuration with the best performance has been identified by a systematic optimization-based comparison of the various cases. The following conclusions are obtained in this study:

- There exists an optimal match between the number of compression stages and expansion stages in a standalone LAES system. When the number of expansion stages is 3, 4 and 5, the highest RTE is obtained with 2, 3, and 4 compression stages, respectively. Among these, the LAES system with a 2-stage compression and a 3-stage expansion has the highest RTE of 66.7%, which compares nicely with the original work of Guizzi et al. in 2015 (54.4%).
- ORCs are used to recover compression heat that is not fully utilized for preheating air in the expansion section. The largest net work output obtained for the case with 4-stage compression and 4-stage expansion is 605.01 kW, unfortunately this work is less than the reduced expansion work when increasing the number of compression stages from 3 to 4, i.e. the optimal match for the case with 4-stage expansion. This shows that ORCs can never improve the energy efficiency of standalone LAES systems.

- For cases with optimal matches between the number of compression stages and expansion stages, the exergy efficiency of the compression part is reduced with increasing number of compression stages (from 89.4% via 88.5% to 87.5%), while the expansion section exergy efficiency is increased (from 84.3% via 85.0% to 85.4%). The larger reduction in exergy efficiency of the charging part compared to the discharging part explains the reduction in RTE (from 66.7% via 65.37% to 64.17%). This clearly indicates that exergy efficiency is a valuable and comprehensive performance indicator for LAES systems.

The best configuration of the LAES is the system with 2-stage compression and 3-stage expansion (66.7%). Such high RTE makes the LAES more competitive among various energy storage technologies in terms of energy efficiency. However, the pressure ratios of compressors in the best configuration of the LAES are relatively high, and the cost for unconventional compressors with high pressure ratios is obviously higher than the conventional ones. Thus, there are several challenges that can be considered in future work:

- A cost analysis can be conducted and used to indicate the profitability and feasibility of the LAES system with high pressure ratio compressors.
- More case studies are needed to analyze the LAES with additional thermodynamic cycles.
- Going beyond the standalone LAES system, integration with external hot and cold thermal energy sources can significantly boost the RTE of the system.

The next chapter will discuss different approaches to utilize the unused compression heat in the LAES.

Chapter 6 Improved Heat Recovery in Liquid Air Energy Storage

Abstract

In Chapter 5, it was found that part of the compression heat is not efficiently utilized in some layouts for the Liquid Air Energy Storage (LAES) and this limits the round-trip efficiency (RTE) of the system. In this chapter, Organic Rankine Cycle (ORC), Absorption Refrigeration Cycle (ARC) and High Temperature Heat Pump (HTHP) are considered to utilize the surplus compression heat in the LAES system. The ORC and the ARC are adopted in the LAES system with a 4-stage compressor and a 4-stage expander, while the HTHP is used to utilize the medium grade compression heat in an LAES system with a 6-stage compressor and a 3-stage expander. The reason is the limited number of working fluids available for high temperature heat pump systems. Results indicate that the ORC, the ARC and the HTHP can effectively improve the performance of the LAES system with the available surplus compression heat.

This chapter is based on the publication:

- Liu Z, He T, Kim D, Gundersen T. Optimal utilization of compression heat in liquid air energy storage. Applied Energy (under review, 2022).

As mentioned in Chapter 5, the number of compressors and expanders in the charging and discharging parts has a significant influence on the performance of the LAES. The temperature and amount of compression heat are varying with different number of compression stages in the charging part. For example, 54% of compression heat at 109.3°C is not utilized in the preheaters in the expansion section of an LAES system with a 6-stage compressor and a 3-stage expander. The corresponding numbers for an LAES system with a 4-stage compressor and a 4-stage expander are 17% of compression heat at 168.2°C not being utilized in the discharging part. Based on the reviewed papers [60-66], it is known that Organic Rankine Cycles (ORCs) are widely studied to utilize the unused part of compression heat to produce power. This has proven to be an efficient method for system improvement. Furthermore, an absorption refrigeration cycle (ARC) provides another alternative for the utilization of excess compression heat.

However, most of the studies related to the ORC-based utilization of compression heat focus on the improvement of RTE for an LAES with a specific configuration. For an LAES system with a 4-stage compressor and a 4-stage expander, there is a lack of research on comparing and selecting different working fluids for the ORC. In addition, the ARC-based utilization of compression heat in the mentioned papers is aimed to produce a cold stream [60, 63-65]. The cold stream is either regarded as the heat sink of an ORC or provided as a cold energy product. It is known that the cold energy from the discharging part is not enough to liquefy air, so electricity is required to compress air in the charging part. In the available literature, no research on the utilization of the cold duty produced by an ARC in the cold box for air liquefaction have been conducted. In addition to ORC and ARC, high temperature heat pumps (HTHPs) are also promising technologies to utilize waste heat and thereby increase system efficiency [133-141]. HTHPs can efficiently raise the process stream temperature and provide another possibility for the utilization of compression heat in the LAES. The temperature of compression heat can be upgraded in the HTHP, and the upgraded compression heat is used to preheat air to increase the power output in the discharging part. To be profitable, the additional power output must be greater than the power input to the heat pump. In addition, the investment cost for the heat pump must be considered.

In this chapter, three technologies for the utilization of compression heat (ORC, ARC and HTHP) are applied to different LAES configurations. For the LAES system with a 4-stage compressor and a 4-stage expander, the temperature of compression heat is around 170ºC. An ORC and an ARC are considered to utilize this high temperature heat source. The ORC is used for converting excess compression heat to power, while the ARC is aimed at providing cold duty to the cold box in the charging part. An HTHP is adopted in an LAES configuration with medium grade compression heat (around 110ºC), such as the system with a 6-stage compressor and a 3-stage expander. The reason is that very few working fluids are available for high temperature heat pump cycles. Furthermore, different working fluids for the ORC and the HTHP are selected and compared to identify the best working fluids for these technologies.

6.1 System description

The LAES system with a 4-stage compressor and a 4-stage expander has a high-grade compression heat (Case I), while the system with a 6-stage compressor and a 3-stage expander has a medium grade compression heat (Case II). These configurations have been thoroughly studied in Chapter 5, and they are regarded as reference cases with available surplus compression heat. Thus, an ORC and an ARC are introduced to utilize the surplus high-grade compression heat in Case I, while an HTHP is selected to utilize the surplus medium grade compression heat in Case II.

6.1.1 LAES system with an ORC for utilization of surplus high-grade compression heat

The process flow diagram of the LAES system with an ORC is shown in Figure 6.1. Surplus compression heat (stream H4) is used as heat source for the ORC. The working fluid in the ORC is first pumped to high pressure, and then it is preheated and evaporated by recovering surplus compression heat. After the working fluid is fully regasified, it is expanded to generate power. The exhaust stream from the expander provides heat to a preheater before the stream is

liquified by a water cooler. In this work, subcritical ORCs are selected with the consideration of operational feasibility, safety and investment cost. To ensure stable operation of the ORC, the pressure of working fluids in the ORC should be below the near-critical region, here set to be below 90% of the critical pressure [142, 143]. Eight substances have been considered as working fluids for the ORC in the LAES system. The performance of different working fluids of the ORC is discussed in Section 6.3.1.

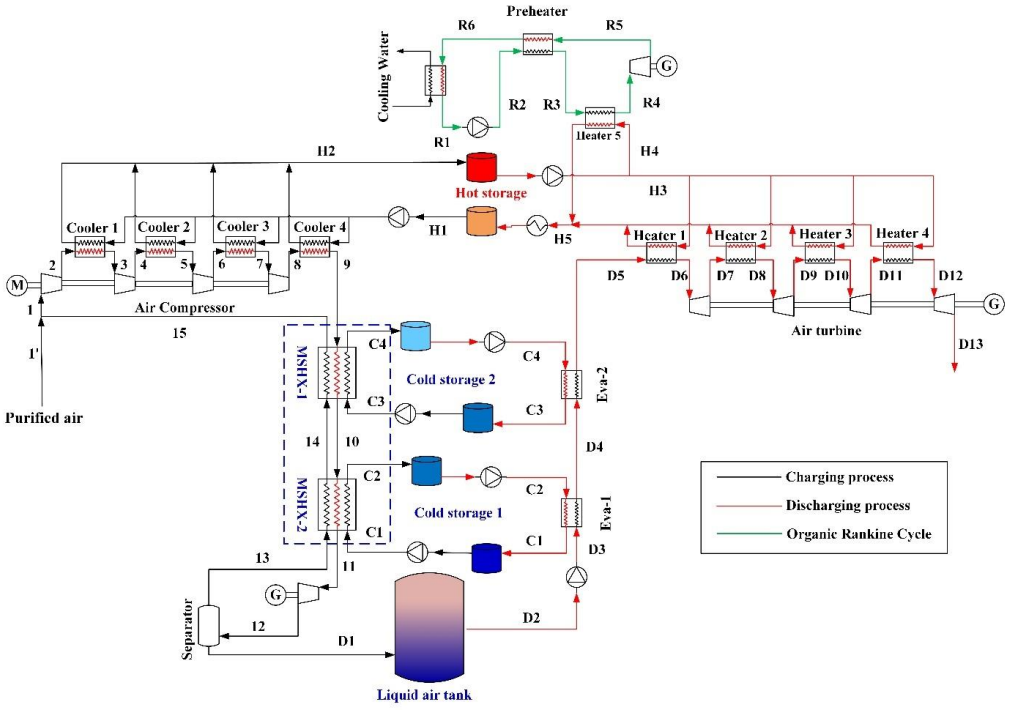

Figure 6.1 Flow diagram of liquid air energy storage with an ORC.

6.1.2 LAES system with an ARC for utilization of surplus high-grade compression heat

The flowsheet of the LAES system with an ARC is shown in Figure 6.2. Ammonia-water is the working fluid of the ARC. The ammonia solution (A1) is pumped and preheated before entering a distillation column to be separated. The pure ammonia stream obtained at the top of the column is first precooled by cooling water and then throttled to generate refrigeration capacity for the cold box. After the cold energy of the ammonia regasification is delivered to the cold box, the ammonia stream is sent back to an absorber. The product in the bottom of the distillation column is a lean ammonia solution, which is then sent to a preheater to heat the feed stream to the column. The lean ammonia stream is next throttled before it is sent back to the absorber to be mixed with pure ammonia. It is worth noting that the heat source of the ARC is surplus compression heat (stream H4), which provides the heat duty in the reboiler of the column. The cold energy generated from the ARC is sent to the cold box to liquefy more air.

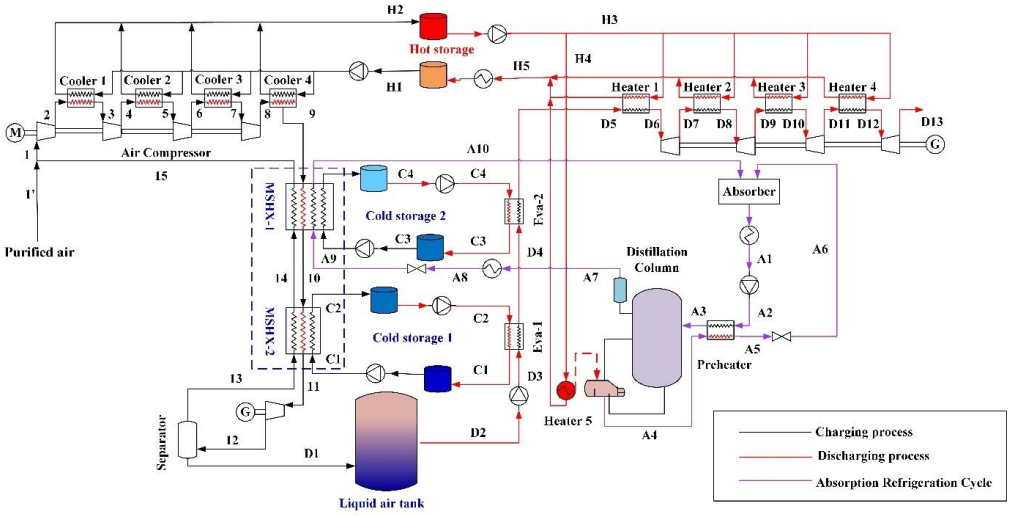

Figure 6.2 Flow diagram of liquid air energy storage with an ARC.

6.1.3 LAES system with an HTHP for utilization of surplus medium grade compression heat

As discussed in Chapter 5, a medium grade compression heat of 109.3°C is obtained when there is a 6-stage compressor in the charging part. The schematic of the LAES system with an HTHP to utilize the medium grade compression heat is shown in Figure 6.3. The medium grade compression heat is split into two streams H3 and H4. Stream H4 is sent to heat exchanger HP-Eva, where surplus compression heat is used to evaporate the working fluid of the HTHP. The vapor is then pressurized in a compressor, and the outlet stream of the compressor is at high temperature, which is used to increase the temperature of stream H3. The enhanced stream H3 is sent to heat exchangers to preheat air before expansion stages and thereby increase the power production. Eight substances have been selected as potential working fluids of the HTHP, and the results will be discussed in detail in Section 6.3.3.

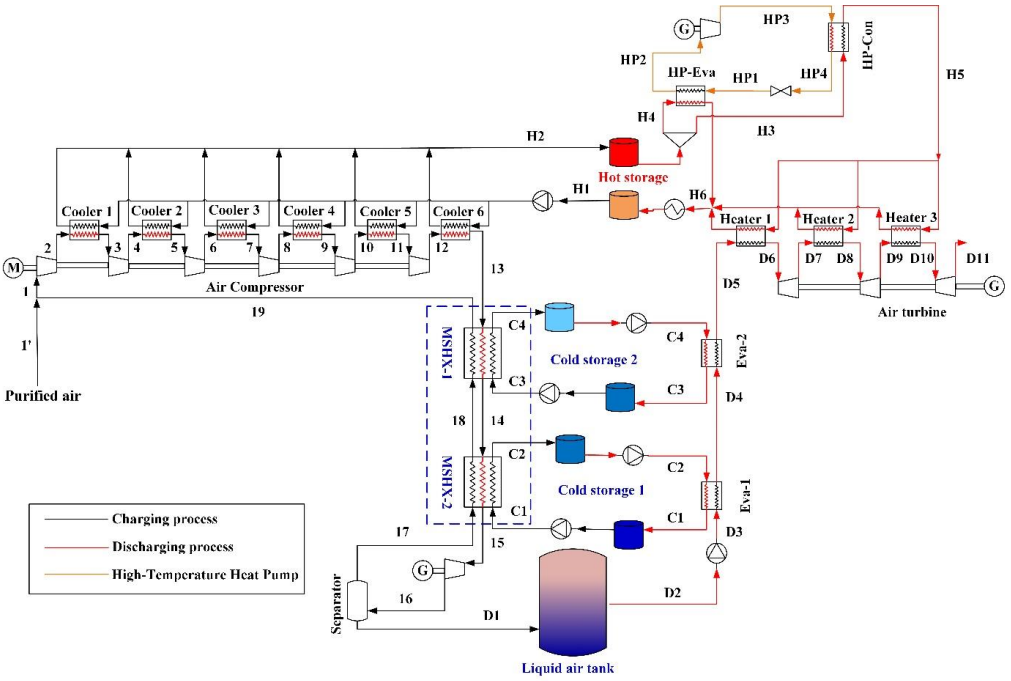

Figure 6.3 Flow diagram of liquid air energy storage with an HTHP.

6.2 Process evaluation and optimization

This section introduces the detailed definitions of key performance indicators (KPIs) that are used to evaluate different configurations of the LAES. The optimization algorithm for the LAES is then provided.

6.2.1 Process evaluation

The performance of the LAES system can be evaluated by round-trip efficiency and exergy efficiency. The definition of the round-trip efficiency was given in Section 3.1, thus, this will

not be discussed in detail to avoid repetition. Detailed exergy efficiencies for different LAES systems will be provided in this chapter. In addition, the thermal efficiency of the ORC and the Coefficient of Performance (COP) of the ARC and the HTHP are calculated to indicate the performance of different thermodynamic cycles.

The exergy efficiencies of the charging and discharging parts ($\eta_{\dot{E}_{\mathrm{ch}}}$ and $\eta_{\dot{E}_{\mathrm{dc}}}$) of the LAES-ORC, LAES-ARC and LAES-HTHP systems are given by Equations (6.1) - (6.6).

$$\eta_{\dot{E}\,\mathrm{ch,ORC}} = \frac{\dot{W}_{\mathrm{cryotur,ch}} + \dot{E}_{\mathrm{liq}} + \dot{E}_{\mathrm{h}}}{\dot{W}_{\mathrm{comp,ch}} + \dot{E}_{\mathrm{c}} + \dot{E}_{\mathrm{fa}}} \tag{6.1}$$

$$\eta_{\dot{E}\,\mathrm{dc,ORC}} = \frac{\dot{W}_{\mathrm{tur,dc}} + \dot{E}_{\mathrm{c}} + \dot{W}_{\mathrm{ORC}}}{\dot{W}_{\mathrm{pump,dc}} + \dot{E}_{\mathrm{liq}} + \dot{E}_{\mathrm{h}}} \tag{6.2}$$

$$\eta_{\dot{E}\,\mathrm{ch,ARC}} = \frac{\dot{W}_{\mathrm{cryotur,ch}} + \dot{E}_{\mathrm{liq}} + \dot{E}_{\mathrm{h}}}{\dot{W}_{\mathrm{comp,ch}} + \dot{E}_{\mathrm{c}} + \dot{E}_{\mathrm{fa}} + \dot{W}_{\mathrm{ARC}}} \tag{6.3}$$

$$\eta_{\dot{E}\,\mathrm{dc,ARC}} = \frac{\dot{W}_{\mathrm{tur,dc}} + \dot{E}_{\mathrm{c}}}{\dot{W}_{\mathrm{pump,dc}} + \dot{E}_{\mathrm{liq}} + \dot{E}_{\mathrm{h}}} \tag{6.4}$$

$$\eta_{\dot{E}\,\mathrm{ch,HTHP}} = \frac{\dot{W}_{\mathrm{cryotur,ch}} + \dot{E}_{\mathrm{liq}} + \dot{E}_{\mathrm{h}}}{\dot{W}_{\mathrm{comp,ch}} + \dot{E}_{\mathrm{c}} + \dot{E}_{\mathrm{fa}} + \dot{W}_{\mathrm{HTHP}}} \tag{6.5}$$

$$\eta_{\dot{E}\,\mathrm{dc,HTHP}} = \frac{\dot{W}_{\mathrm{tur,dc}} + \dot{E}_{\mathrm{c}}}{\dot{W}_{\mathrm{pump,dc}} + \dot{E}_{\mathrm{liq}} + \dot{E}_{\mathrm{h}}} \tag{6.6}$$

Here, $\dot{W}_{\mathrm{tur,dc}}$, $\dot{W}_{\mathrm{pump,dc}}$ and $\dot{W}_{\mathrm{ORC}}$ are the expansion work of expanders, the work consumed in the pump and the net work production in the ORC in the discharging part. $\dot{W}_{\mathrm{ARC}}$ is the work consumed by the pump in the ARC, and $\dot{W}_{\mathrm{HTHP}}$ is the compression work in the HTHP. The performance of the ORC, the ARC and the HTHP is provided by Equations (6.7) - (6.9).

$$\eta_{\mathrm{ORC}} = \frac{\dot{W}_{\mathrm{ORC}}}{\dot{Q}_{\mathrm{ORC}}} \tag{6.7}$$

$$COP_{\mathrm{ARC}} = \frac{\dot{Q}_{\mathrm{ARC}}}{\dot{W}_{\mathrm{ARC}} + \dot{Q}_{\mathrm{Heater5}}} \tag{6.8}$$

$$COP_{\mathrm{HTHP}} = \frac{\dot{Q}_{\mathrm{HTHP}}}{\dot{W}_{\mathrm{HTHP}}} \tag{6.9}$$

Here, $\dot{Q}_{\mathrm{ORC}}$ represents the heat duty of the evaporator (Heater 5) in the ORC in Figure 6.1. $\dot{Q}_{\mathrm{ARC}}$ is the cold energy produced in the ARC and then delivered to the cold box, and $\dot{Q}_{\mathrm{Heater5}}$ is the heat input to the reboiler of the column in Figure 6.2. $\dot{Q}_{\mathrm{HTHP}}$ is the heat duty of the condenser (HP-Con) in the HTHP in Figure 6.3.

6.2.2 Process optimization

The LAES system with different thermodynamic cycles is optimized by using a Particle Swarm Optimization (PSO) algorithm. The PSO is executed in Matlab, version R2018a [121], which provides the input to the HYSYS model and collects stream data from the simulated LAES system. The objective is to maximize the RTE of the LAES with different thermodynamic cycles to utilize the surplus compression heat. The equation for the objective function can be found in Section 3.3. The constraints for different LAES systems are listed in Table 6.1. It is worth noting that the optimization is performed only for the ORC and the HTHP cycles in the LAES-ORC and the LAES-HTHP systems, since only hot oil stream H4 is affected. However, the situation is different for the LAES-ARC system. The cold duty generated from the ARC is provided to the cold box, which affects the performance of the overall system. Thus, the optimization is implemented for the entire LAES-ARC system. In order to balance heat transfer efficiency and cost of heat exchangers in all three cases (ORC, ARC and HTHP), the minimum temperature difference (ΔT_{min}) of heaters and coolers is assumed to be 10°C, while the ΔT_{min} of low temperature heat exchangers (the cold box and evaporators) is set to 1°C [122]. For the LAES-ARC, the purity of ammonia in the top of the distillation column is constrained to be larger than 0.999. In addition, to ensure that the surplus compression heat is transferred to the reboiler, the outlet temperature of Heater 5 is assumed to be 10°C larger than the bottom stream

of the column. The decision variables for the LAES system with different thermodynamic cycles are listed in Table 6.2, where the upper and lower bounds for the variables are provided.

Table 6.1 Constraints for the LAES-ORC, LAES-ARC and LAES-HTHP systems.

	Constraints
LAES-ORC	$\Delta T_{con/eva} \geq 10°C$
	$VF_{in,pump,ORC} = 0$
	$VF_{in,tur,ORC} = 1$
	$VF_{out,tur,ORC} = 1$
LAES-ARC	$\Delta T_{heater/cooler} \geq 10°C$
	$\Delta T_{MSHX/eva} \geq 1°C$
	$x_{NH3} \geq 0.999$
	$T_{out,Heater\ 5} - T_{A4} \geq 10°C$
LAES-HTHP	$\Delta T_{con/eva} \geq 10°C$
	$VF_{in,comp,HP} = 1$
	$VF_{out,comp,HP} = 1$
	$T_{out,comp} \leq T_{cr}$
	$p_{out,comp} \leq p_{cr}$

6.3 Results and discussion

The Organic Rankine Cycle (ORC), the Absorption Refrigeration Cycle (ARC) and the High Temperature Heat Pump (HTHP) are selected to utilize the waste compression heat at different temperature levels in the LAES system. The performance of these thermodynamic cycles is discussed in the following.

6.3.1 Analysis of the LAES system with an ORC

As illustrated in Figure 6.1, a part of the high temperature compression heat in Case I will be recovered by the ORC rather than wasted. Stream data for the optimized LAES system with available surplus compression heat for the ORC is shown in Table 6.3. From this table, it is observed that around 17% of the compression heat at 168.2°C is in surplus. ORC is regarded to be one of the solutions to utilize this surplus high temperature compression heat in the LAES.

Table 6.2 Lower and upper bounds for decision variables of the LAES-ORC, LAES-ARC and LAES-HTHP systems.

Variables	Lower Bounds	Upper Bounds
Condensation pressure (bar) [a]	1.0	$0.9p_{cr}$
Evaporation pressure (bar) [a]	1.1	$0.9p_{cr}$
Working fluid evaporation temperature (°C) [a]	50	T_{cr}
Working fluid molar flowrate (kmol/h) [a]	0.1	800
Pressure ratio for compressors [b]	1.0	5
Pressure ratio for expanders [b]	1.0	10
Thermal oil temperature (°C) [b]	100	230
Cold box outlet air temperature (°C) [b]	-185	-165
Cold box outlet recycled air temperature (°C) [b]	-10	29
Working fluid operating temperature (higher) (°C) [b]	-90	-20
Working fluid molar flowrate (kmol/h) [b]	0.1	3000
Working fluid operating temperature (lower) (°C) [b]	-186	-166
Condensation pressure (bar) [c]	1.1	p_{cr}
Evaporation pressure (bar) [c]	1.0	p_{cr}
Working fluid evaporation temperature (°C) [c]	50	T_{cr}
Working fluid molar flowrate (kmol/h) [c]	0.1	800

[a] variable bounds for the LAES-ORC system

[b] variable bounds for the LAES-ARC system

[c] variable bounds for the LAES-HTHP system

The thermodynamic properties of the working fluid are crucial for the ORC and will thereby affect the performance of the LAES system. A comparison of working fluids should be conducted to identify the most suitable medium that leads to the largest net work production of the ORC and the highest RTE of the LAES. Working fluids for typical ORCs have been investigated widely, and a large number of candidates can be considered for the selection in this chapter. Thus, a pre-selection is needed to reduce the workload of screening working fluids for the ORC in the LAES system. The criteria for selection of working fluid for the ORC take physical properties, environmental impact, economics and operational feasibility into consideration, and the most important ones are the following:

1) Freezing point of the working fluid should be lower than ambient temperature to avoid the formation of solids in the ORC.
2) Ozone Depletion Potential (ODP) of the working fluid should be 0 and the Global Warming Potential (GWP) of the fluid should be low.
3) The working fluids should be non-corrosive, non-toxic and innoxious to humans.
4) Low cost working fluids are more favorable.
5) In order to avoid a pinch limitation in the evaporation heat exchanger (Heater 5) in the ORC, the critical temperature of the working fluid should be lower than the temperature of the heat source (stream H4). However, the critical temperature should not be too low, since that would result in large exergy losses in Heater 5.

Based on the criteria listed above, eight working fluids that are studied as candidates for the ORC are listed in Table 6.4. As mentioned in Section 6.1.1, subcritical operation is applied for the ORC. Figure 6.4 illustrates the net power output of ORCs with different working fluids that utilize the high temperature surplus compression heat in the LAES system. It is shown that R600a and R152a are the top 2 working fluids in terms of net power output. Table 6.5 shows the optimal operating variables for the eight working fluids, such as condensation and evaporation pressures, temperature, heat duty and logarithmic mean temperature difference (LMTD) of the evaporator, and work of the turbine and pump. The smallest LMTD of the evaporator and the largest pressure ratio between evaporation and condensation are obtained

in the cycle using R600a as the working fluid. This leads to the smallest exergy loss in the evaporator and the largest net power output and thermal efficiency of the cycle. This also results in the largest RTE of 64.5% in the LAES-ORC system.

Table 6.3 Stream data for the heat recovery cycle in Case I.

Stream	T °C	p bar	$\dot{m}$ kmol/h	Fluids	Stream	T °C	p bar	$\dot{m}$ kmol/h	Fluids
1	21.02	1.01	2469.05	Air	D3	-186.72	159.81	2131.62	Air
2	174.58	3.74	2469.05	Air	D4	-64.39	159.81	2131.62	Air
3	30.00	3.74	2469.05	Air	D5	26.39	159.81	2131.62	Air
4	188.03	13.77	2469.05	Air	D6	158.17	159.81	2131.62	Air
5	30.00	13.77	2469.05	Air	D7	38.97	45.09	2131.62	Air
6	188.69	50.76	2469.05	Air	D8	158.17	45.09	2131.62	Air
7	30.00	50.76	2469.05	Air	D9	40.68	12.72	2131.62	Air
8	189.27	187.12	2469.05	Air	D10	158.17	12.72	2131.62	Air
9	30.00	187.12	2469.05	Air	D11	41.62	3.59	2131.62	Air
10	-57.20	187.12	2469.05	Air	D12	158.17	3.59	2131.62	Air
11	-176.00	187.12	2469.05	Air	D13	41.93	1.01	2131.62	Air
12	-194.31	1.01	2469.05	Air	H1	15.00	1.01	336.87	Thermal oil
13	-194.31	1.01	337.43	Air	H2	168.22	1.01	336.87	Thermal oil
14	-63.34	1.01	337.43	Air	H3	168.22	1.01	278.83	Thermal oil
15	27.45	1.01	337.43	Air	H4	168.22	1.01	58.04	Thermal oil
D1	-194.31	1.01	2131.62	Air	H5	47.27	1.01	336.87	Thermal oil
D2	-194.31	1.01	2131.62	Air					

Table 6.4 Properties of working fluids investigated in this study.

Fluids	Chemical formula	T_{cr} (°C)	p_{cr} (bar)	T_{nb} (°C)	ODP	GWP_{100}
R125	C_2HF_5	66.02	36.19	-48.11	0	3500
R143a	$C_2H_3F_3$	72.73	37.64	-47.34	0	4470
R1270	C_3H_6	92.44	46.64	-47.69	0	2
R290	C_3H_8	96.67	42.42	-42.08	0	3
R134a	$C_2H_2F_4$	101.03	40.56	-26.07	0	1100
R152a	$C_2H_4F_2$	113.55	45.00	-24.95	0	124
R600a	C_4H_{10}-2	134.83	36.54	-11.79	0	3
R600	C_4H_{10}-1	152.00	37.96	-0.51	0	4

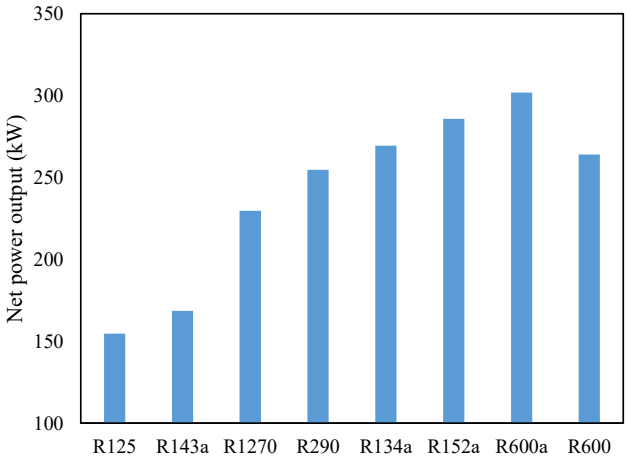

Figure 6.4 Net power output of different working fluids for the ORC when utilizing the surplus high temperature compression heat in the LAES.

It can be noticed that the LMTD of the evaporator in the cycle with R134a is slightly smaller than the cycle using R152a as the working fluid, while the net power output is larger for the cycle with R152a. This is because the critical pressure of working fluid R152a is quite high (45 bar, see Table 6.4), and the pressure ratio of the expander in the ORC using R152a as the working fluid is larger than the cycle with R143a. As a result, the power output of the cycle with R152a is larger than the cycle with R134a. The working fluid R600 has the second largest thermal efficiency for the ORC in converting compression heat to power. However, the power output of the cycle with R600 is lower compared to the cases using R600a, R152a and R134a as working fluids, since the heat recovered in the evaporator (1663.6 kW) is the smallest. This is due to the fact that there exists a trade-off between the amount of recovered heat and the pressure ratio of the turbine in the ORC. A higher evaporation pressure is preferred to have a larger power output.

However, to avoid pinch limitation in the evaporator, the amount of recovered heat in the evaporator may not be satisfactory, as the case using R600 as the working fluid shows. For other working fluids with a low critical temperature (e.g., R125, R143a and R1270), the amount of recovered heat in the evaporator is large, while the pressure ratio of the turbine in the ORC is limited, and therefore the power output and thermal efficiency of the cycle is low. In addition, the high GWP_{100} for R125, R143a and R134a makes them less competitive than other working fluids in this chapter. Thus, it is the working fluid with proper critical temperature and pressure (R600a) and a moderate amount of recovered heat in the evaporator that has the maximum power output.

Table 6.5 Performance of the ORC with different working fluids in the LAES system.

Fluids	$\dot{W}_{net}$ (kW)	p_{con} (bar)	p_{eva} (bar)	$\dot{m}$ (kmol/h)	$\dot{Q}_{eva}$ (kW)	T_{eva} (°C)	$LMTD_{eva}$ (°C)	$\dot{W}_{tur}$ (kW)	$\dot{W}_{pump}$ (kW)	η_{ORC} (%)	RTE (%)
R125	154.65	12.10	27.55	451.34	2074.77	66.32	34.65	178.54	23.89	7.45	63.36
R143a	168.60	12.00	28.24	450.52	2077.38	72.99	31.09	187.19	18.59	8.12	63.47
R1270	229.64	10.31	32.04	427.15	2068.38	91.42	21.40	256.07	26.43	11.10	63.96
R290	254.79	8.42	32.65	401.67	2066.45	96.27	19.86	284.62	29.83	12.33	64.16
R134a	269.43	5.82	31.00	323.89	2073.97	101.24	18.15	293.14	23.72	12.99	64.28
R152a	285.78	5.34	41.00	270.23	1859.20	113.22	18.47	310.01	24.23	15.37	64.41
R600a	301.95	3.11	29.45	263.01	1856.82	121.79	15.84	327.07	25.12	16.26	64.54
R600	264.11	2.14	17.01	216.67	1663.57	105.49	23.33	275.38	11.27	15.88	64.24

6.3.2 Analysis of the LAES system with an ARC

Stream data of the optimized LAES-ARC are provided in Table 6.6. Figure 6.5 shows the composite curves of the cold box in the LAES system without and with an ARC. It is noticed that the LMTD for MSHX-1 is larger for the LAES system with an ARC (4.05°C) compared to the system without an ARC (1.71°C) due to the constant temperature during ammonia phase changing. However, the increased cold energy from ammonia regasification in MSHX-1 leads to a larger liquid yield and a slightly lower charging pressure in the charging part of the LAES-ARC system, as shown in Table 6.7. A higher liquid yield of air means that less air needs to be re-compressed, and less compression work is required in the charging part of the LAES-ARC system compared to the system without an ARC. Thus, with the ARC to utilize the surplus compression heat, the RTE of the system is increased to 63.5% due to the reduced compression work in the charging part.

Table 6.6 Stream data of the optimized LAES-ARC system.

Stream	T °C	p bar	$\dot{m}$ kmol/h	Fluids	Stream	T °C	p bar	$\dot{m}$ kmol/h	Fluids
1	19.08	1.01	2384.24	Air	D8	156.25	42.63	2131.62	Air
2	171.51	3.73	2384.24	Air	D9	40.75	12.26	2131.62	Air
3	30.00	3.73	2384.24	Air	D10	156.25	12.26	2131.62	Air
4	187.82	13.73	2384.24	Air	D11	41.64	3.52	2131.62	Air
5	30.00	13.73	2384.24	Air	D12	156.25	3.52	2131.62	Air
6	188.47	50.54	2384.24	Air	D13	41.94	1.01	2131.62	Air
7	30.00	50.54	2384.24	Air	H1	15.00	1.01	328.04	Thermal oil
8	189.06	186.03	2384.24	Air	H2	166.30	1.01	328.04	Thermal oil
9	30.00	186.03	2384.24	Air	H3	166.30	1.01	280.52	Thermal oil
10	-66.36	186.03	2384.24	Air	H4	166.30	1.01	47.53	Thermal oil
11	-180.00	186.03	2384.24	Air	H5	53.83	1.01	328.04	Thermal oil
12	-194.31	1.01	2384.24	Air	A1	20	1.4	868.54	Ammonia solution
13	-194.31	1.01	252.62	Air	A2	20.11	10	868.54	Ammonia solution
14	-72.90	1.01	252.62	Air	A3	93.29	10	868.54	Ammonia solution
15	11.28	1.01	252.62	Air	A4	108.3	10.1	807.29	Ammonia solution
D1	-194.31	1.01	2131.62	Air	A5	29.73	10.1	807.29	Ammonia solution
D2	-194.31	1.01	2131.62	Air	A6	29.92	1.4	807.29	Ammonia solution
D3	-187.27	148.26	2131.62	Air	A7	25.18	10	61.25	Ammonia
D4	-73.92	148.26	2131.62	Air	A8	20	10	61.25	Ammonia
D5	8.22	148.26	2131.62	Air	A9	-26.36	1.4	61.25	Ammonia
D6	156.25	148.26	2131.62	Air	A10	10.28	1.4	61.25	Ammonia
D7	39.07	42.63	2131.62	Air					

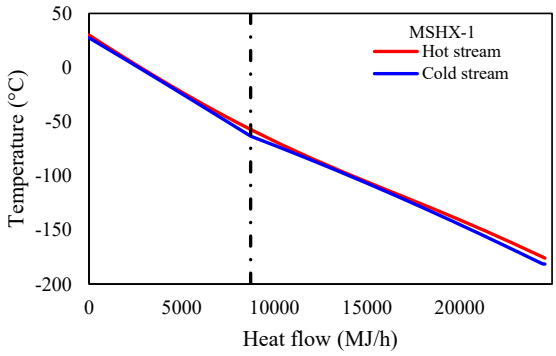

(a) LAES system without ARC

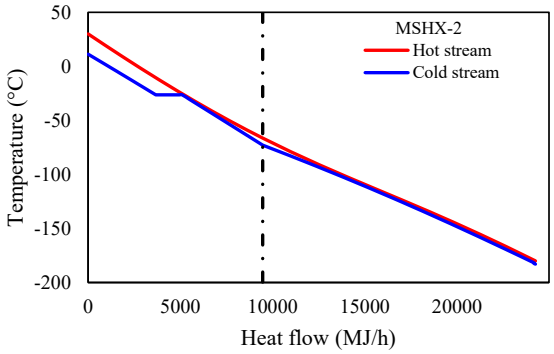

(b) LAES system with ARC

Figure 6.5 Composite curves of the cold box in LAES configurations (a) without and (b) with an ARC system.

Table 6.7 Performance of the LAES system with an ARC.

	LAES	LAES-ARC
COP	-	0.64
$\dot{Q}_{\text{coldbox}}$ (kJ/kg)	346.24	353.26
$LMTD_{\text{MSHX-1}}$ (°C)	1.71	4.05
$LMTD_{\text{MSHX-2}}$ (°C)	2.50	2.41
p_{ch} (bar)	187.12	186.02
p_{dc} (bar)	159.81	148.26
η_{LY} (%)	86.57	89.60
$\dot{W}_{\text{ch}}$ (MW)	12.50	12.06
$\dot{W}_{\text{dc}}$ (MW)	7.76	7.65
RTE (%)	62.13	63.47

6.3.3 Analysis of the LAES system with an HTHP

The temperature and amount of thermal oil vary with different number of compression stages in the charging part of the LAES system. A lower temperature of thermal oil at 109.3°C is obtained in the LAES with a 6-stage compressor compared to the system with a 4-stage compressor (168.2°C). Stream data for the heat recovery cycle in Case II, which is illustrated in Figure 6.3, are shown in Table 6.8. In this work, the HTHP is selected to utilize the medium grade compression heat in the LAES system. As for the selection of working fluid for the HTHP, in addition to the mentioned concerns about physical properties and economics mentioned in Section 3.1, three significant criteria should be considered for the working fluid selection:

Table 6.8 Stream data for the heat recovery cycle in the LAES system with an HTHP.

Stream	T °C	p bar	$\dot{m}$ kmol/h	Fluids	Stream	T °C	p bar	$\dot{m}$ kmol/h	Fluids
1	20.95	1.01	2486.28	Air	19	26.66	1.01	354.66	Air
2	110.01	2.28	2486.28	Air	D1	-194.32	1.01	2131.62	Air
3	30.00	2.28	2486.28	Air	D2	-194.32	1.01	2131.62	Air
4	121.63	5.11	2486.28	Air	D3	-189.02	111.71	2131.62	Air
5	30.00	5.11	2486.28	Air	D4	-76.48	111.71	2131.62	Air
6	121.74	11.47	2486.28	Air	D5	25.65	111.71	2131.62	Air
7	30.00	11.47	2486.28	Air	D6	131.92	111.71	2131.62	Air
8	121.95	25.77	2486.28	Air	D7	-2.14	23.30	2131.62	Air
9	30.00	25.77	2486.28	Air	D8	131.92	23.30	2131.62	Air
10	122.26	57.86	2486.28	Air	D9	0.32	4.86	2131.62	Air
11	30.00	57.86	2486.28	Air	D10	131.92	4.86	2131.62	Air
12	122.30	129.93	2486.28	Air	D11	1.09	1.01	2131.62	Air
13	30.00	129.93	2486.28	Air	H1	15.00	1.01	497.82	Thermal oil
14	-68.55	129.93	2486.28	Air	H2	109.34	1.01	497.82	Thermal oil
15	-176.00	129.93	2486.28	Air	H3	109.34	1.01	214.26	Thermal oil
16	-194.32	1.01	2486.28	Air	H4	109.34	1.01	283.56	Thermal oil
17	-194.32	1.01	354.66	Air	H5	62.12	1.01	497.82	Thermal oil
18	-75.31	1.01	354.66	Air					

1) Operational feasibility: The evaporation temperature of the heat pump should be lower than the temperature of the medium grade compression heat in the LAES. Moreover, the critical temperature of the working fluids of the heat pump should be higher than the temperature of the compression heat.
2) Coefficient of Performance: The COP reveals the efficiency to convert work to heat in heat pumps.
3) Environmental impact: To mitigate the progress of global warming, potential greenhouse gases should be avoided.

Taking the above concerns into consideration, eight working fluid candidates with critical temperature higher than 109.3°C are considered and listed in Table 6.9. Some key parameters and the performance of the HTHP with different working fluids are shown in Table 6.10, such as the mass flow rate of the working fluid, heat duties and temperatures of evaporators and condensers, the work consumed in the compressor and the heat pump, the work consumed in the charging part, and the work produced in the discharging part of the LAES system. It is observed that the system using R1233zd as the working fluid in the heat pump has the highest upgraded temperature of the compression heat (155.1°C), and thereby the highest RTE of the LAES-HTHP system. The reason is that the heat duty of the evaporator in the heat pump is the main factor that influences the temperature of the upgraded compression heat, and the power production in the LAES-HTHP system as well. The heat source for the heat pump is a part of surplus compression heat in the LAES system, which is regarded as free. The largest heat recovery in the evaporator will lead to the largest condensation heat in the heat pump, which is beneficial for the power generation in the discharging part of the LAES system. For the cycle using R1233zd as working fluid, the heat recovered in the evaporator achieves a maximum of 2.0 MW, and the largest heat duty of 2.7 MW is obtained in the condenser to be released to upgrade the compression heat. Although compression work is the largest and COP is the smallest for the heat pump cycle with R1233zd, the additional work produced in the discharging part of the LAES system can justify the compression work in the heat pump due to the upgraded compression heat. Another advantage of selecting R1233zd is that it is a

hydrofluoroolefin (HFO) with low environmental impact, achieving the phase-out of hydrofluorocarbons (HFCs) [144].

Table 6.9 Properties of working fluid candidates for the HTHP.

Fluids	Chemical formula	T_{cr} (°C)	p_{cr} (bar)	T_{nb} (°C)	ODP	GWP_{100}
R600a	C_4H_{10}-2	134.83	36.54	-11.79	0	3
R600	C_4H_{10}-1	152.00	37.96	-0.51	0	4
R1234ze	$C_3H_2F_4$-N2	150.12	35.37	9.80	0	1
R245fa[a]	$C_3H_3F_5$	154.05	36.40	14.90	0	858
R1233zd	$C_3H_2CLF_3$-N1	165.60	35.70	18.30	0.00034	1
R601a	C_5H_{12}-2	187.25	33.34	27.88	0	4
R601	C_5H_{12}-1	196.45	33.75	36.06	0	4
n-Hexane	C_6H_{14}	234.75	30.32	68.73	0	<6

[a] Even though R245fa has a large GWP_{100}, it is selected as a traditional refrigerant to be compared with other low-GWP refrigerants in this work.

Table 6.10 Performance of the LAES system with HTHP with using different working fluids.

Fluids	$\dot{m}$ (kmol/h)	$\dot{Q}_{eva}$ (MW)	T_{eva} (°C)	$\dot{Q}_{con}$ (MW)	T_{con} (°C)	T_{H5} (°C)	$\dot{W}_{comp}$ (MW)	$\dot{W}_{ch}$ (MW)	$\dot{W}_{dc}$ (MW)	COP	RTE (%)
R600a	255.03	0.59	90.49	0.71	129.19	120.92	0.11	10.99	6.14	6.45	55.89
R600	507.89	1.51	78.60	1.96	149.10	141.97	0.45	11.33	6.52	4.35	57.55
R1234ze	368.05	1.28	81.77	1.61	142.80	136.09	0.33	11.21	6.42	4.88	57.24
R245fa	442.67	1.59	77.64	2.08	151.00	143.99	0.48	11.36	6.56	4.33	57.71
R1233zd	532.91	2.01	72.11	2.73	161.60	155.19	0.72	11.59	6.76	3.79	58.27
R601a	246.31	1.13	79.33	1.40	142.59	132.57	0.27	11.15	6.35	5.19	56.96
R601	225.54	1.14	79.34	1.41	142.69	132.67	0.27	11.15	6.35	5.21	56.99
n-Hexane	78.36	0.50	79.34	0.59	129.05	119.02	0.09	10.97	6.11	6.55	55.68

6.3.4 Comparison of LAES combined with ORC, ARC and HTHP Cycles

Table 6.11compares the performance of different LAES configurations studied in Chapter 5 and the work presented in this chapter. Based on the analysis of different thermodynamic cycles in the LAES system in Sections 6.3.1-6.3.3, the best performance of LAES-ORC, LAES-ARC and LAES-HTHP systems are selected to be compared with the standalone LAES system. It is seen that the optimal LAES case with a 2-stage compressor and a 3-stage expander still has the best performance. However, the operational and economic feasibility of this optimal case can be questioned due to the large pressure ratios in compressors.

For the LAES systems with more feasible pressure ratios and available surplus compression heat (i.e. 4-stage compressor and 4-stage expander), the largest power generation from the additional ORC is 302.0 kW. The exergy efficiency of the discharging part in the system with an ORC is increased from 84.3 to 86.4%, while the exergy efficiency of the charging part is unchanged. The reason is that the power produced in the ORC leads to an increase in the total power production and the exergy efficiency in the discharging part. The RTE of the LAES system with an ORC is increased from 62.1 to 64.5%.

For the system with an ARC to utilize the surplus compression heat, the compression work in the charging part is reduced, and the liquid yield of air is increased to 89.6% since the cold duty generated from the ARC is provided to the cold box for the liquefaction of air. The RTE of the LAES-ARC system is increased from 62.1 to 63.5% compared to the standalone LAES system with the same number of compression and expansion stages. It is worth noting that a part of surplus compression heat is required to provide heat duty to the reboiler of the distillation column, and pump work is also needed to pressurize the working fluid (ammonia-water solution) in the ARC. Thus, the decreased compression heat from the charging part and the additional pump work in the ARC result in a reduced exergy efficiency in the charging part of the LAES-ARC system compared to the system without an ARC. The exergy efficiency of the discharging part is increased due to the reduction of the exergy input associated with reduced compression heat.

Table 6.11 Comparison between different LAES configurations investigated in Chapter 5 and the work presented in this chapter.

KPIs	Optimal LAES	LAES	LAES-ORC	LAES-ARC	LAES	LAES-HTHP
Compression stages	2	4	4	4	6	6
Expansion stages	3	4	4	4	3	3
Additional cycle	-	-	ORC	ARC	-	HTHP
$\dot{W}_{ch}$ (MW)	15.00	12.50	12.50	12.06	10.88	11.59
$\dot{W}_{dc}$ (MW)	10.00	7.76	8.07	7.65	5.94	6.76
η_{LY} (%)	86.21	86.57	86.57	89.60	85.98	85.98
$\eta_{\dot{E}_{ch}}$ (%)	88.31	86.67	86.67	84.45	86.06	84.44
$\eta_{\dot{E}_{dc}}$ (%)	86.65	84.28	86.35	86.76	80.29	85.91
RTE (%)	66.65	62.13	64.54	63.47	54.56	58.27

High temperature heat pumps are considered to utilize medium grade compression heat in the LAES system. It is observed that the compression work is increased, and the exergy efficiency is reduced for the charging part of the LAES-HTHP system. This is due to the fact that the compressor in the HTHP provides heat to upgrade the compression heat in the LAES system by consuming work, which will be added to the work consumed in the charging part. Thus, the power consumption in the charging part is increased and, as a result, the exergy efficiency of the charging part is decreased. However, the enhanced compression heat results in an increase in the work production in the discharging part. The increased work production can justify the increased work consumption in the LAES-HTHP system. The RTE of the LAES-HTHP system reaches 58.3%, which is an increment of 3.7% points compared to the system without an HTHP.

6.4 Conclusions

This chapter presents three thermodynamic cycles to utilize the surplus compression heat in the LAES system in order to improve the performance of the overall system. The three thermodynamic cycles are Organic Rankine Cycle (ORC), Absorption Refrigeration Cycle (ARC) and High Temperature Heat Pump (HTHP). The ORC and ARC are considered for the utilization of the high temperature compression heat in the LAES system with a 4-stage compressor and a 4-stage expander, while the HTHP is utilizing medium grade compression heat in an LAES system with a 6-stage compressor and 3-stage expander. The three processes are simulated in Aspen HYSYS and optimized by using a Particle Swarm Optimization algorithm. The conclusions are summarized as follows:

- For the ORC to utilize the high temperature surplus compression heat, eight working fluids are selected and compared to identify the best working fluid for the ORC in the LAES system with a 4-stage compressor and a 4-stage expander. Optimization results show that the cycle using R600a as working fluid has the largest net power output of 302.0 kW, and the RTE of the overall system is improved from 62.1 to 64.5% compared to the system without an ORC.
- The ARC utilizes part of the surplus high temperature compression heat to generate cold duty. The cold duty is then supplied to the cold box to increase the liquid yield of air, which is improved from 86.6% to 89.6%. The exergy efficiency of the charging part is reduced from 86.7 to 84.5%, while the exergy efficiency of the discharging part is increased from 84.3 to 86.8%. The RTE of the LAES-ARC system reaches 63.5%.
- In the HTHP cycle, the heat source is part of the medium grade surplus compression heat. The LAES with eight suitable working fluids for the HTHP are optimized and compared, indicating that the additional power production in the discharging part due to the upgraded compression heat can justify the work consumption in the heat pump. The largest RTE of the LAES-HTHP is obtained by using R1233zd as working fluid, and the RTE is improved from 54.6 to 58.3% compared to the LAES without an HTHP.

Optimization results show that the ORC, the ARC and the HTHP are effective methods to improve the performance of the LAES system by utilizing available surplus compression heat. It is worth noting that the LAES system with additional thermodynamic cycles is not comparable to the optimal LAES system with a 2-stage compressor and a 3-stage expander from an energy efficiency point of view. However, the pressure ratios of compressors in the thermodynamically optimal LAES system are relatively large, and the feasibility in a real application of the process can be questioned. In addition, cost evaluation of the optimal LAES case and the LAES system with ORC, ARC and HTHP should be conducted to identify the most profitable LAES configuration. An LAES with an ARC is more complex with a larger number of units compared to the other configurations, which is expected to give a higher capital cost. Also, even with an improvement of 3.7%, the use of an HTHP in LAES systems may not be a good idea, as a multi-stage compressor is required in order to have compression heat temperatures that the HTHP can handle. To evaluate different LAES configurations comprehensively, an economic analysis of the LAES is conducted in the next chapter.

Chapter 7 Economic Analysis of some Liquid Air Energy Storage Configurations with Combined Hot Water and Power Supply

Abstract

In order to evaluate the economic feasibility and identify the most economic layout for a standalone LAES system, this chapter presents an economic comparative analysis of four LAES configurations with a storage capacity of 10 MW / 80 MWh. The net present value (NPV), payback period and levelized cost of storage (LCOS) are used as financial evaluation indexes. In addition, a comparison between the LAES and other energy storage technologies indicates that the LAES system has a better economic performance than Li-ion and Pb batteries, but it has a larger LCOS than Pumped Hydroelectric Energy Storage (PHES) and Compressed Air Energy Storage (CAES). This means that the LAES is a promising energy storage technology, but still needs to be further investigated to improve its competitiveness.

This chapter is based on the following publication.

- Liu Z, Kim D, Gundersen T. Techno-economic analysis of different liquid air energy storage configurations. Chemical Engineering Transactions. 2022;94:241-246.

The thermodynamic performance of the LAES has been thoroughly studied in Chapters 4-6. However, it is also important for a real-life application of the LAES to perform an economic evaluation. Most existing publications perform economic analyses either on a specific layout for the LAES system or on an integrated system between the LAES and external hot and cold thermal energy sources [74-83]. There is a lack of comparison between different configurations for a standalone LAES, which will also be valuable for integrated systems. In Chapter 5, the thermodynamic optimum was found to be when there are few compression stages with large pressure ratios. However, a system with maximum energy efficiency is not necessarily the most economic option. The cost for unconventional compressors with high pressure ratios is obviously considerably higher than the conventional ones, a fact that is neglected in most studies. An extra cost factor is applied in our studies to compressors with high pressure ratios for more realistic comparison with other processes. In this chapter, the economic performance of four different layouts for a standalone LAES is investigated and compared. The net present value (NPV), the payback period and the levelized cost of electricity (LCOE) are used for the evaluation of different LAES configurations. The purpose of this study is to investigate the economic feasibility of a standalone LAES system.

7.1 System description

In this chapter, hot water is an additional product besides electricity for making profit. This is achieved by utilizing waste heat in the LAES system to heat cold tap-water from 20°C to 65°C. The waste heat in the system consists of the remaining compression heat carried by thermal oil after the expansion part and the heat in the exhaust air after the last expansion stage.

Table 7.1 Main parameters and key performance indicators of some LAES configurations.

Parameters	Unit	Case 1	Case 2	Case 3	Case 4
Molar flow rate of air	kmol/h	2131.62	2563.35	2745.96	2650.67
Pressure ratios of compressors	-	13.05	5.29	3.69	3.69
Charging pressure	bar	171.85	149.84	187.12	187.12
Discharging pressure	bar	148.41	129.13	159.81	159.81
Compression work	MW	15.00	15.31	16.09	15.53
Expansion work	MW	10.00	10.00	10.00	9.65
Net work output from ORC	MW	-	-	-	0.40
$\dot{Q}_{\mathrm{wh}}$	MW	4.22	3.32	3.14	-
$\Delta T_{\mathrm{ac/pre}}$	°C	10.00	10.00	10.02	10.02
$\Delta T_{\mathrm{coldbox/eva}}$	°C	1.00	1.02	1.01	1.01
Liquid yield	%	86.21	86.26	86.62	86.62
RTE	%	66.65	65.32	62.16	64.41

From the results of the thermodynamic analysis for different LAES configurations in Chapter 5, the highest RTE is obtained for an LAES system with a 2-stage compressor and a 3-stage expander, which is selected as Case 1 in this study. This is followed by a system with a 3-stage compressor and a 4-stage expander, which is regarded as Case 2. One of the challenges for the top two LAES configurations is that the pressure ratios for the compressors are so high that conventional compressors are not suitable. Moreover, cost data for unconventional compressors with high pressure ratios and outlet temperatures are not available. Thus, an extra cost factor is applied for these units, and this is discussed in detail in Section 7.2.1. Case 3 is an LAES system with a 4-stage compressor and a 4-stage expander, which has moderate pressure ratios of less than 4 and conventional compressors can be used. From the results shown in Chapter 5, it can be seen that the performance of the LAES is improved when an additional Organic Rankine Cycle (ORC) is used to convert the unused compression heat to work.

Therefore, Case 4 is testing the economic feasibility of Case 3 with the additional ORC. Cases 1 - 3 are variants of a standalone LAES system shown very simplified (symbolic) in Figure 7.1, and the only difference between the three configurations is the number of compression and expansion stages. An additional ORC used in Case 4 makes it different from Cases 1 - 3, as illustrated in Figure 7.2. It is worth noting that there is no available waste heat from neither thermal oil nor exhaust air to produce hot water in Case 4, since the waste compression heat is used to drive the ORC. Thus, the heat duty of the water heater is left blank in Table 7.1 for Case 4. In this work, it is assumed that the LAES system has a storage capacity of 10 MW / 80 MWh aimed at providing auxiliary services to renewable power plants. The main parameters and key performance indicators of the four cases are listed in Table 7.1.

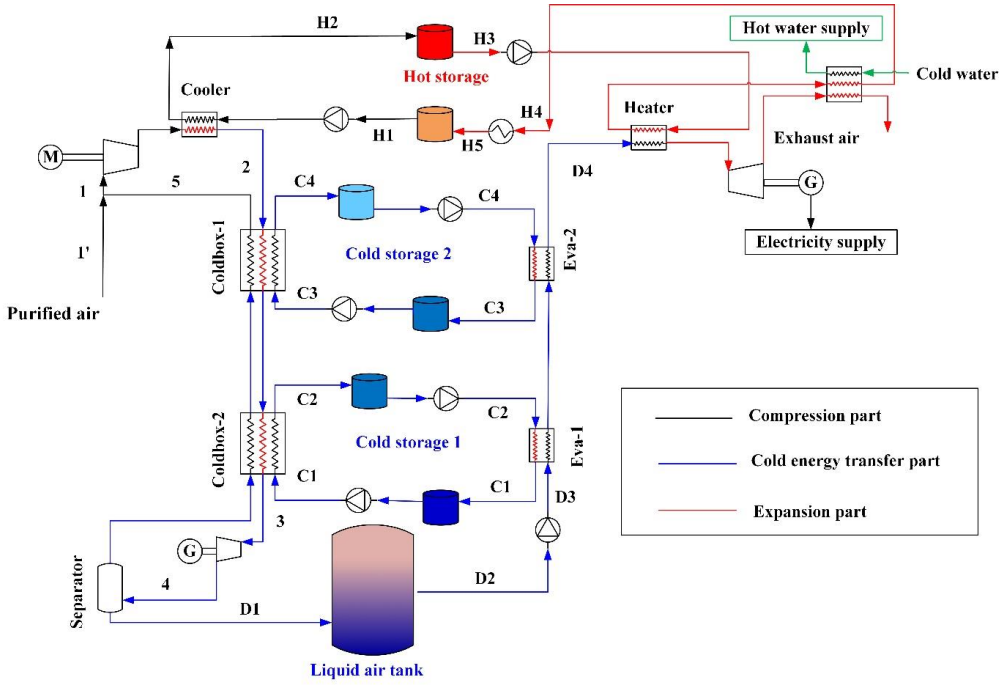

Figure 7.1 Simplified flowsheet of a standalone LAES system with hot water production.

7.2 Methodology and data

First in this section, models for total capital investment cost, annualized post-production cost, and annual income are introduced. Then economic evaluation indexes are presented. Finally, the initial conditions and assumptions for economic assessment of the LAES system are provided.

7.2.1 Economic model

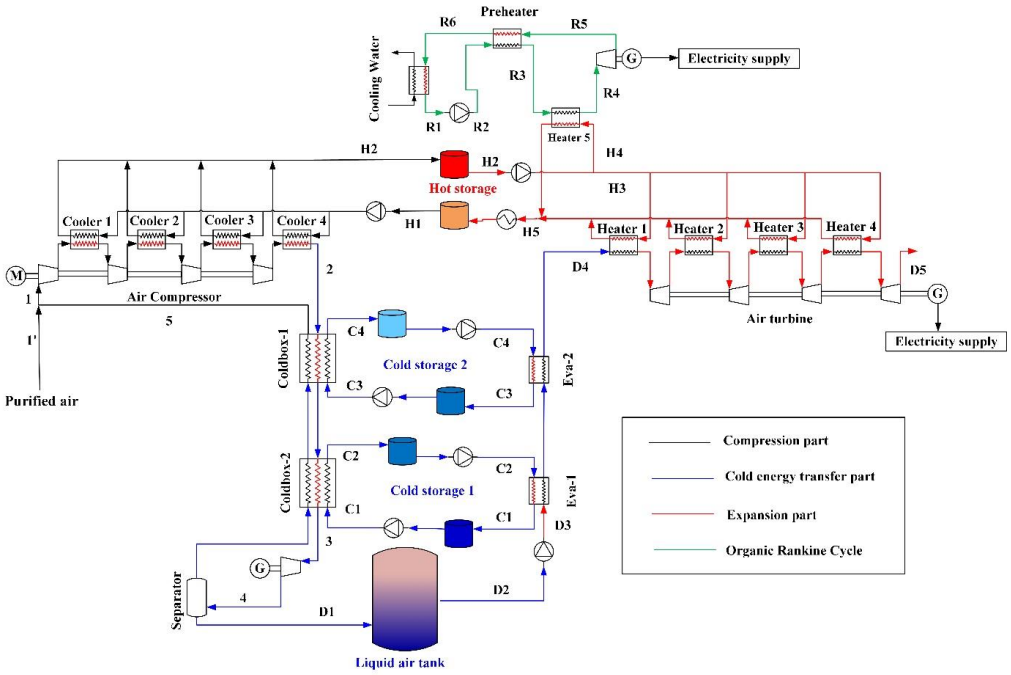

Figure 7.2 Flowsheet of an LAES system with an additional ORC.

7.2.1.1 Total capital investment cost

The total capital investment cost (C_{TCI}) consists of the total bare-module investment cost (C_{BM}), the contingency cost and contractor fee (C_{CC}), the land acquisition cost (C_{LA}), and the working

capital cost (C_{WC}), as given by Equation (7.1). The working capital cost is a part of start-up capital used to fund the initial operating phase of the plant before it earns revenue. This part of the cost is recoverable at the end of the project; thus, it is excluded from depreciation. The calculation methods for total capital investment cost of an LAES plant are provided in Table 7.2.

$$C_{TCI} = C_{BM} + C_{CC} + C_{LA} + C_{WC} \tag{7.1}$$

Table 7.2 Parameters, equations and assumptions for cost calculations of an LAES plant.

Component	Main variable	Method	Assumptions	Reference
Compressors	Capacity, $\dot{W}_C$ (kW)	246 \$/kW[a]	CS, Centrifugal	[145]
Turbines	Capacity, $\dot{W}_T$ (kW)	268.5 \$/kW	CS, Axial gas turbine	[145]
Cryo-turbine	Capacity, $\dot{W}_{CT}$ (kW)	$11514 \cdot \dot{W}_{CT}^{0.67}$ \$/kW	SS, Radial gas and liquid expander	[146]
Hot storage	Volume, V (m^3)	$(242 \cdot V + 619300)$ \$/m^3	Large field erected storage tank	[147]
Aftercoolers and preheaters	Area, A (m^2)	$(f_p \cdot 1.43 + 2.068) \cdot \frac{65 \cdot A}{1000}$ \$/m^2	f_p=1, CS/CS, Shell/tube	[146]
Cold box and evaporators	Area, A (m^2)	$(160.6 + 80.3 \cdot (f_m + f_p)) \cdot \frac{A}{2000}$ \$/m^2	f_m=2.3 and f_p=1.2, SS, Flat-plate	[146]
Cold storage	Duty, $\dot{Q}$ (kWh)	15125 \$/kWh	Rock packed-bed	[148]
Liquid air storage tank	Mass of liquid air, $\dot{m}$ (ton)	2480.5 \$/ton	SS, Cryotank, Atmospheric pressure	[148]
Liquid pump	Capacity, $\dot{W}_P$ (kW)	$2820 \cdot \dot{W}_P^{0.6}$ \$/kW	Reciprocating pump	[146]
C_{CC}	-	$0.18 \cdot C_{BM}$ \$	18% of total bare-module cost	[149]
C_{LA}	-	66686 \$	Plant covers 19 218 m^2 with a land price of 3.47 \$/m^2	[75]
C_{WC}	-	$0.15 \cdot C_{BM}$ \$	15% of total bare-module cost	[149]

[a] An extra cost factor f_c is applied to the compressor with a high pressure ratio in the LAES system. The cost formula for the compressors with high pressure ratios is: $246 \cdot f_c$ \$/kW. The f_c is assumed to be 1.9 and 1.3 for Cases 1 and 2.

7.2.1.2 Annualized post-production cost

Annualized post-production cost (C_{APC}) is the sum of the total annual operating cost and the depreciation of capital investment, as given by Equation (7.2). The estimation of the annualized post-production cost is summarized in Table 7.3.

$$C_{APC} = C_{AOC} + C_D \tag{7.2}$$

The total annual operating cost (C_{AOC}) is composed of maintenance cost (C_{MC}), labor cost (C_{LC}), and utility cost (C_{UC}), as shown in Equation (7.3).

$$C_{AOC} = C_{MC} + C_{LC} + C_{UC} \tag{7.3}$$

Table 7.3 Estimation of annualized post-production cost of an LAES plant.

Term	Assumptions	Reference
C_{MC}	6% of total capital investment cost	[149]
C_{LC}	Plant operates with 20 workers with an annual salary of 56,310 $/person	[150]
C_{UC}	Sum of the electricity cost at low demand times and the cooling water cost for cooling duties.	
C_D	$\eta = 0.85$; $\beta = 0.05$	[75]

The depreciation of capital investment (C_D) is the difference between the purchase and installation cost before the plant is put into operation and the gains obtained by selling equipment when the plant is closed. This is taken as an expense each year. In this work, the C_D is calculated by using the straight-line method, which is provided by Equation (7.4).

$$C_D = \frac{C_{TCI} \cdot \eta \cdot (1 - \beta)}{N} \tag{7.4}$$

Here, η is the conversion ratio of the total capital investment to depreciable assets (excluding the working capital cost); β is the residual value ratio; and N denotes the depreciation period (year).

7.2.1.3 Annual income model

The profit can be obtained by selling stored electricity at high demand times and hot water supplied to domestic hot water systems. The annual income model (C_{AI}) is given by Equation (7.5).

$$C_{AI} = \dot{W} \cdot C_{hd} \cdot h_{an} + \dot{Q}_{wh} \cdot C_{hw} \tag{7.5}$$

Here, $\dot{W}$ denotes the power production in the discharging process (kW); $\dot{Q}_{wh}$ is the heat duty of the water heater (kW); C_{hd} and C_{hw} are the electricity price during high demand periods and the hot water price ($/kWh); and h_{an} represents the annual number of hours for power generation (h/year).

7.2.1.4 Financial evaluation index

The economic performance of the LAES system is evaluated by net present value (NPV), payback period and levelized cost of storage (LCOS). The definitions of the three financial evaluation indexes are provided in Section 3.1.

7.2.2 Initial conditions and assumptions

In order to apply the economic estimation to an LAES system as given by Equations (7.1) - (7.5) and Equations (3.8) - (3.10), the key input parameters for the calculations are summarized in Table 7.4. The operating strategy for the LAES is to store electricity during off-peak periods at a low electricity price and recover electricity during on-peak periods at a high price. The hot water can also be supplied for domestic hot water systems. However, the cost of cold water is neglected.

Table 7.4 Key input parameters for cost estimation of an LAES plant.

Parameters	Unit	Value
Plant life time	years	30
Electricity storage time	h	8
Electricity release time	h	8
Annual operating time	h	4800
Interest rate	%	8
Off-peak electricity price[a]	$/kWh	0.20
On-peak electricity price[a]	$/kWh	0.58
Hot water price [152]	$/kWh	0.081

[a] Electricity prices for on-peak and off-peak periods are for the Hawaii area [151].

7.3 Results and discussion

The economic analysis of the four case studies is discussed in Section 7.3.1. A sensitivity analysis of the on-peak and off-peak electricity prices, the extra cost factor, and the annual operating hours for the LAES system is carried out in Section 7.3.2. Finally, the comparison between the LAES and other energy storage technologies is provided in Section 7.3.3.

7.3.1 Comparison of different LAES configurations

The total capital investment cost of some LAES configurations is shown in

Figure 7.3. It is observed from

Figure 7.3 that the cost of the compression part accounts for the largest portion in the LAES

configurations. This indicates that the extra cost factor for compressors with high pressure ratios has a significant effect on the LAES system, and a sensitivity analysis for the extra cost factor will be conducted in Section 7.3.2. Moreover, the total capital investment cost, the annualized post-production cost, the annual income, and the economic evaluation indexes of the four case studies are shown in Table 7.5. It can be seen that the total investment cost in the best LAES configuration from an energy point of view (Case 1) is the highest, followed by Case 2 and Case 3, while Case 4 has the lowest. The reason is that an extra cost factor of 1.9 that is applied to the cost model of compressors with the highest pressure ratios leads to the highest price of the compression units in Case 1 among the four case studies. However, due to the high RTE of Case 1, the mass flow of air feed is lower compared to Cases 2 - 4 to achieve the power output of 10 MW in the LAES system, which results in a smaller size and cost of equipment other than compressors. The total investment cost for Case 2 is larger than Cases 3 and 4 with conventional compressors, since the pressure ratios of compressors in Case 2 are slightly larger than conventional units and the extra cost factor applied to this case is 1.3. By comparing Cases 3 and 4, it is observed that the total investment cost of Case 3 is larger than Case 4, which means that the total investment cost of the LAES system is reduced when an additional ORC is adopted to utilize the unused compression heat. This is due to the fact that the RTE of Case 4 is higher than Case 3, and the mass flow rate of air feed in Case 4 is slightly smaller than that of Case 3, as shown in Table 7.1. Thus, the cost of equipment other than compressors in Case 4 is smaller than Case 3. Since the reduction in the cost of LAES equipment can justify an increase in the cost associated with the ORC, the total investment cost in Case 4 is lower compared to Case 3.

Table 7.5 Total investment cost, annualized post-production cost, annual income and economic evaluation indexes of some LAES configurations

Parameters	Unit	Case 1	Case2	Case 3	Case 4
C_{TCI}	M$	27.77	25.37	25.23	24.70
C_{AOC}	M$/year	9.99	10.00	10.36	10.06
C_{D}	M$/year	0.56	0.51	0.51	0.50
C_{AI}	M$/year	14.74	14.57	14.53	13.93
NPV	M$	31.97	31.81	27.45	24.35
Payback period	years	7.05	6.63	7.33	7.85
LCOS	$/kWh	0.496	0.489	0.503	0.490

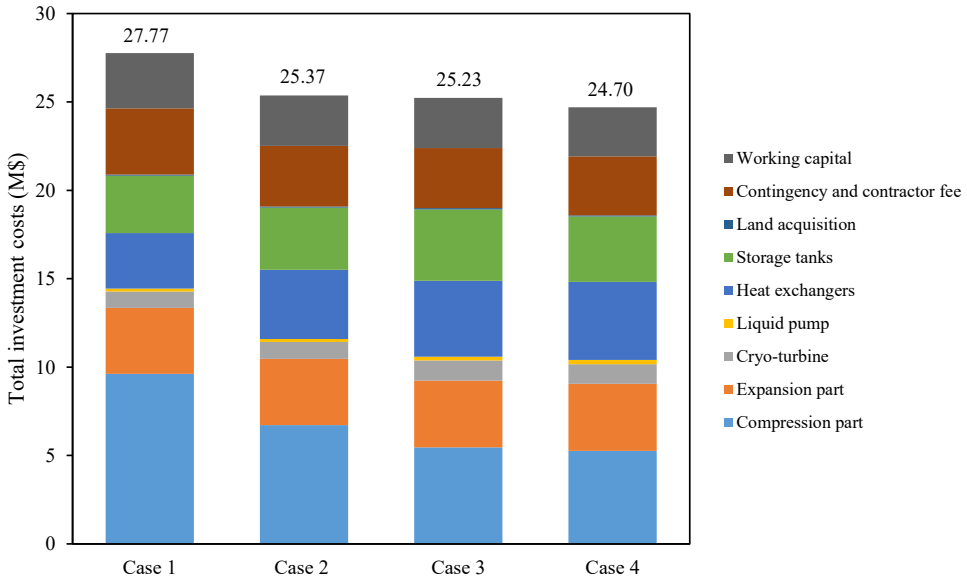

Figure 7.3 Total investment costs of some LAES configurations.

The annualized post-production cost, which is related to the total annual operating cost (maintenance cost, labor cost and utility cost) and the depreciation of capital cost of some LAES configurations are presented in Figure 7.4. It is worth noting that the utility cost is related to compression work in the charging mode, while the annual income is the result of electricity export and hot water supply in the discharging mode. A dominant part of the annualized post-production cost is utility cost, which accounts for more than 65% of the annualized post-production cost. The amount of consumed electricity during the charging phase in Case 3 is the highest among the four case studies. Thus, the corresponding utility cost and the annualized post-production cost in Case 3 is the largest (see Figure 7.4), followed by Case 4 in terms of utility cost and annualized post-production cost. The utility cost, shown as the values next to the grey bars in Figure 7.4, is the smallest in Case 1 due to the high RTE of system. However, the maintenance cost and the depreciation of capital cost in Case 1 are slightly larger than for the other cases. As a result, the annualized post-production cost of Case 1 is slightly lower than Case 4. The lower maintenance cost and the depreciation of capital makes the annualized post-production cost of Case 2 smaller than Case 1, and Case 2 has the smallest annualized post-production cost.

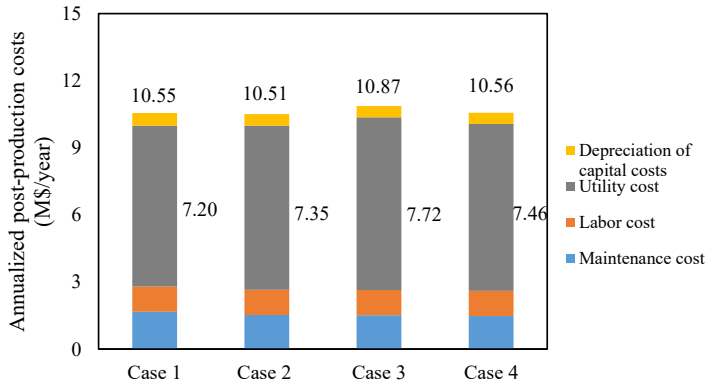

Figure 7.4 Annualized post-production costs of some LAES configurations.

The annual income of different LAES configurations is related to the amount of electricity export and hot water supply in the discharging mode. As shown in Table 7.5, Case 4 has the lowest annual income compared to Cases 1 - 3. This is due to the fact that the revenue for Case 4 is only from electricity production, while hot water is another profitable product in Cases 1 - 3. In this chapter, LCOS, NPV and payback period are used to evaluate the four selected configurations for the LAES. According to the definition of the LCOS, the income of the LAES plant is not included. It turns out that Case 2 has a lower LCOS of 0.489 $/kWh compared to Cases 1, 3 and 4. However, for the NPV and payback period, the income of the LAES is included, and this obviously has an impact on the evaluation of the four cases studied. The NPV of the four cases for a 30 years lifespan is positive, which means that all of them are profitable. The NPV for different LAES configurations as a function of the number of years in operation is illustrated in Figure 7.5. It is observed that the NPV for Case 4 is larger than the other cases in the beginning of the project, as the total capital investment cost for Case 4 is the smallest among different layouts of the LAES system. However, from year 1 to year 24, Case 2 has a larger NPV than other LAES configurations, which means that Case 2 is the most economical layout of the LAES during this period. The NPV for Case 1 is the smallest in the beginning due to its large total capital cost. However, the NPV for Case 1 is larger than the other cases after year 25 due to the large profit obtained by selling electricity and hot water in. In year 30, the highest NPV of 32.0 M$ is achieved for Case 1, followed by Case 2 (31.8 M$) and Case 3 (27.5 M$), while Case 4 has the smallest NPV of 24.4 M$. Moreover, the payback period, which is a parameter to indicate the time required for completely recovering total investment cost, is also provided for the four cases studied in Table 7.5. It is shown that a shorter return on the investment cost is obtained in Case 2 (6.63 years) compared to Cases 1, 3 and 4.

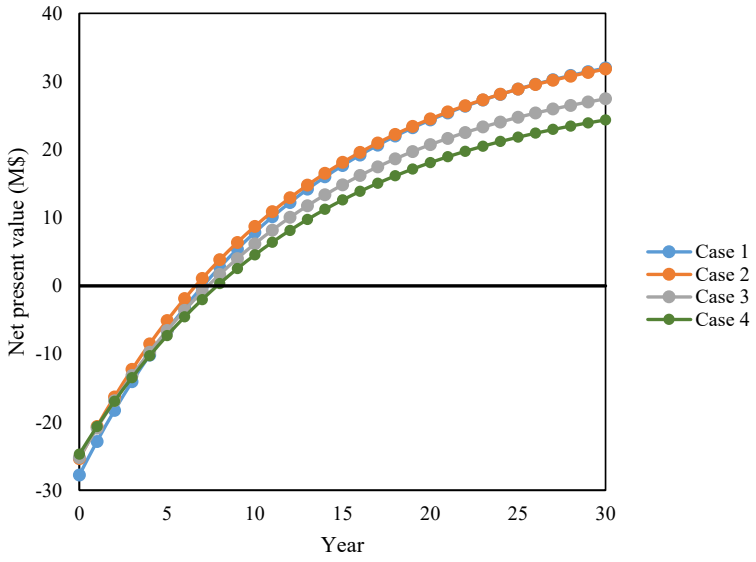

Figure 7.5 NPV for different LAES configurations.

According to the results from the above analysis, Case 2 has a slightly lower LCOS compared to the other cases without considering the revenue of the LAES plant. However, when the revenue of the LAES is considered, Case 2 is more profitable than the other options from year 1 to year 24. Case 1 has better economic performance than other case studies from year 25, so it is more profitable in long-term operation. In addition, by comparing Cases 3 and 4, it can be found that the energy efficiency is increased (the RTE is improved from 62.16 to 64.41%), but the NPV is reduced with an additional ORC in the LAES system that has a 4-stage compressor and a 4-stage expander. This is because electricity is the only revenue source for Case 4 with an additional ORC to utilize the surplus compression heat. Although the increased RTE leads to lower total capital investment and annualized post-production cost, the annual income is smaller for Case 4 compared to Case 3. The extra profit gained by selling hot water can justify

the increase in the total expenses regardless of a slightly lower RTE in Case 3 compared to Case 4.

7.3.2 Sensitivity analysis

There are several important parameters for the cost evaluation of the LAES system, such as on-peak electricity price and the extra cost factor discussed in Section 7.2.1. In this section, a sensitivity analysis is carried out to measure the effect of the mentioned parameters on the system performance.

7.3.2.1 Effects of the on-peak electricity price on some LAES configurations

As mentioned in Section 7.2.2, the electricity consumed in the LAES is purchased during off-peak periods and the electricity produced in the system will be sold during on-peak periods. Thus, the on-peak electricity price is critical for evaluating the profitability of the LAES system. In the economic analyses above, the electricity prices for on-peak and off-peak periods are 0.58 and 0.20 $/kWh. The on-peak electricity price will be varied between -30% and +30% of the nominal value. When the off-peak electricity price is fixed at 0.20 $/kWh, the variations of the NPV with changing on-peak electricity price are shown in Figure 7.6. NPVs and payback periods under different on-peak electricity prices are listed in Table 7.6 and Table 7.7. It is worth noting that the NPV will be negative, and the payback period will be longer than the lifespan of the LAES plant when the on-peak electricity price is below the break-even point, which of course is a range not worth studying. Thus, the first point for Cases 1 - 4 in Figure 7.6 is their break-even points, where the profit is equal to total expenses. The break-even on-peak electricity prices for the four case studies are listed in Table 7.8. It is observed that the break-even on-peak electricity prices for Cases 1 and 2 are 0.462 $/kWh, which are smaller than the electricity prices for Cases 3 and 4. Obviously, a higher on-peak electricity price will lead to a higher NPV and a quicker return on investment for the four cases. From Figure 7.6, when the electricity is sold at 0.754 $/kWh, the most profitable layout of the LAES is Case 1 with the largest revenue of 79.0 M$, very closely followed by Case 2 with a revenue of 78.8

M$.

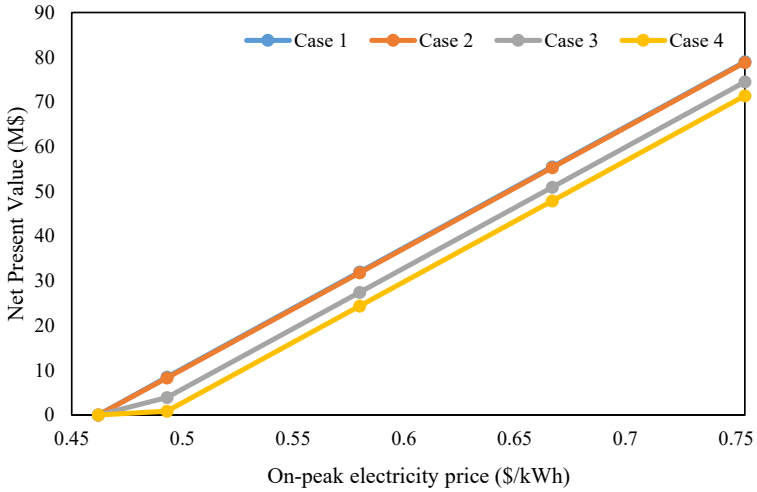

Figure 7.6 Comparison of NPV under different on-peak electricity prices.

Table 7.6 NPVs under different on-peak electricity prices.

On-peak electricity price ($/kWh)	NPV (M$)			
	Case 1	Case 2	Case 3	Case 4
0.493	8.46	8.31	3.94	0.83
0.58	31.97	31.81	27.45	24.35
0.667	55.47	55.32	50.96	47.87
0.754	78.97	78.83	74.47	71.39

7.3.2.2 Effects of the extra cost factor on some LAES configurations

As discussed in Section 7.3.1, a major part of the total investment cost is allocated to the compression part. It is obvious that the extra cost factor applied to compressors in Cases 1 and 2 significantly affects the economic performance of the LAES system. The base values for the extra cost factors in Cases 1 and 2 are 1.9 and 1.3, respectively. The variation of the extra cost factors is in the range between -20% and +20% of the nominal value, and the sensitivity of the cost factors on the NPV for the LAES is shown in Table 7.9. Since the extra cost factors only apply to Cases 1 and 2, Cases 3 and 4 are not part of this sensitivity analysis. It is observed that Case 1 has the most economic layout of the LAS systems when the extra cost factor is below the nominal value. The largest revenue of 35.7 M$ is achieved in Case 1 with the minimum extra cost factor of 1.52, which is much larger than Cases 3 and 4. When the extra cost factors are decreased from their nominal values, the second largest NPV is obtained in Case 2 (34.4 M$), followed by Case 3 (27.5 M$), while Case 4 (24.4 M$) is the smallest. A different situation can be found when the extra cost factors are larger than their nominal values, where Case 2 replaces Case 1 as the most profitable layout for the LAES system. In addition, Table 7.10 lists the payback period for some LAES configurations under different extra cost factors.

Table 7.7 Payback periods under different on-peak electricity prices.

On-peak electricity price ($/kWh)	Payback period (year)			
	Case 1	Case 2	Case 3	Case 4
0.493	15.23	14.74	19.62	26.63
0.580	7.05	6.63	7.33	7.85
0.667	4.64	4.33	4.60	4.76
0.754	3.47	3.22	3.36	3.42

Table 7.8 Break-even on-peak electricity prices for the selected cases studied.

Break-even index	Unit	Case 1	Case 2	Case 3	Case 4
On-peak electricity price	$/kWh	0.462	0.462	0.478	0.490

Table 7.9 NPVs for some LAES configurations under different extra cost factors.

Variation range of cost factors	NPV			
	Case 1	Case 2	Case 3	Case 4
-20%	35.67	34.4	27.45	24.35
-10%	33.82	33.11	27.45	24.35
0	31.97	31.81	27.45	24.35
10%	30.12	30.52	27.45	24.35
20%	28.27	29.23	27.45	24.35

Table 7.10 Payback periods for some LAES configurations under different extra cost factors.

Variation range of cost factors	Case 1	Case 2	Case 3	Case 4
-20%	6.06	5.93	7.33	7.85
-10%	6.54	6.27	7.33	7.85
0	7.05	6.63	7.33	7.85
10%	7.58	7.00	7.33	7.85
20%	8.15	7.39	7.33	7.85

7.3.3 LAES versus other energy storage technologies

In this section, the LCOS for Cases 1 - 4 is compared with mature energy storage technologies, such as PHES, CAES, Li-ion and Pb batteries. The LCOS of the four mature energy storage technologies are calculated and provided by Jülch [153]. In order to objectively compare Cases 1 - 4 with other energy storage technologies, the storage capacity and the cost of electricity in the charge mode are equal to 100 MW and 0.033 $/kWh, which are the same as in the work of Jülch [153]. The main cost components contributing to the LCOS for each system is shown in Figure 7.7. It is observed that Case 2 has a lower LCOS compared to the other three LAES configurations. Moreover, the LCOS for the LAES is considerably less than for Li-ion batteries and slightly less than for Pb batteries, but LAES cannot compete with PHES and CAES.

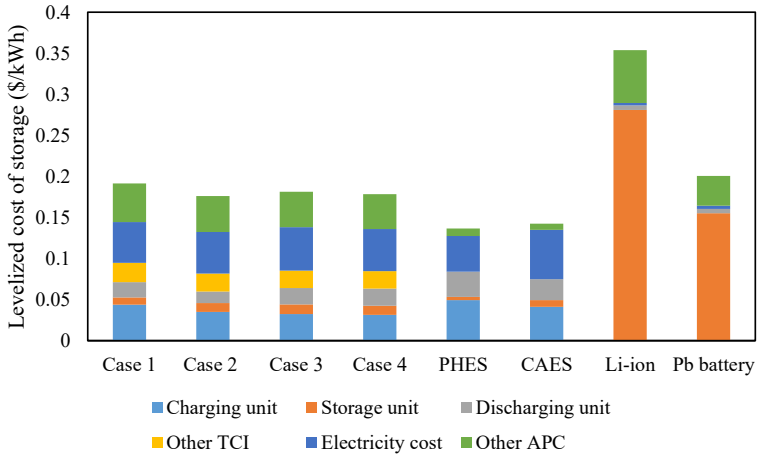

Figure 7.7 Cost comparison between the LAES and other energy storage technologies.

7.4 Conclusions

An economic analysis of four different layouts for a standalone liquid air energy storage (LAES) is performed and the four configurations are compared. The net present value (NPV), payback period and levelized cost of storage (LCOS) are selected as economic evaluation indexes to present the economic benefit of different LAES processes. Results indicate that the LAES system with a 3-stage compressor and a 4-stage expander (Case 2) has the lowest LCOS among the four case studies without considering the income of the LAES plant from power export and hot water supply. However, when the income of the LAES is considered, the LAES system with a 2-stage compressor and a 3-stage expander (Case 1) has a better economic performance than the other cases. The NPV of 32.0 M$ is achieved for Case 1, which is 0.5%, 16.5% and 31.3% larger than Cases 2, 3 (LAES with a 4-stage compressor and a 4-stage expander) and 4 (system with a 4-stage compressor and a 4-stage expander and an Organic Rankine Cycle), respectively. In addition, by comparing Cases 3 and 4, with an additional ORC in Case 4, the NPV is reduced and the return on investment is increased compared to Case 3 where hot water production gives extra profit.

Results of the sensitivity analysis show that the largest NPV of 79.0 M$ is obtained in Case 1 when the electricity is sold at 0.754 $/kWh, which is 1.5 times more profitable than selling electricity at 0.580 $/kWh. In addition, when the extra cost factor is decreased from the nominal values (1.9 for Case 1 and 1.3 for Case 2) to lower values, the largest revenue of 35.7 M$ is achieved in Case 1 with the minimum extra cost factor of 1.52.

The economic analysis of the LAES system shows that the four studied cases with a storage capacity of 10 MW / 80 MWh are economically feasible. The economic comparison between the LAES and other energy storage technologies indicates that the LAES is a promising technology, which has a better economic performance than Li-ion and Pb batteries, but LAES has a larger LCOS than PHES and CAES. Thus, further research on the LAES is required to improve its cost competitiveness.

Chapter 8 Conclusions and future work

8.1 Conclusions

The main purpose of the research reported in this thesis is to improve the performance of a standalone Liquid Air Energy Storage (LAES) system by developing novel cold energy recovery cycles, analyzing different configurations for the compression and expansion sections, and being integrated with additional thermodynamic cycles. This thesis mainly focuses on developing process models of the modified LAES for systematic optimization in order to objectively assess measures for performance improvement. The economic models of the proposed system are also provided to comprehensively evaluate the feasibility of this technology.

Different cold energy recovery cycles are optimized and compared by using a stochastic search optimization method (Particle Swarm Optimization, PSO) to analyze the effect of structural differences. A single multi-component fluid cycle (MCFC) to be used as the cold energy recovery cycle is not recommended since the temperature difference between the hot and cold composite curves of the low-temperature heat exchangers is relatively large, resulting in poor performance for the entire system. Two cold energy recovery cycles, however, are able to considerably improve the performance of the LAES system. Among several studied combinations, dual MCFC is the preferred configuration to transfer the cold regasification energy from liquid air to air liquefaction in the LAES. Organic Rankine Cycles (ORCs) were also tested for transferring cold thermal energy between the charging and discharging processes. This was, however, proven not to be an interesting option, since the power output

of the ORC was achieved at the expense of an increase in the temperature difference of low-temperature heat exchangers, reducing the system performance.

For the LAES, it is found that the expansion section is strongly influenced by the compression section since there is a hot thermal energy transfer and storage between these two sections in the standalone system. Various LAES configurations related to different number of compression and expansion stages are optimized and compared. A better performance of the LAES is obtained when the hot and cold streams have composite curves that are close to parallel in the preheaters. Moreover, the thermodynamic optimum is found when there are few compression stages with large pressure ratios. Of course, large pressure ratios affect the technical feasibility and investment cost. In cases where compression heat from the charging part cannot be fully utilized in the preheaters, an ORC can be used to turn this surplus heat into power. Exergy analysis of the LAES indicates that the performance of the expansion part is mainly related to the heat transfer efficiency in preheaters and the performance of the ORC, both significantly affecting the RTE.

The mentioned part of compression heat that for some LAES configurations (i.e. the number of compression stages is equal to or larger than the number of expansion stages) is not efficiently utilized in the preheaters, has been subject to a more detailed investigation. The unused compression heat can be used in additional thermodynamic cycles for power generation or to produce hot or cold streams. An ORC and an Absorption Refrigeration Cycle (ARC) are suggested to utilize high-grade surplus compression heat, while a High Temperature Heat Pump (HTHP) is considered in LAES configurations with medium grade compression heat, since working fluids available for high temperature heat pump systems are limited. Optimization results show that the ORC, the ARC and the HTHP are effective methods to improve the performance of the LAES system by utilizing the available surplus compression heat.

Although the LAES system is commonly optimized to maximize RTE, it is also important to evaluate the economic feasibility of this technology. An economic analysis of four different layouts for a standalone LAES is performed. The LAES with fewer compression stages and

higher pressure ratios are found to be more profitable compared to the system with compressor pressure ratios within the normal range. The economic comparison between the LAES and other energy storage technologies indicates that the LAES has a lower levelized cost of storage (LCOS) than batteries, but LAES has a larger LCOS than pumped hydroelectric energy storage (PHES) and compressed air energy storage (CAES), which validates the economic viability of this technology.

8.2 Future work

Although the structural optimization of the LAES provides interesting and promising results in this thesis, there are still potential areas that require further investigation. The main future research topics are summarized as follows:

The thermodynamic analysis of the LAES is carried out based on steady-state models of the process. However, as an energy storage technology, the LAES must be flexible enough to handle the intermittent renewable energy sources and the fluctuating electricity demand. Thus, dynamic models of the LAES should be developed to correctly predict the transient phenomena in actual operation.

It makes sense to include energy losses in the analysis of the LAES, especially in hot and cold thermal energy storage cycles. In addition, materials for the low-temperature energy storage and equipment with excellent thermal insulation have not been tested and analyzed.

To analyze the LAES with additional thermodynamic cycles, more case studies are needed. In particular, all possible combinations between the LAES and the ARC / HTHP have not been discussed. For the ARC and HTHP in the LAES, the unused compression heat is first converted to cold energy (in ARC) or enhanced heat (in HTHP). Either the cold energy or the enhanced heat needs to be utilized somewhere in the LAES to increase the performance of the system. In this thesis, we use the cold energy from the ARC in the cold box, while this can also be used to precool the compressed air in the compression part, which can be considered in future work.

The enhanced heat from the HTHP is used to preheat air before expansion, but there are also other methods to utilize this enhanced heat. One example is to use the enhanced heat in an ORC rather than the expansion stages.

An economic analysis has been performed to evaluate the economic feasibility of the modified LAES system. The cost data available in literature should only be seen as an estimation of the CAPEX and OPEX, and a more accurate method should be considered. Besides, cost uncertainties related to unconventional units (such as compressors with high pressure ratios) and materials may have significant effects on the economics of the proposed system. It would be interesting to optimize the cost of the LAES, which may result in different optimal operating conditions for the system. In this thesis, the revenue of the LAES is achieved by selling electricity and hot water. Another possible revenue of the LAES can be obtained by participating in ancillary service markets with incentive policies, which can be considered in future work.

In the standalone LAES system, the cold energy from liquid air is insufficient to liquefy air, so electricity is required to compress air in the charging part. Thus, the integration of the LAES with external cold energy sources (such as LNG regasification processes and air separation units) could significantly increase the round-trip efficiency of the system. Although a part of compression heat is not efficiently used in the discharging part in some layouts for the LAES, external heat sources at high temperatures can also be considered to increase the inlet temperature of air to expanders, improving the performance of the LAES. Geothermal energy and the waste heat from nuclear power plants are possible options for heat sources that can be applied to the LAES.

References

[1] REN21 Secretariat. Renewables 2020 Global Status Report. Paris, France. 2020.

[2] British Petroleum. BP Statistical Review of World Energy Report. BP: London, UK. 2020.

[3] Alanne K, Saari A. Distributed energy generation and sustainable development. Renewable Sustainable Energy Reviews. 2006;10(6):539-558.

[4] Rozali NEM, Wan Alwi SR, Manan ZA, Klemeš JJ, Hassan MY. Optimisation of pumped-hydro storage system for hybrid power system using power pinch analysis. Chemical Engineering Transactions. 2013;35:85-90.

[5] Aneke M, Wang M. Energy storage technologies and real life applications–A state of the art review. Applied Energy. 2016;179:350-377.

[6] Rehman S, Al-Hadhrami LM, Alam MM. Pumped hydro energy storage system: A technological review. Renewable and Sustainable Energy Reviews. 2015;44:586-598.

[7] Arabkoohsar A, Machado L, Farzaneh-Gord M, Koury RNN. Thermo-economic analysis and sizing of a PV plant equipped with a compressed air energy storage system. Renewable Energy. 2015;83:491-509.

[8] Chen H, Cong TN, Yang W, Tan C, Li Y, Ding Y. Progress in electrical energy storage system: A critical review. Progress in Natural Science. 2009;19:291-312.

[9] Rahman MM, Oni AO, Gemechu E, Kumar A. Assessment of energy storage technologies: A review. Energy Conversion and Management. 2020;223:113295.

[10] U.S. Department of Energy, Office of Fossil Energy. Electricity Storage Technology Review. Washington, U.S.. 2020.

[11] IRENA. Innovative Operation of Pumped Hydropower Storage. Abu Dhabi, United Arab Emirates. 2020.

[12] Damak C, Leducq D, Hoang HM, Negro D, Delahaye A. Liquid air energy storage (LAES) as a large-scale storage technology for renewable energy integration –A review of investigation studies and near perspectives of LAES. International Journal of Refrigeration. 2020;110:208-218.

[13] Linde C. Process of producing low temperatures, the liquefaction of gases, and the separation of the constituents of gaseous mixtures. U.S. Patents 727,650; 1895.

[14] Claude G. Process for separation of the constituents of gaseous mixtures. U.S. Patents 607,775; 1902.

[15] Kapitza PL. Method and means for distillation of low boiling point liquids. U.S. Patents 625,107; 1939.

[16] Roberts MJ, Agrawal R, Daugherty TL. Single mixed refrigerant gas liquefaction process. U.S. Patent No. 6,347,531 B1; 2002.

[17] Swenson LK. Single mixed refrigerant, closed loop process for liquefying natural gas. U.S. Patent No. 4,033,735; 1977.

[18] Barclay MA, Gongaware DF, Dalton K, Skrzypkowski MP. Thermodynamic Cycle Selection for Distributed Natural Gas Liquefaction. AIP Conference Proceedings. 2004;710:75-82.

[19] Fredheim A, Paurola P. Natural Gas Liquefaction Process. U.S. Patent No. 7,386,996 B2; 2008.

[20] Foglietta JH. LNG Production Using Dual Independent Expander Refrigeration Cycles. U.S. Patent No. 6,412,302 B1; 2002.

[21] Roberts MJ, Agrawal R. Dual Mixed Refrigerant Cycle for Gas Liquefaction. U.S. Patent No. 6,269,655 B1; 2001.

[22] Bukowski J, Liu YN, Boccella S, Kowalski L. Innovations in Natural Gas Liquefaction Technology for Future LNG Plants and Loating LNG Facilities. Proceedings of International Gas Union Research Conference 2011. Seoul, Korea: International Gas Union (IGU); 2011.

[23] Grootjans HF, Nagelvoort RK, Vink KJ. Liquefying a Stream Enriched in Methane. U.S. Patent No. 6,370,910 B1; 2002.

[24] Paradowski H, Rojey A. Multi-steps Cooling by Heat Exchanging with the Compressed Coolant. U.S. Patent No. 6,150,389; 2000.

[25] Paradowski H, DuFresne JP. Process analysis shows how to save energy. Hydrocarbon

Process. 1983;62(7):103-108.

[26] Gaumer L, Newton C. Combined cascade and multicomponent refrigeration system and method. U.S. Patent No. 3,763,658; 1973.

[27] Bauer H, Franke H, Sapper R, Schier M, Bolt M, Pettersen J, et al. Natural Gas Liquefaction Process. U.S. Patent No. 2008/0006053 A1; 2008.

[28] Roberts MJ, Agrawal R. Hybrid cycle for the production of liquefied natural gas. U.S. Patent No. 6,308,531; 2001.

[29] Paradowski H, Vovard S. Process for the Production of a Subcooled Liquefied Natural Gas Stream from a Natural Gas Feed Stream, and associated Installation. U.S. Patent No. 2010/0126214 A1; 2010.

[30] Knowlen C, Hertzberg A, Mattick A. Automotive propulsion using liquid nitrogen. 30th Joint Propulsion Conference and Exhibit. 1994;2967.

[31] Knowlen C, Mattick AT, Bruckner AP, Hertzberg A. High efficiency energy conversion systems for liquid nitrogen automobiles. SAE transactions. 1998;1837-1842.

[32] Knowlen C, Williams J, Mattick AT, Deparis H, Hertzberg A. Quasi-isothermal expansion engines for liquid nitrogen automotive propulsion. SAE paper. 1997;972649.

[33] Kim H, Hong S. Review on economical efficiency of LNG cold energy use in South Korea. 23rd World Gas Conference. 2006;1285-1294.

[34] Bai F, Zhang Z. Integration of low-level waste heat recovery and liquefied nature gas cold energy utilization. Chinese Journal of Chemical Engineering. 2008;16(1):95-99.

[35] Wang Q, Li Y, Wang J. Analysis of power cycle based on cold energy of liquefied natural gas and low-grade heat source. Applied Thermal Engineering. 2004;24(4):539-548.

[36] Szargut J, Szczygiel I. Utilization of the cryogenic exergy of liquid natural gas (LNG) for the production of electricity. Energy. 2009;34(7):827-837.

[37] Bisio G, Tagliafico L. On the recovery of LNG physical exergy. Collection of Technical Papers. 35th Intersociety Energy Conversion Engineering Conference and Exhibit (IECEC). 2000;1: 309-317.

[38] Bisio G, Tagliafico L. On the recovery of LNG physical exergy by means of a simple cycle or a complex system. Exergy, An International Journal. 2002;2(1):34-50.

[39] Agazzani A, Massardo AF, Korakianitis T. An assessment of the performance of closed cycles with and without heat rejection at cryogenic temperatures. Journal of Engineering for Gas Turbines and Power. 1999;121(3):458-465.

[40] Zhang N, Liu W, Cai R. Thermodynamic Analysis of Closed Brayton Cycle Working on LNG Cryogenic Exergy and Waste Heat Utilization. Proceedings-Chinese Society of Electrical Engineering. 2003;23(7):173-177.

[41] Gómez MR, Garcia RF, Gómez JR, Carril JC. Review of thermal cycles exploiting the exergy of liquefied natural gas in the regasification process. Renewable and Sustainable Energy Reviews. 2014;38:781-795.

[42] Kaneko K, Ohtani K, Tsujikawa Y, Fujii S. Utilization of the cryogenic exergy of LNG by a mirror gas-turbine. Applied Energy. 2004;79(4):355-369.

[43] Otsuka T. Evolution of an LNG terminal: Senboku terminal of Osaka GAS. Proceedings of the 23rd world gas conference. 2006;1:14.

[44] Oliveti G, Arcuri N, Bruno R, De Simone M. A rational thermodynamic use of liquefied natural gas in a waste incinerator plant. Applied Thermal Engineering. 2012;35:134-144.

[45] Dispenza C, Dispenza G, La Rocca V, Panno G. Exergy recovery during LNG regasification: electric energy production-part two. Applied Thermal Engineering. 2009;29(2-3):388-399.

[46] Dispenza C, Dispenza G, La Rocca V, Panno G. Exergy recovery during LNG regasification: electric energy production-part two. Applied Thermal Engineering. 2009;29(2-3):388-399.

[47] Hisazumi Y, Yamasaki Y, Sugiyama S. Proposal for a high efficiency LNG power-generation system utilizing waste heat from the combined cycle. Applied Energy. 1998;60(3):169-182.

[48] Guizzi GL, Manno M, Tolomei LM, Vitali RM. Thermodynamic analysis of a liquid air energy storage system. Energy. 2015;93:1639-1647.

[49] Guo H, Xu Y, Chen H, Zhou X. Thermodynamic characteristics of a novel supercritical compressed air energy storage system. Energy Conversion and Management. 2016;115:167-177.

[50] Hamdy S, Morosuk T, Tsatsaronis G. Cryogenics-based energy storage: Evaluation of cold exergy recovery cycles. Energy. 2017;138:1069-1080.

[51] Hamdy S, Morosuk T, Tsatsaronis G. Exergoeconomic optimization of an adiabatic cryogenics-based energy storage system. Energy. 2019;183:812-824.

[52] Farres-Antunez P, Xue H, White AJ. Thermodynamic analysis and optimisation of a combined liquid air and pumped thermal energy storage cycle. Journal of Energy Storage. 2018;18:90-102.

[53] An B, Chen J, Deng Z, Zhang T, Wang J, Yang L, Chang X. Design and testing of a high performance liquid phase cold storage system for liquid air energy storage. Energy Conversion and Management. 2020;226:113520.

[54] Hüttermann L, Span R. Influence of the heat capacity of the storage material on the efficiency of thermal regenerators in liquid air energy storage systems. Energy. 2019;174:236-245.

[55] Borri E, Tafone A, Romagnoli A, Comodi G. A review on liquid air energy storage: History, state of the art and recent developments. Renewable and Sustainable Energy Reviews. 2021;137:110572.

[56] Vecchi A, Li Y, Ding Y, Mancarella P, Sciacovelli A. Liquid air energy storage (LAES): A review on technology state-of-the-art, integration pathways and future perspectives. Advances in Applied Energy. 2021;3:100047.

[57] Morgan R, Nelmes S, Gibson E, Brett G. An analysis of a large-scale liquid air energy storage system. Proceedings of the Institution of Civil Engineers - Energy. 2015;168(2):135-144.

[58] Borri E, Tafone A, Romagnoli A, Comodi G. A preliminary study on the optimal configuration and operating range of a “microgrid scale” air liquefaction plant for Liquid Air Energy Storage. Energy Conversion and Management. 2017;143:275-285.

[59] Chen J, An B, Yang L, Wang J, Hu J. Construction and optimization of the cold storage process based on phase change materials used for liquid air energy storage system. Journal of Energy Storage. 2021;41:102873.

[60] Peng X, She X, Cong L, Zhang T, Li C, Li Y, et al. Thermodynamic study on the effect of cold and heat recovery on performance of liquid air energy storage. Applied Energy. 2018;221:86-99.

[61] She X, Peng X, Nie B, Leng G, Zhang X, Weng L, et al. Enhancement of round trip efficiency of liquid air energy storage through effective utilization of heat of compression. Applied Energy. 2017;206:1632-1642.

[62] Zhang T, Zhang X, He Y, Xue X, Mei S. Thermodynamic analysis of hybrid liquid air energy storage systems based on cascaded storage and effective utilization of compression heat. Applied Thermal Engineering. 2020;164:114526.

[63] Tafone A, Borri E, Comodi G, van den Broek M, Romagnoli A. Liquid air energy storage performance enhancement by means of organic Rankine cycle and absorption chiller. Applied Energy. 2018;228:1810-1821.

[64] Cui S, Song J, Wang T, Liu Y, He Q, Liu W. Thermodynamic analysis and efficiency assessment of a novel multi-generation liquid air energy storage system. Energy. 2021;235:121322.

[65] Xue X, Zhang T, Zhang X, Ma L, He Y, Li M, et al. Performance evaluation and exergy analysis of a novel combined cooling, heating and power (CCHP) system based on liquid air energy storage. Energy. 2021;222:119975.

[66] Nabat M, Zeynalian M, Razmi A, Arabkoohsar A, Soltani M. Energy, exergy, and economic analyses of an innovative energy storage system; liquid air energy storage (LAES) combined with high-temperature thermal energy storage (HTES). Energy Conversion and Management. 2020;226:113486.

[67] Li Y, Cao H, Wang S, Jin Y, Li D, Wang X, et al. Load shifting of nuclear power plants using cryogenic energy storage technology. Applied Energy. 2014;113:1710-1716.

[68] Cetin TH, Kanoglu M, Yanikomer N. Cryogenic energy storage powered by geothermal energy. Geothermics. 2019;77:34-40.

[69] Lee I, Park J, Moon I. Conceptual design and exergy analysis of combined cryogenic energy storage and LNG regasification processes: Cold and power integration. Energy. 2017;140:106-115.

[70] Lee I, You F. Systems design and analysis of liquid air energy storage from liquefied natural gas cold energy. Applied Energy. 2019;242:168-180.

[71] Qi M, Park J, Kim J, Lee I, Moon I. Advanced integration of LNG regasification power plant with liquid air energy storage: Enhancements inflexibility, safety, and power generation. Applied Energy. 2020;269:115049.

[72] Antonelli M, Barsali S, Desideri U, Giglioli R, Paganucci F, Pasini G. Liquid air energy storage: Potential and challenges of hybrid power plants. Applied Energy. 2017;194:522-529.

[73] Liu Z, Gundersen T, Liquid Air Energy Storage - Integration Opportunities, AIChE Annual Meeting, Boston and Virtual, USA. 2021.

[74] Wang C, Akkurt N, Zhang X, Luo Y, She X. Techno-economic analyses of multi-functional liquid air energy storage for power generation, oxygen production and heating. Applied Energy. 2020;275:115392.

[75] Cui S, He Q, Liu Y, Wang T, Shi X, Du D. Techno-economic analysis of multi-generation liquid air energy storage system. Applied Thermal Engineering. 2021;198:117511.

[76] Park J, Heo J, Lee J. Techno-economic study of nuclear integrated liquid air energy storage system. Energy Conversion and Management. 2022;251:114937.

[77] Xie C, Hong Y, Ding Y, Li Y, Radcliffe J. An economic feasibility assessment of decoupled energy storage in the UK: With liquid air energy storage as a case study. Applied Energy. 2018;225:244-257.

[78] Lin B, Wu W, Bai M, Xie C, Radcliffe J. Liquid air energy storage: Price arbitrage operations and sizing optimization in the GB real-time electricity market. Energy Economics. 2019;78:647-55.

[79] Tafone A, Ding Y, Li Y, Xie C, Romagnoli A. Levelised Cost of Storage (LCOS) analysis of liquid air energy storage system integrated with Organic Rankine Cycle. Energy. 2020;198:117275.

[80] Hamdy S, Morosuk T, Tsatsaronis G. Exergetic and economic assessment of integrated cryogenic energy storage systems. Cryogenics. 2019;99:39-50.

[81] Georgiou S, Shah N, Markides C. A thermo-economic analysis and comparison of pumped-thermal and liquid-air electricity storage systems. Applied Energy. 2018;226:1119-1133.

[82] Kim J, Noh Y, Chang D. Storage system for distributed-energy generation using liquid air combined with liquefied natural gas. Applied energy. 2018;212:1417-1432.

[83] Qyyum MA, Minh LQ, Ali W, Hussain A, Bahadori A, Lee M. Feasibility study of environmental relative humidity through the thermodynamic effects on the performance of natural gas liquefaction process. Applied Thermal Engineering. 2018;128:51-63.

[84] Nguyen T-V, Rothuizen ED, Markussen WB, Elmegaard B. Thermodynamic comparison of three small-scale gas liquefaction systems. Applied Thermal Engineering. 2018;128:712-724.

[85] Na J, Lim Y, Han C. A modified DIRECT algorithm for hidden constraints in an LNG process optimization. Energy. 2017;126:488-500.

[86] Park K, Won W, Shin D. Effects of varying the ambient temperature on the performance of a single mixed refrigerant liquefaction process. Journal of Natural Gas Science and Engineering. 2016;34:958-968.

[87] Ghorbani B, Hamedi M-H, Amidpour M, Mehrpooya M. Cascade refrigeration systems in integrated cryogenic natural gas process (natural gas liquids (NGL), liquefied natural gas (LNG) and nitrogen rejection unit (NRU)). Energy. 2016;115:88-106.

[88] Park JH, Khan MS, Lee M. Modified coordinate descent methodology for solving process design optimization problems: Application to natural gas plant. Journal of Natural Gas Science and Engineering. 2015;27:32-41.

[89] Lee I, Tak K, Lee S, Ko D, Moon I. Decision Making on Liquefaction Ratio for Minimizing Specific Energy in a LNG Pilot Plant. Industrial & Engineering Chemistry Research. 2015;54(51):12920-12927.

[90] Xu X, Liu J, Cao L. Optimization and analysis of mixed refrigerant composition for the PRICO natural gas liquefaction process. Cryogenics. 2014;59:60-69.

[91] Uwitonze H, Han S, Jangryeok C, Hwang KS. Design process of LNG heavy hydrocarbons fractionation: Low LNG temperature recovery. Chemical Engineering and Processing: Process Intensification. 2014;85:187-195.

[92] Khan MS, Chaniago YD, Getu M, Lee M. Energy saving opportunities in integrated NGL/LNG schemes exploiting: Thermal-coupling common-utilities and process knowledge. Chemical Engineering and Processing: Process Intensification. 2014;82(0):54-64.

[93] Tesch S, Morosuk T, Tsatsaronis G. Advanced exergy analysis applied to the process of regasification of LNG (liquefied natural gas) integrated into an air separation process. Energy. 2016;117, Part 2:550-561.

[94] Marmolejo-Correa D, Gundersen T. A comparison of exergy efficiency definitions with focus on low temperature processes. Energy. 2012;44(1):477-89.

[95] Morosuk T, Tsatsaronis G. Comparative evaluation of LNG – based cogeneration systems using advanced exergetic analysis. Energy. 2011;36(6):3771-3778.

[96] Shin J, Yoon S, Kim J-K. Application of exergy analysis for improving energy efficiency of natural gas liquids recovery processes. Applied Thermal Engineering. 2015;75:967-977.

[97] Szablowski L, Krawczyk P, Wolowicz M. Exergy analysis of adiabatic Liquid Air Energy Storage (A-LAES) system based on Linde-Hampson cycle. Energies. 2021;14(4):945.

[98] Kandezi MS, Naeenian SM. Investigation of an efficient and green system based on liquid air energy storage (LAES) for district cooling and peak shaving: Energy and exergy analyses. Sustainable Energy Technologies and Assessments. 2021;47:101396.

[99] Dzido A, Krawczyk P, Wołowicz M, Badyda K. Comparison of advanced air liquefaction systems in Liquid Air Energy Storage applications. Renewable Energy. 2022;184:727-739.

[100] Manesh MH, Ghorbani B. Energy and exergy analyses of an innovative energy storage configuration using liquid air integrated with Linde-Hampson liquefaction system, molten carbonate fuel cell, and organic Rankine cycle. Journal of Energy Storage. 2022;47:103676.

[101] Derakhshan S, Khosravian M. Exergy optimization of a novel combination of a liquid air energy storage system and a parabolic trough solar collector power plant. Journal of Energy Resources Technology. 2019;141(8):081901.

[102] Al-Zareer M, Dincer I, Rosen MA. Analysis and assessment of novel liquid air energy storage system with district heating and cooling capabilities. Energy. 2017;141:792-802.

[103] Krawczyk P, Szabłowski Ł, Karellas S, Kakaras E, Badyda K. Comparative thermodynamic analysis of compressed air and liquid air energy storage systems. Energy. 2018;142:46-54.

[104] Kotas TJ. The exergy method of thermal plant analysis. Exergon Publishing Company with Paragon Publishing. London, UK. 2012.

[105] Marmolejo-Correa D, Gundersen T. A new efficiency parameter for exergy analysis in low temperature processes. International Journal of Exergy. 2015;17(2):135-170.

[106] Kim D, Gundersen T. Development and use of exergy efficiency for complex cryogenic processes. Energy conversion and management. 2018;171:890-902.

[107] Kim D, Gundersen T. Use of exergy efficiency for the optimization of LNG processes with NGL extraction. Energy. 2020; 197:117232.

[108] Abdollahi-Demneh F, Moosavian MA, Omidkhah MR, Bahmanyar H. Calculating exergy in flowsheeting simulators: A HYSYS implementation. Energy. 2011;36(8):5320-5327.

[109] Lee I, Moon I. Economic Optimization of Dual Mixed Refrigerant Liquefied Natural Gas Plant Considering Natural Gas Extraction Rate. Industrial & Engineering Chemistry Research. 2017;56(10):2804-2814.

[110] Mousavi SB, Ahmadi P, Hanafizadeh P, Khanmohammadi S. Dynamic simulation and techno-economic analysis of liquid air energy storage with cascade phase change materials as a cold storage system. Journal of Energy Storage. 2022;50:104179.

[111] Gao Z, Ji W, Guo L, Fan X, Wang J. Thermo-economic analysis of the integrated bidirectional peak shaving system consisted by liquid air energy storage and combined cycle power plant. Energy Conversion and Management. 2021;234:113945.

[112] Wu S, Zhou C, Doroodchi E, Moghtaderi B. Techno-economic analysis of an integrated liquid air and thermochemical energy storage system. Energy Conversion and Management. 2020;205:112341.

[113] Nabat MH, Sharifi S, Razmi AR. Thermodynamic and economic analyses of a novel liquid air energy storage (LAES) coupled with thermoelectric generator and Kalina cycle. Journal of Energy Storage. 2022;45:103711.

[114] Gao Z, Guo L, Ji W, Xu H, An B, Wang J. Thermodynamic and economic analysis of a trigeneration system based on liquid air energy storage under different operating modes. Energy Conversion and Management. 2020;221:113184.

[115] HYSYS A. Version 10.0. Aspen Technology Inc. Burlington, MA. 2017.

[116] Mofid H, Jazayeri-Rad H, Shahbazian M, Fetanat A. Enhancing the performance of a parallel nitrogen expansion liquefaction process (NELP) using the multi-objective particle swarm optimization (MOPSO) algorithm. Energy. 2019;172:286-303.

[117] Wang M, Khalilpour R, Abbas A. Thermodynamic and economic optimization of LNG mixed refrigerant processes. Energy Conversion and Management. 2014;88:947-961.

[118] Jin C, Lim Y. Economic evaluation of NGL recovery process schemes for lean feed compositions. Chemical Engineering Research and Design. 2018;129:297-305.

[119] Sayyaadi H, Babaelahi M. Thermoeconomic optimization of a cryogenic refrigeration cycle for re-liquefaction of the LNG boil-off gas. International Journal of Refrigeration. 2010;33(6):1197-1207.

[120] Eberhart R, Kennedy J. A new optimizer using particle swarm theory. Proceedings of the Sixth International Symposium on Micro Machine and Human Science. 1995:39-43.

[121] MATLAB. 9.4.0.813654 (R2018a). The MathWorks Inc.. Natick, Massachusetts. 2018.

[122] Higginbotham P, White V, Fogash K, Guvelioglu G. Oxygen supply for oxyfuel CO2 capture. International Journal of Greenhouse Gas Control. 2011;5:S194-S203.

[123] Yu H, Feng X, Wang Y, Biegler LT, Eason J. A systematic method to customize an efficient organic Rankine cycle (ORC) to recover waste heat in refineries. Applied Energy. 2016;179:302-315.

[124] Walraven D, Laenen B, D'Haeseleer W. Economic system optimization of air-cooled organic Rankine cycles powered by low-temperature geothermal heat sources. Energy. 2015;80:104-113.

[125] Jang Y, Lee J. Optimizations of the organic Rankine cycle-based domestic CHP using biomass fuel. Energy Conversion and Management. 2018;160:31-47.

[126] Bellos E, Tzivanidis C. Investigation of the Environmentally-Friendly Refrigerant R152a for Air Conditioning Purposes. Applied Sciences. 2019;9(1):119.

[127] Jensen JB, Skogestad S. Problems with Specifying ΔTmin in the Design of Processes with Heat Exchangers. Industrial & engineering chemistry research. 2008;47(9):3071-3075.

[128] Austbø B, Gundersen T. Optimal distribution of temperature driving forces in low-temperature heat transfer. AIChE Journal, 2015;61(8):2447-2455.

[129] Kim D, Gundersen T. Constraint Formulations for Optimisation of Dual Mixed Refrigerant LNG Processes. Chemical Engineering Transcations. 2017;61:643-648.

[130] RWE Power AG. Adele - adiabatic compressed-air energy storage for electricity supply. 2010.<https://wecanfigurethisout.org/ENERGY/Web_notes/Round_Pegs/Power_Cycles_and_Energy_Storage_Supporting_Files/ADELE%20%E2%80%93%20Adiabatic%20Compressed-Air%20Energy%20Storage%20for%20Electricity%20Supply.pdf > accessed 14.04.2022

[131] Zunft S. Adiabatic CAES: The ADELE-ING project. SCCER Heat & Electricity Storage Symposium. Villigen, Switzerland. 2015.

[132] U.S. Department of Energy. Gas Turbine Handbook. West Virginia, U.S. 2006.

[133] Wu D, Hu B, Wang R, Fan H, Wang R. The performance comparison of high temperature heat pump among R718 and other refrigerants. Renewable Energy. 2020;154:715-722.

[134] Cao X, Yang W, Zhou F, He Y. Performance analysis of different high-temperature heat pump systems for low-grade waste heat recovery. Applied Thermal Engineering. 2014;71(1):291-300.

[135] Bamigbetan O, Eikevik TM, Nekså P, Bantle M. Review of vapour compression heat pumps for high temperature heating using natural working fluids. International journal of refrigeration. 2017;80:197-211.

[136] Frate GF, Ferrari L, Desideri U. Analysis of suitability ranges of high temperature heat pump working fluids. Applied Thermal Engineering. 2019;150:628-640.

[137] Mateu-Royo C, Arpagaus C, Mota-Babiloni A, Navarro-Esbrí J, Bertsch SS. Advanced high temperature heat pump configurations using low GWP refrigerants for industrial waste heat recovery: A comprehensive study. Energy conversion and management. 2021;229:113752.

[138] Mikielewicz D, Wajs J. Performance of the very high-temperature heat pump with low GWP working fluids. Energy. 2019;182:460-470.

[139] Alhamid MI, Aisyah N, Nasruddin N, Lubis A. Thermodynamic and Environmental Analysis of a High-temperature Heat Pump using HCFO-1224yd (Z) and HCFO-1233zd (E). International Journal of Technology. 2019;10(8):1585.

[140] Wu Z, Wang X, Sha L, Li X, Yang X, Ma X, Zhang Y. Performance analysis and multi-objective optimization of the high-temperature cascade heat pump system. Energy. 2021;223:120097.

[141] Jiang J, Hu B, Wang RZ, Liu H, Zhang Z, Li H. Theoretical performance assessment of low-GWP refrigerant R1233zd (E) applied in high temperature heat pump system. International Journal of Refrigeration. 2021;131:897-908.

[142] Yu H, Kim D, Gundersen T. A study of working fluids for Organic Rankine Cycles (ORCs) operating across and below ambient temperature to utilize Liquefied Natural Gas (LNG) cold energy. Energy. 2019;167:730-739.

[143] Yu H, Kim D, Hu X, Gundersen T Organic Rankine Cycle with pure and mixed working fluids for LNG cold energy recovery. Chemical Engineering Transactions. 2019;76:607-612.

[144] United States Environmental Protection Agency. Protecting Our Climate by Reducing Use of HFCs. <www.epa.gov/climate-hfcs-reduction> accessed 27.05.2022.

[145] Latz J. Ökonomische Bewertung der zentralen und der dezentralen Druckluft-speicherung zur verbesserten Netzintegration von Windenergie (in German). Study thesis, Institute for Future Energy Consumer Needs and Behavior (FCN)/E.ON Energy Research Center, RWTH Aachen University; September 2008.

[146] Ulrich G. Vasudevan P. Chemical engineering-process Design and economics: a practical guide. John Wiley & Sons, Inc.. New York. US. 2004;352-419.

[147] Peters M. Timmerhaus K. West R. Chapter 12 materials-handling equipment - design and costs. Plant design and economics of chemical engineers. McGraw-Hill Companies, Inc.. New York. US. 2003;485-589.

[148] Morgan R, Nelmes S, Gibson E, Brett G. An analysis of a large-scale liquid air energy storage system. Proceedings of the Institution of Civil Engineers - Energy. 2015;168(2):135-144.

[149] Turton R. Analysis, synthesis, and design of chemical processes. fourth ed. Upper Saddle River, N.J: Pearson Education; 2013.

[150] Bureau of Labor Statistics. May 2020 national occupational employment and wage estimates. 2020. <www.bls.gov/oes/current/oes_nat.htm#00-0000> accessed 31.06.2022.

[151] Hawaii electric. Time of Use Rate History. 2022. <www.hawaiianelectric.com/products-and-services/save-energy-and-money/time-of-use-program/time-of-use-rate-history> accessed 31.06.2022.

[152] Office of Energy Efficiency & Renewable Energy. Energy Cost Calculator for Electric and Gas Water Heaters. <www.energy.gov/eere/femp/energy-cost-calculator-electric-and-gas-water-heaters> accessed 13.06.2022

[153] Jülch V. Comparison of electricity storage options using levelized cost of storage (LCOS) method. Applied Energy. 2016;183:1594-1606.